A173.4(Bell)

REPORT NO. 8578-950001

LOW FREQUENCY PRESSURE OSCILLATION STUDY

Phase I Interim Report

July 1970

Contract No. NAS9-10381

Bell Aerospace Company DIVISION OF textron

Bell Aerospace Company DIVISION OF textron

POST OFFICE BOX 1 BUFFALO, NEW YORK 14240

REPORT NO. 8578-950001

LOW FREQUENCY PRESSURE OSCILLATION STUDY

Phase I Interim Report

July 1970

Contract No. NAS9-10381

WRITTEN BY: T. Shew
T. Shew

WRITTEN BY: A. Lytle
A. Lytle

APPROVED BY: J. M. Senneff
J. M. Senneff
Program Manager

1.0 INTRODUCTION

Low frequency pressure oscillations (LFO), which are the subject of this study, have been observed during the Apollo program on both the SPS and APS engines. These oscillations normally display a periodic frequency. The amplitude tends to increase and decrease in such a manner that the envelope of the pressure/time instrumentation recordings tend to describe a shape similar to "footballs". The general characteristics of these oscillations are amplitudes of 10 to 50 psi, periodic frequencies ranging from 300 to 500 Hz, and durations from 0.1 to 2.0 seconds. If the oscillations occur, they generally occur immediately after the start transient overshoot. The occurrence of the oscillations appears to be very sensitive to the amount of helium contained in the fuel. Under extreme operating conditions of helium saturation and chamber pressure, the start "football" did not dampen, resulting in sustained oscillations.

This study was undertaken to isolate and identify the parameters which control the occurrence of LFO.

The objective of the first phase of this contract was to utilize the applicable test data gathered at Bell Aerospace Company during the development of the LM Ascent engine to achieve such correlations. The objective of the second phase was to modify previously developed analogue models to make them consistent with the observations and correlations derived in Phase I.

This document presents the results of the Phase I effort. The effort includes a data review and analysis as well as an assessment of the changes required to update the analogue model. Phase I of the program has been subdivided into five tasks (A through E). These tasks were as follows:

Task A - Review and Correlation of Past Engine Test Data

This task consisted of a review of the engine data generated during the Ascent engine development program. The purpose of this data review was to determine the relation between LFO's and operating parameters.

Task B - Review and Analysis of Photographic Studies

This task consisted of review and analysis of the photographic coverage of tests conducted on a single element LM type triplet with and without helium injection. The intent of this effort was to determine the effect of helium on the operating characteristics of the triplet tested.

Task C - Definition of Controlling Parameters and Basic Mechanisms

This task consists of applying the controlling parameters (defined in Tasks A and B) and determining the mechanisms creating LFO's. These theories were then tested to be applicable for use with the analogue model.

Task D - Analogue Model Analysis

This task consists of reviewing applicable analogue models: This consisted primarily of an evaluation of the BAC model used to analyze LFO's during the ascent engine development program in terms of its basic capabilities to predict the controlling parameters determined in Task A. The identification of required changes were to serve as the basis for the Task E recommendations.

Task E - Conclusions and Recommendations

This task provides the rationale for additional work to be conducted in the area of LFO simulations.

This portion of the report is a summary of the Phase I information; the details for each task are reported in individual appendices. The recommendations and conclusions (Task E) are included in a separate section.

2.0 SUMMARY

A critical analysis of the data generated during the Bell Aerospace Company's LM Ascent Engine Development Program was conducted to isolate and correlate the circumstances under which low frequency oscillations were noted.

Previous analysis conducted during the development program had indicated that sensitivity was a function of the fuel propellant circuit, chamber pressure (for a fixed configuration), and the quantity of helium in the fuel. The fuel circuit was identified as a controlling parameter in a series of tests where helium was injected into the individual propellant lines. No significant response was detected from the oxidizer system while injection of helium into the fuel system produced LFO's.

There appear to be discrete fuel pressure drop values below which LFO's are always produced. The specific value is related to the helium saturation of the fuel. This critical pressure ($C\Delta P$) is also influenced by the particular cell in which the tests were conducted. At an overall injector pressure drop below 27 psi, all injectors tested produced a start "football". It was determined furthermore that the pressure drop across the injector orifices is the most sensitive portion of the overall value. An orifice critical pressure drop value of approximately 21 psi was found to exist when the propellants were saturated with helium at the maximum LM tank pressure level.

The available data were derived from tests in which propellants containing substantial amount of helium were used. Sustained LFO's were not found with propellants that had not been exposed to an helium pressure environment above chamber pressure. Furthermore, it was observed that "footballs" become more predominant as pressurization methods were used which would trap or contain greater quantities of helium.

A significant amount of evidence is evolving which indicates that, at least over pertinent portions of the operating regime, the critical pressure drop and the local gas evolution potential are directly related. This means that the critical pressure drop increases as the helium saturation level of the fuel circuit is increased.

In terms of these observations, one can therefore propose an explanation for the occurrence of start "footballs", which must answer such questions as: Why are "footballs" of limited

time duration and how are they related to continuous low frequency oscillations? It can be shown that the start "football" is representative of the period of time when "dirty" fuel, produced by the outgassing during the transient period, passes through the injector. Obviously, the lower the initial saturation level of the propellant, the smaller is the likelihood of a transient "football" and vice versa. The cross-correlationship between the injector pressure drop and the level of "dirtiness" of the propellant becomes evident from such observations that for the same injector configuration, the start "football" duration at the same chamber pressure would increase as the helium saturation level is increased; similarly it also increases as the chamber pressure is decreased for propellants conditioned to the same saturation value. The same general relationship has also been observed for continuous oscillations. Below a given critical pressure drop, stabilization cannot be achieved if a saturation level corresponding to 190 psi exists in the fuel; however, normal operation proceeds if the saturation level is, for example, lowered to 140 psi. It would appear, therefore, that the start "football" and the continuous oscillations are aspects of the same mechanism. In either case, they represent states when the orifice pressure drop of the injector becomes too low to stabilize the existing level of "dirtiness" of the fuel passing through the injector. In either case, thermodynamic states exist where large evolution of helium can occur. For the start "football", this is caused by the temporary low ambient pressure seen during the start transient by the propellant downstream of the trim orifices. The saturation levels at which continuous oscillations have been observed correspond to conditions where gas evolution can readily occur as pressure drops are encountered anywhere in the system. It appears that a functional relationship exists, at ranges of helium saturation which allow local two-phase condition at the injector orifices to occur, which takes the form

$$\frac{C\Delta p}{F(\rho_p)} = K$$

where

$C\Delta p$ is the critical orifice pressure drop.

ρ_p is the local gas evolution potential.

K is a constant for a given injector.

F represents a function

The examination of the photographic data for the single element combustion sheds further light on these considerations. When helium was injected into the upstream fuel circuit, oscillations in the liquid streams, the impinging point and the combustion pattern could be observed. These oscillations were not at the same frequency as the main chamber LFO's, however the existence of the oscillations suggests that the coupling between the injector orifice flow and the combustion is the mechanism producing the sustained oscillations and that the gas (helium) content is the sustaining trigger.

The examination of the Bell Analogue Model indicated that while LFO's could be produced by manipulation of injector drop and propellant acoustic velocity assumption, a critical pressure drop value could not be derived. The inclusion of this criteria into the model then became the recommendation for the Phase II effort. The additional recommendations include a further examination of the method of coupling producing the sustained oscillations. The three methods of coupling suggested for further examination include:

1. As a result of helium evolution, the discharge coefficient, C_D, of the fuel injection orifices changes discontinuously at a given value of back pressure or ΔP. The resultant stream emission oscillation produces a variable rate of combustion.

2. As a result of helium evolution, element blow apart, changing the combustion rate and spatial location, occurs in a discrete manner as the pressure drop or velocity of the fuel jet varies.

3. The fuel propellant manifold upstream of the propellant orifices and the combustion reaction zone form a resonant system. The free gas content in the fuel modifies the acoustic velocity of the fluid.

The portion of this program devoted to the analyses of applicable analogue models was conducted exclusively on the analogue model constructed by BAC and utilized to investigate the LFO phenomena during the LM ascent engine development program.

The review and analysis of this model has indicated its ability to provide correlation with test data in the following areas:

1. Simulate the LFO frequency.

2. Correlate with fuel system variations and LFO occurrence.

3. Correlate the observation that increased chamber pressure reduces LFO incidence.

The BAC analogue model has also been shown to have the ability of simulating what the work statement defines as basic requirements of a model. These requirements include the ability of the model to simulate the following conditions and parameters.

a. Helium saturated propellants.

b. The pressure drops and volumes in various parts of the injector.

c. The pressure drops and volumes in various parts of the propellant feed lines, valve, and test stand.

d. Changes in operating conditions such as mixture ratio, chamber pressure, propellant temperatures, acoustic velocities, impingement angles, fuel and oxidizer propellants leads.

e. Combustion dynamics such as propellant stay times, combustion ignition delay.

3.0 DISCUSSION

As discussed previously, it had been established as a result of tests conducted during the LM ascent engine development program that the occurrence of low frequency chamber pressure oscillations are related to the fuel propellant circuit and become more sensitive at low chamber pressure and in the presence of helium in the fuel. Utilizing this information, the existing test data were reviewed and correlations attempted in order to define the controlling parameters and the basic mechanisms that produce the low frequency oscillations.

Analysis Results of Task A

This effort consisted of the review and correlation of past engine data. During this task, many correlations were attempted in order to isolate the variables that influence the occurrence of both start and continuous low frequency oscillations. The approach taken was to examine the components and variables of the fuel circuit and assess their influence insofar as this was possible with the existing data. The subdivisions of the fuel circuit examined are as follows:

A. Injector Influence

1) Manifold type
2) Manifold volume
3) Baffle type
4) Oxidizer lead
5) Flow rate
6) Pressure drop

B. Feed System Influences

1) Line length
2) Line volume
3) Line pressure drop
4) Prepurge
5) System response

C. Operating Conditions

1) Chamber pressure
2) Feed pressure
3) Propellant temperature
4) Mixture ratio

FIGURE 1

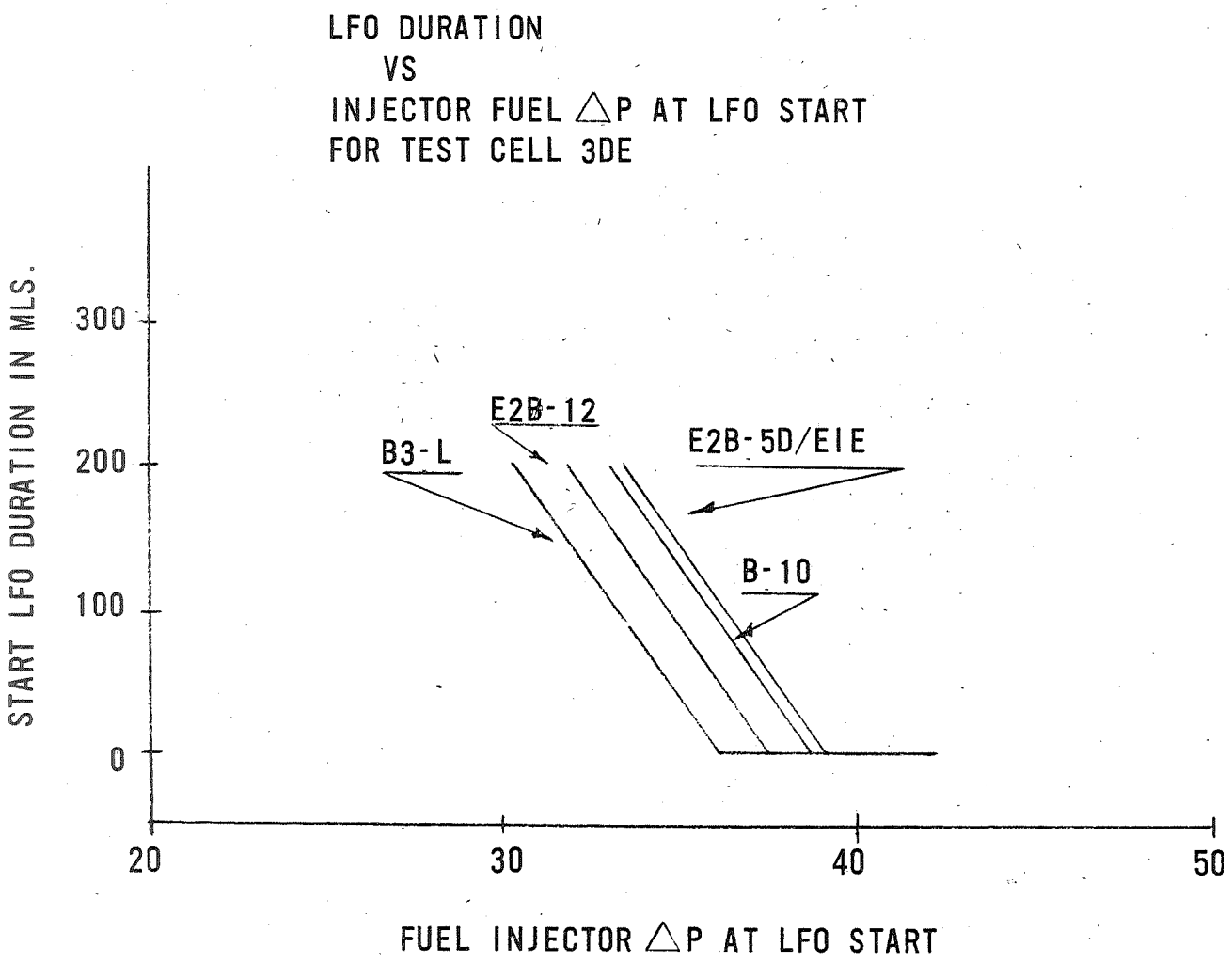
LFO DURATION
VS
INJECTOR FUEL △P AT LFO START
FOR TEST CELL 3DE
START LFO DURATION IN MLS.
300
200
100
0
20
30
40
50
FUEL INJECTOR △P AT LFO START
E2B-12
B3-L
E2B-5D/E1E
B-10

D. Helium Influences

1) Helium injection
2) Circulation method

The only significant correlation relative to injector influences which could be established was with fuel injector pressure drop. This correlation showed that within a given test cell with a given type of helium gas saturation, low frequency oscillations were eliminated when the fuel injector pressure drop was increased above a critical value (Figure 1). This value of fuel injector pressure drop was independent of injector manifold volume, manifold type, baffle type, oxidizer lead, flow rate or design pressure drop. Figure 2 indicates the extremes analyzed in injector type.

The value of critical fuel pressure drop was influenced by the particular test cell used. Figure 3 is a plot of critical fuel pressure drop for each test cell. The analysis conducted to determine the test cell feed system influences (extreme in feed system are shown in Figure 4) indicated that the most significant correlation was with the system response parameters of fuel feed pressure recovery time and fuel transient flow (Figure 5). These effects are understandable when one examines the variations in system response noted in the fuel feed pressure Figure 6.

The test cell effect was considered to be the result of the low static pressure the fuel encounters immediately after opening the propellant valve. As the fuel is accelerated the line pressure decreases until a limiting flow is established. The static pressure at this flow condition is substantially lower than tank pressure and often below chamber pressure. If gas is entrained at a tank pressure value of saturation, the lower pressure would allow the gas to come out of solution, producing an oscillating injection of gas and fuel. The qualifying influence is the rate the gas goes back into solution after the initial chamber pressure rise. The entrained gas in the fuel at start was affected by the response of the test cell and was considered totally responsible for the different start response traces shown in Figure 6.

The operating conditions analyzed failed to yield additional correlations. The propellant temperature did appear to be an influencing parameter; however, these data were masked by the difference between hardware temperature and propellant temperature. The tests conducted with off-nominal propellant temperatures did not incorporate hardware temperature conditioning. Therefore,

FIGURE 2

INJECTOR DESIGN VARIATIONS

B3 TYPE

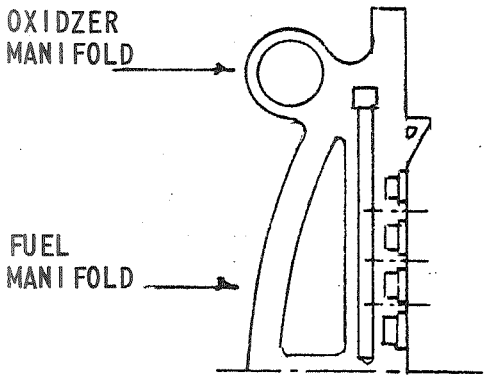

CHARACTERISTICS.

1. MAN TYPE		
	OXID.	SINGLE PASS TORUS
	FUEL	CENTRAL DISC
2. MAN VOL		
	OXID	28 IN^3
	FUEL	28 IN^3
3. BAFFLE TYPE		UNCOOLED 5 LEG
4. PROP. LEAD.		CONCURRENT
5. INJECTOR RATED ΔP		
	FUEL	44

E2 TYPE

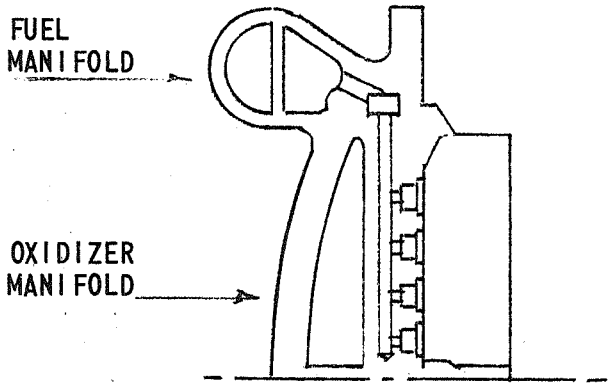

CENTRAL DISC-DOUBLE PASS TORUS

28 IN^3

52 IN^3

FLOW THROUGH 3 LEG

OXIDIZER (50MLS.)

31

FIGURE 3

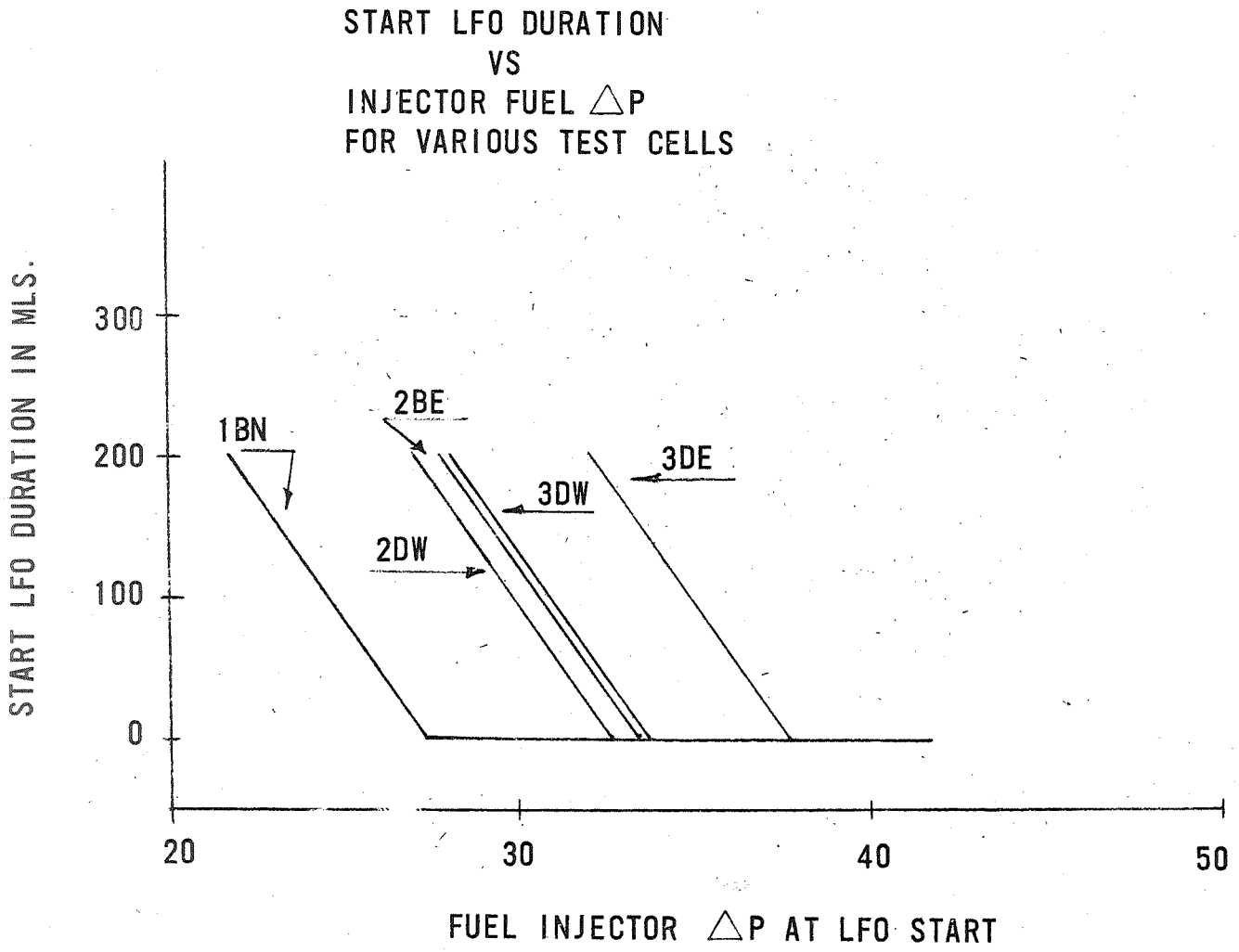
START LFO DURATION
VS
INJECTOR FUEL △P
FOR VARIOUS TEST CELLS
START LFO DURATION IN MLS.
300
200
100
0
1BN
2BE
3DE
3DW
2DW
20
30
40
50
FUEL INJECTOR △P AT LFO START

FIGURE 4

TEST CELL COMPARISON

2DW
VERTICAL S/L

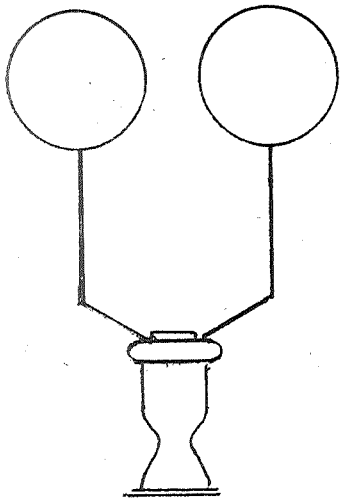

1BN
HORZIONAL ALT.

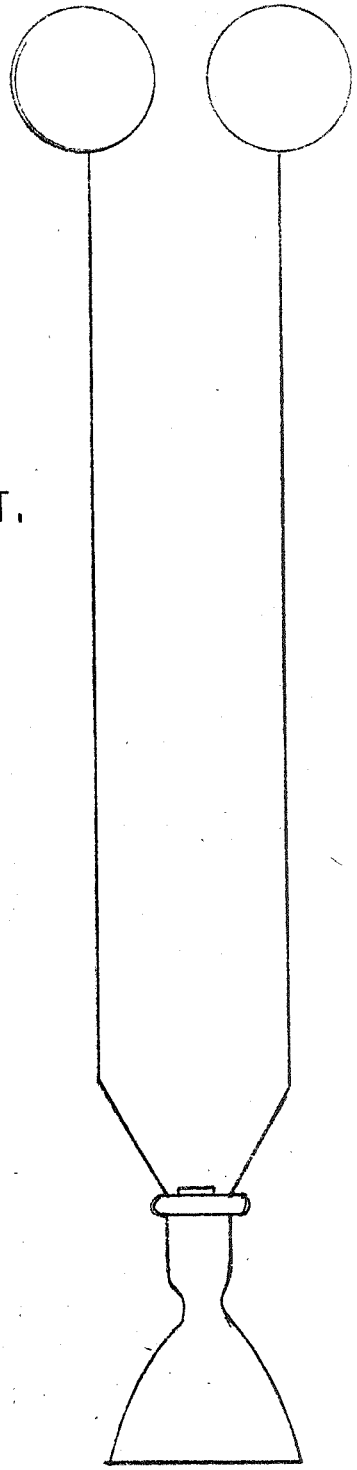

	2DW	1BN
FUEL LINE LENGTH(FT.)	6.5	40.0
FUEL LINE VOLUME(IN^3)	98.0	945.0
FUEL LINE PRESSURE DROP(PSI)	25.0	27.0

FIGURE 5

SYSTEM RESPONSE CHARACTERISTICS

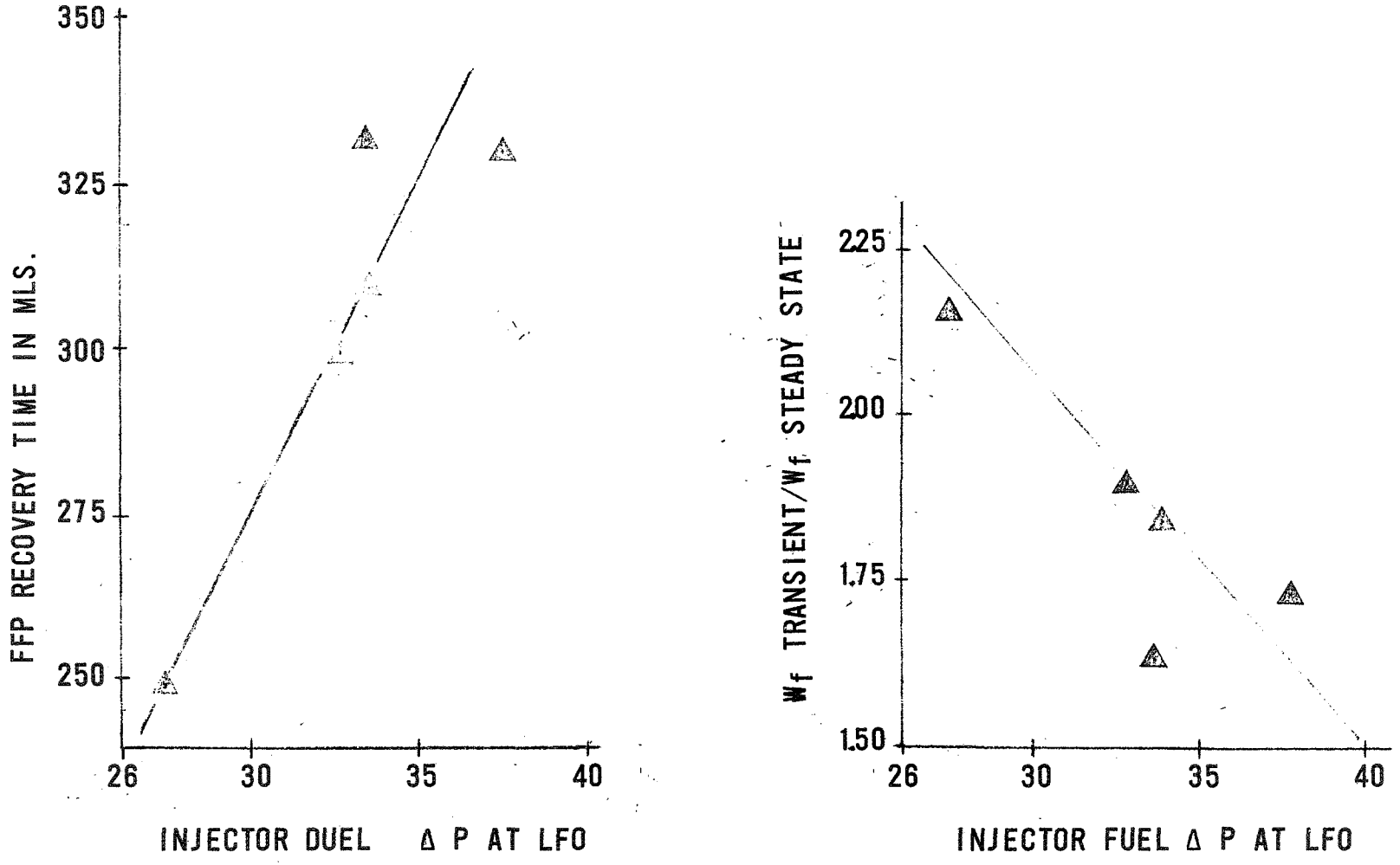

FIGURE 6

SYSTEM RESPONSE VARIATIONS.

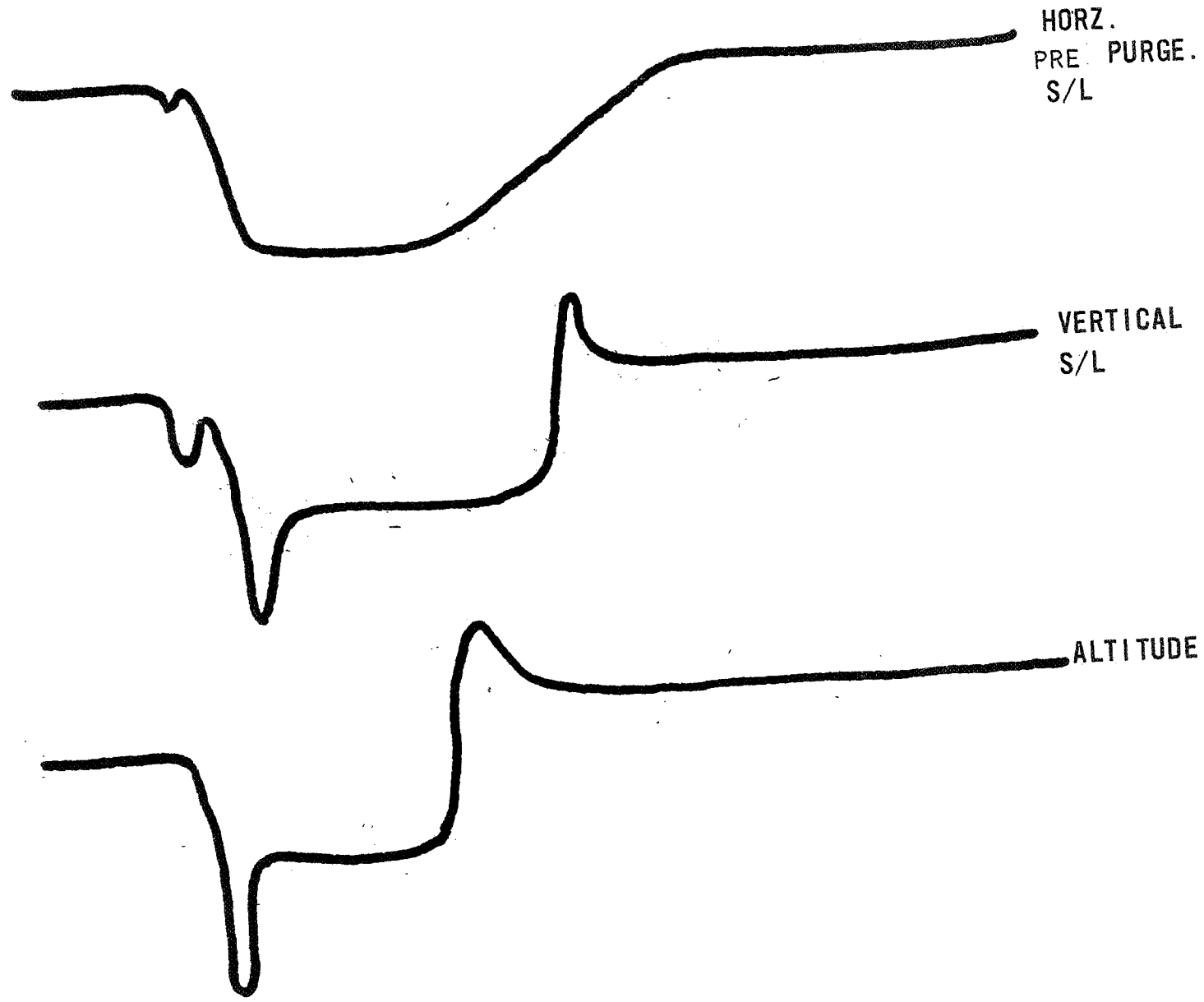

the effect of the propellant temperature was masked by the nonequilibrium heat transfer condition taking place during the start transient.

The examination of the helium saturation methods (Figure 7) showed a significant variation in test results (Figure 8). The examination of Figure 8 indicates that no continuous LFO's would be expected under normal circumstances if a saturation pressure of 50 psi were used. The figure also shows that a LFO would be expected for a saturation pressure of 190 psi when the flow rates (ΔP) was reduced below 4.2 lb/sec.

Examination of data from various types of injectors tested at the 190 psi saturation level has defined the value of the critical pressure drop at which continuous low frequency oscillations are produced. Figure 9 is a tabulation of these injectors and their pressure drops during continuous low frequency oscillations. From this figure we can see that the injection orifice pressure drop is approximately 21 psi for all units examined.

On this basis some concluding observations were listed related to helium saturation. These observations are as follows:

1. Continuous LFO for the same configuration, tested at the same facility, disappear as the helium saturation level is decreased.

2. Start LFO at the same operating test conditions get longer as the saturation level increases.

3. During a given test, an LFO was initiated and terminated at a discrete injector ΔP.

4. It appears that a critical ΔP ($C\Delta p$) exists that is related to the gas evolution potential (ρ_p) in the form

$$\frac{C\Delta p}{F(\rho_p)} = K$$

where $F(\rho_p)$ = F indicates a function of ρ_p.

FIGURE 7

PROPELLANT HELIUM SATURATION

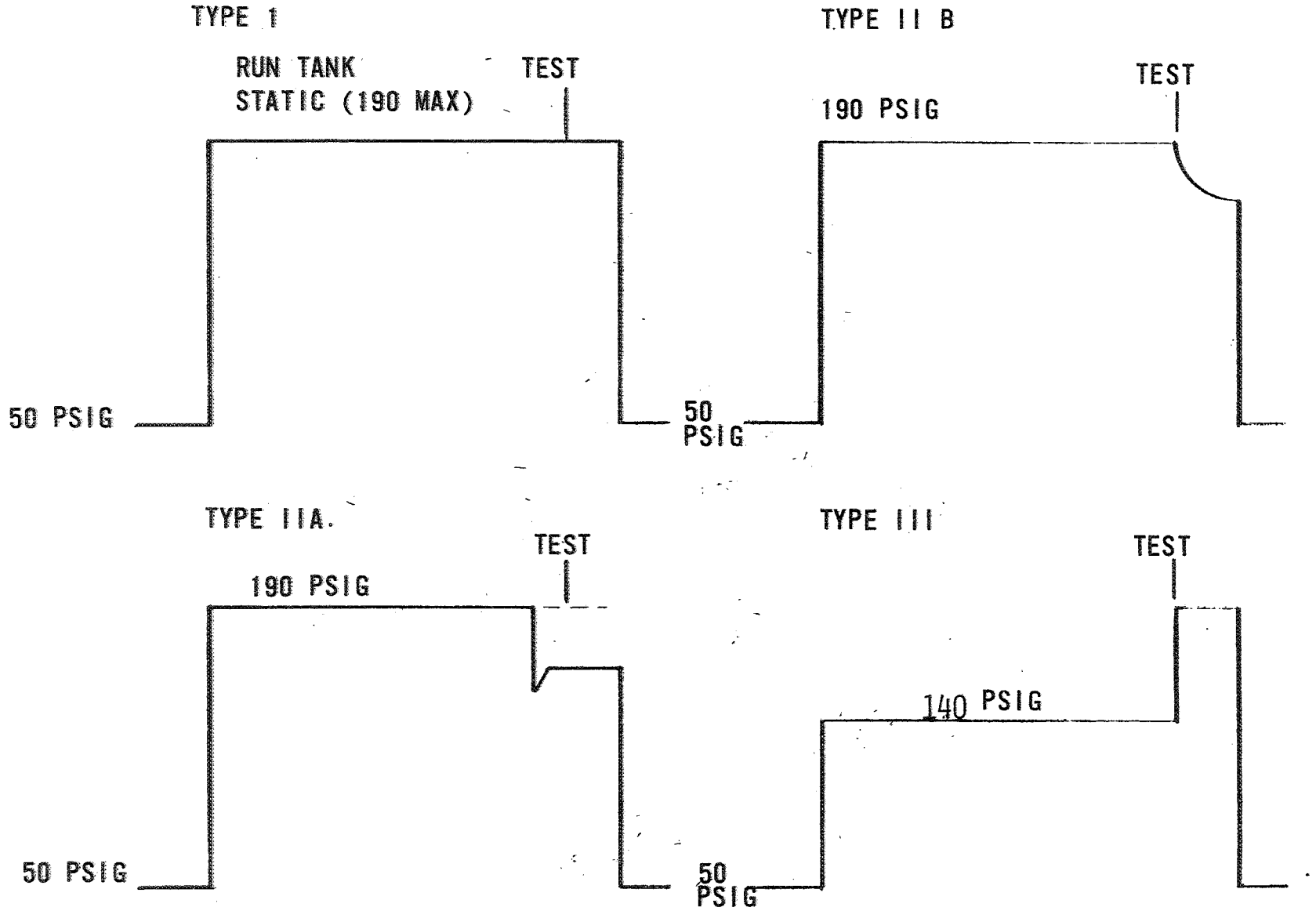

FIGURE 8

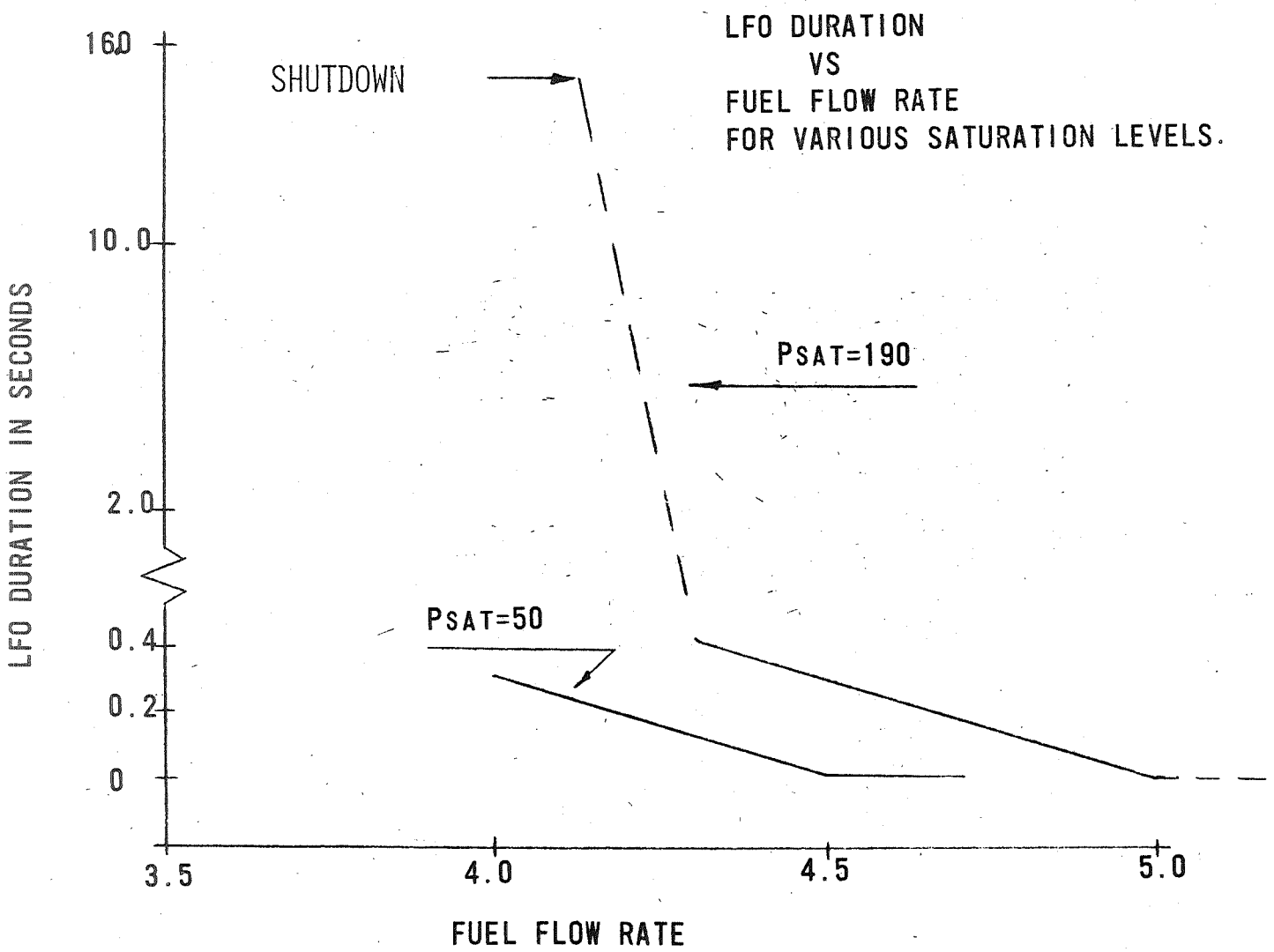
LFO DURATION
VS
FUEL FLOW RATE
FOR VARIOUS SATURATION LEVELS.
SHUTDOWN
PSAT=190
PSAT=50
LFO DURATION IN SECONDS
16.0
10.0
2.0
0.4
0.2
0
3.5
4.0
4.5
5.0
FUEL FLOW RATE

FIGURE 9

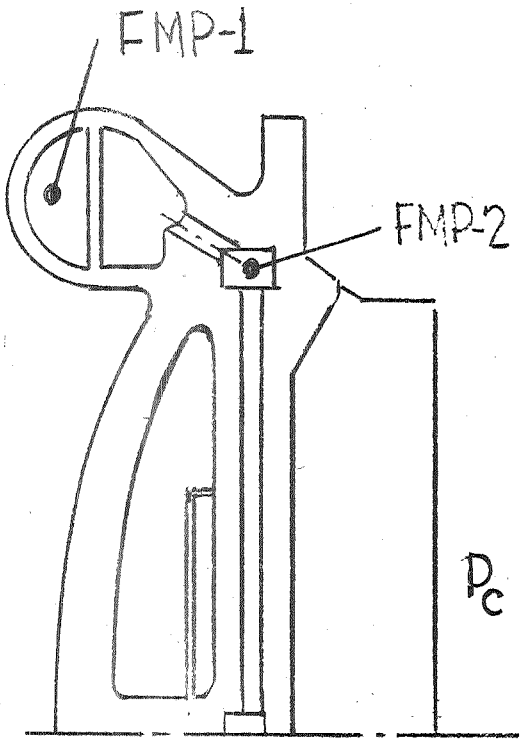

INJECTOR TYPE E2

CONDITIONS PRODUCING CONTINIOUS LFOS AT 190PSI SATURATION PRESSURE(TYPE IIB)

	E2	E2C59	E2CA113HF	E2CA113HF
FFP	154.1	155.5	155.2	152.7
FMP_1	136.5	147.3	144.5	142.8
FMP_2	132.3	131.0	133.8	131.1
P_c	110.5	109.6	112.9	111.9
P_{FMP-P_c}	43.6	43.9	42.3	40.8
P_{FMP-P_c}	21.4	21.4	20.9	19.2

Analysis Results of Task B

Task B of the contract consisted of a review and analysis of the photographic studies, conducted during the LM ascent engine development program. These were high speed photography of a single triplet (two fuel on one oxidizer) of the type used on the BAC injector. The objective of this test series was to observe the effect when helium was injected into the fuel. During the test program, three conditions were examined:

1. Triplet with no helium injection.
2. Triplet with 0.1 percent helium injection in the fuel.
3. Triplet with 0.2 percent helium injection in the fuel.

The film generated during the above tests was examined frame by frame and measurements were made in the areas of the liquid jet, the impingement area and the fan breakup zone to determine any variations due to helium injection.

The examination of these films yielded many interesting observations (Figure 10). The visual review of the data clearly indicated a significant variation in the three cases. With no helium injection the liquid jets were steady with no apparent pulsing or oscillations. The impingement point showed steady impingement at a constant height, and the fan breakup was steady with the breakup area (assumed to be the point where the fan became transparent) steady and nonoscillating. The results with 0.1 percent helium yielded a significant variation in all areas examined. The liquid jets indicated an oscillatory and pulsing phenomena with the average stream diameter being much smaller. The impingement point showed a movement on the average away from the injector and appeared to oscillate in a periodic manner. The fan breakup was also moved downstream and oscillated at a rate of 1000 cps (Figure 11). The results with 0.2 percent helium showed again a drastic change in characteristics. The liquid jets were smaller in diameter than the no helium and the 0.1 percent helium although now the streams were steady with no indications of pulsing or oscillation. The impingement point was moved further downstream and the post impingement fan breakup appears to be retarded. This is surmised on the basis of the complete lack of any observable fan breakup.

FIGURE 10

REVIEW AND ANALYSIS OF PHOTOGRAPHIC STUDIES.

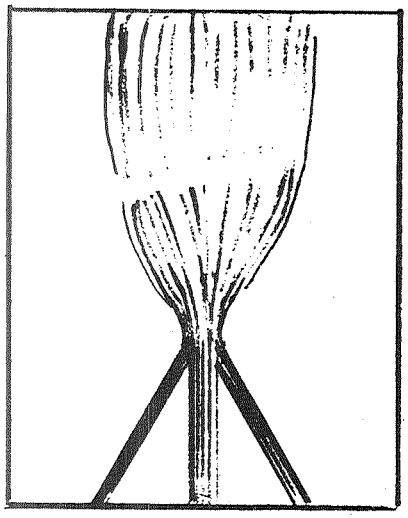

NO HELIUM

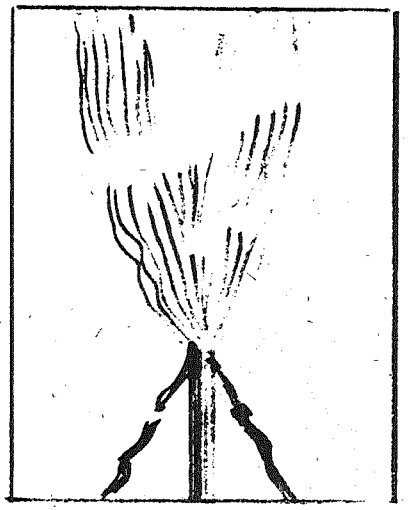

0.1% HELIUM

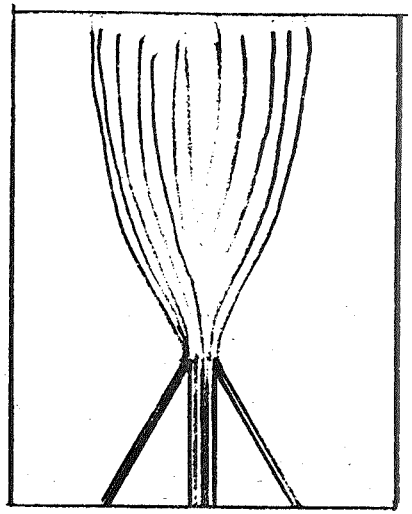

0.2% HELIUM

AREAS INVESTIGATED

LIQUID JET
IMPINGEMENT
FAN BREAKUP

METHOD OF INVESTIGATION

MEASUREMENTS TAKEN FROM PHOTOGRAPHIC REPRODUCTIONS OF HIGH SPEED FILM.

FIGURE 11

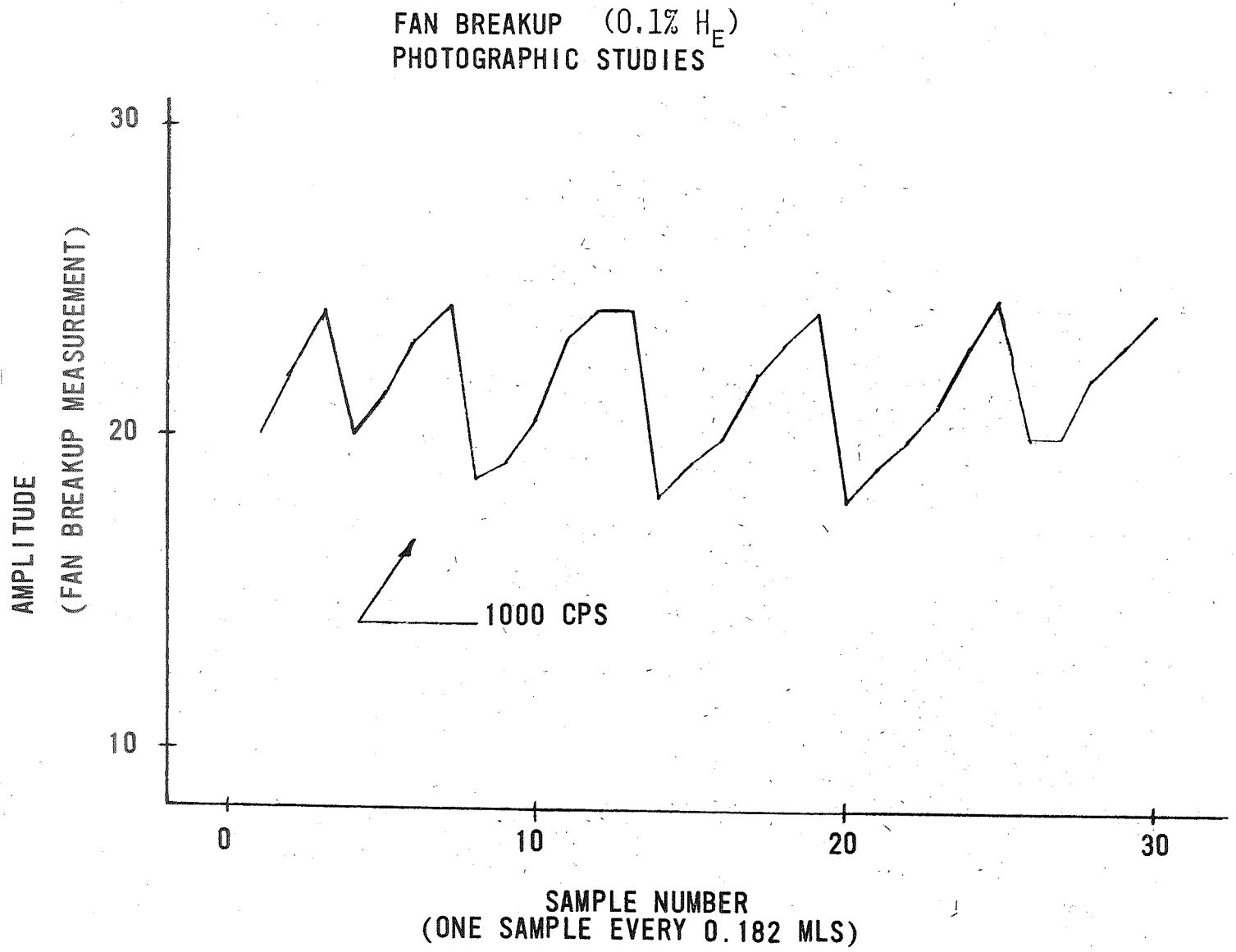
FAN BREAKUP (0.1% H_E)
PHOTOGRAPHIC STUDIES
AMPLITUDE
(FAN BREAKUP MEASUREMENT)
30
20
10
1000 CPS
0
10
20
30
SAMPLE NUMBER
(ONE SAMPLE EVERY 0.182 MLS)

In order to determine further if a predominant frequency could be defined in the impingement point fluctuations under the 0.1 percent condition, a frame-by-frame analysis was conducted. The data for this comparison were collected by measuring the impingement distance on two-hundred consecutive frames for the no-helium and the 0.1 percent helium cases. A Fourier analysis was conducted on the tabulated measurements. The results of the Fourier analysis indicated that some frequency components in the 400 cps range were identifiable in the 0.1 percent case while none were noted in the no-helium case (Figure 12). The frequency data generated for the 0.1 percent helium case was compared to the frequency content of a typical LFO measured during engine testing. Figure 13 shows this comparison. It is interesting to note that the frequency content is almost identical.

It can therefore be concluded that the helium injected into the fuel has the following effects.

1. Reduces the liquid stream diameter and causes the streams to pulse. Exerts a significant effect on the appearance of the fuel jets. At one condition of injection rate (0.1 percent) the jet diameter undergoes nearly periodic diameter variations. At larger values of helium injection (0.2 percent) the flow appears steady. However, the jet diameter is considerably smaller than under no-helium injection conditions.

2. Influences the steadiness and possibly the nature of the triplet impingement. One level of helium injection (0.1 percent) produced oscillatory variations in impimgement that contained the same frequency content of an engine produced LFO.

3. Effects the Fan Breakup

The correlation of the observed data provides an indication that, for the particular configuration to which these data apply, a definite relationship exists between the critical pressure drop and the gas evolution potential. Although the latter term cannot be quantitatively defined at this time, it is observed that periodic, low frequency oscillations will be maintained at levels below a given critical steady-state injector pressure drop when the fuel has been conditioned to a saturation point corresponding to 190 psi at a given temperature. These oscillations will not be maintained in the identical hardware and operating conditions if the saturation conditions are decreased to a value like 140 psi, which is lower than the interface pressure at the valve inlet but, of course, higher than the nominal chamber pressure of 120 psi. In addition, it appears from the successive movie frames that the fuel jet, impingement point and reaction zone

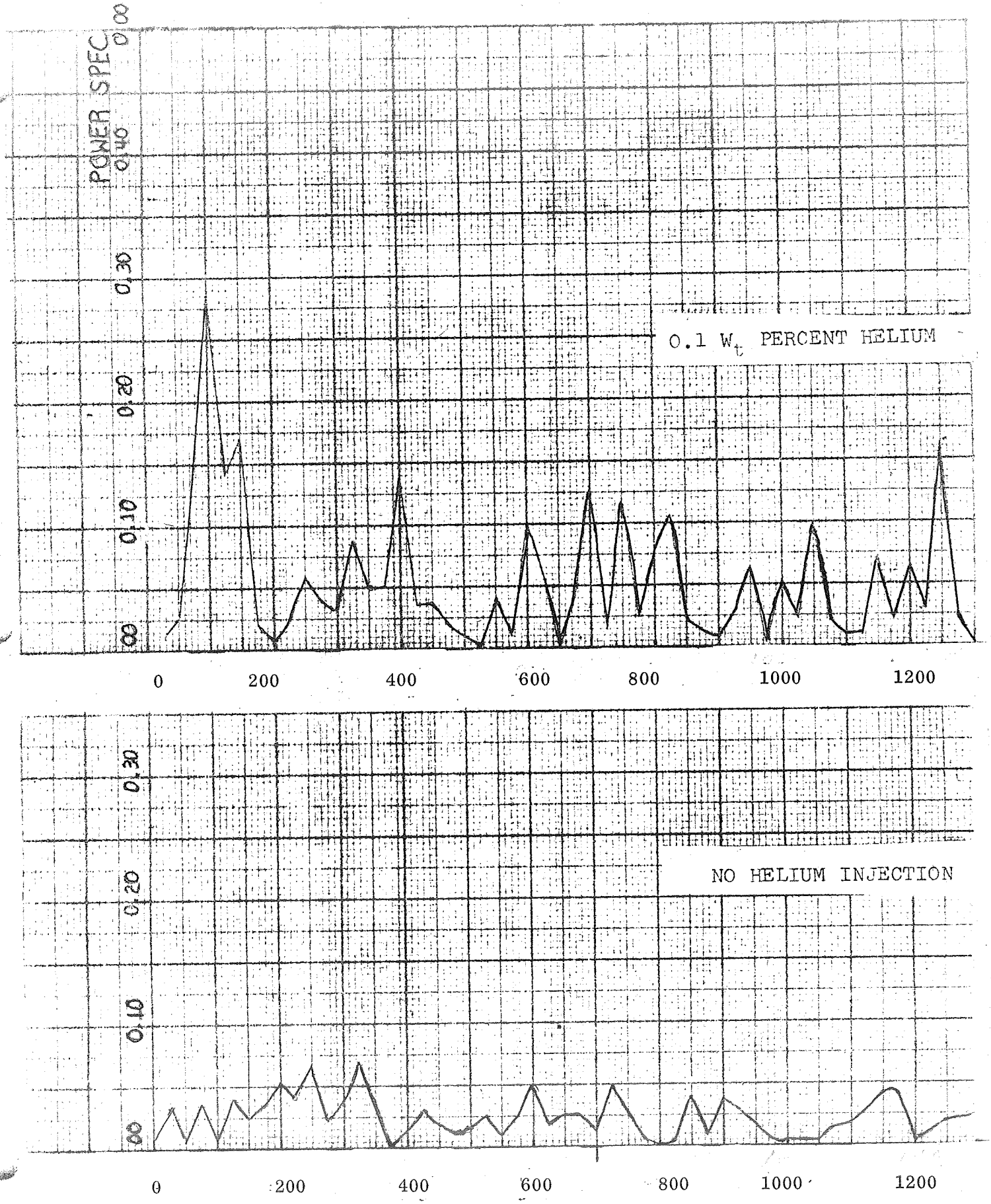

Frequency in CPS

FIGURE 12

FIGURE 13

VARIATIONS IN IMPINGIMENT HEIGHT (FROM PHOTOGRAPIC STUDIES)

AS COMPAIRED TO ENGINE CHAMBER PRESSURE (DEVELOPEMENT TEST)

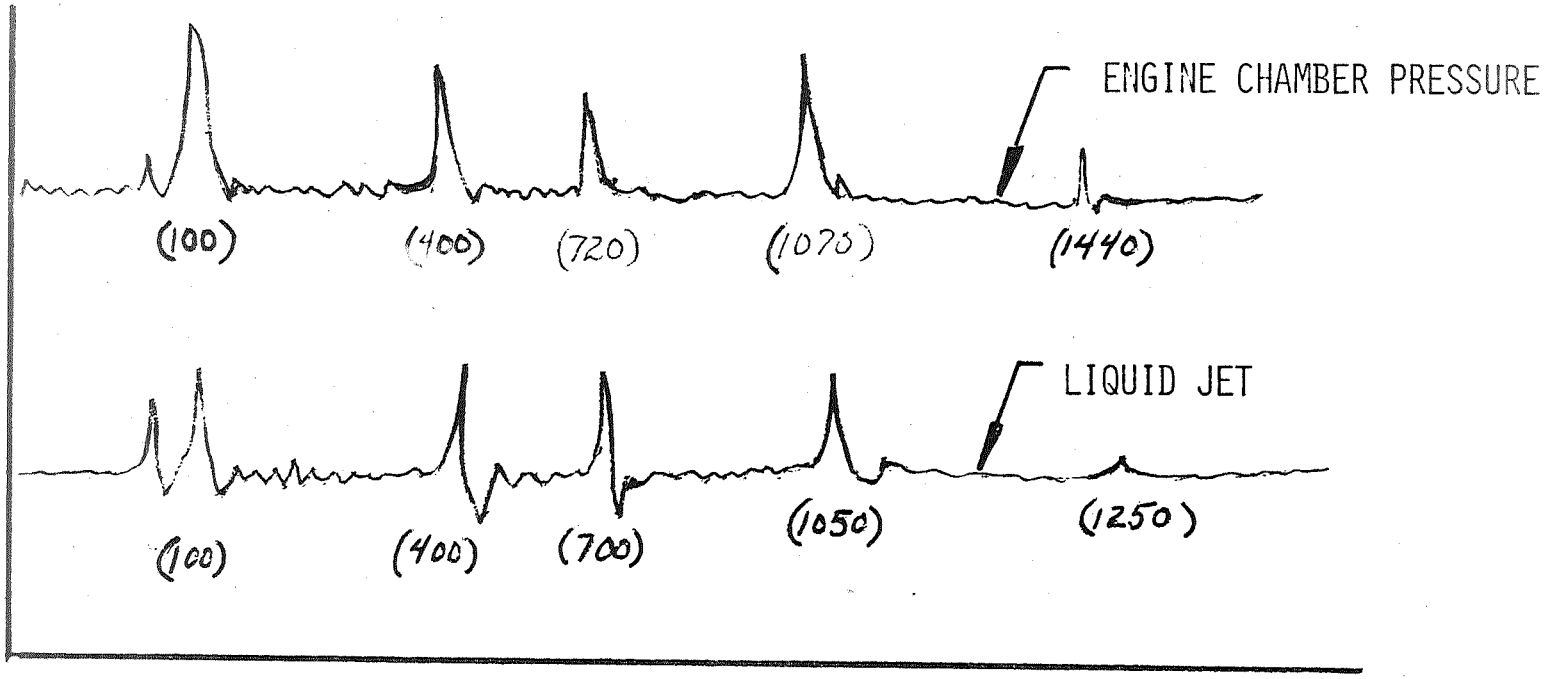

FREQUENCY

luminosity are significantly affected by injection of helium. With these observations in hand, one can speculate on the potential interactions which can establish the feed back mechanism to sustain a periodic oscillatory phenomenon of more or less constant frequency. This frequency, ranging somewhere in the vicinity of 300 to 400 cps, can be approximated by the flight time periodicity of the fuel jets by dividing the jet velocity by twice the distance from the orifice entrance to the impingement point.

Three possible feedback mechanisms have been hypothesized; all are based on the premise that the gas evolution influences the specific operating variables indicated.

1. The discharge coefficient for a fuel jet, having a given helium gas evolution potential, changes discontinuously at a given value of instantaneous back pressure of ΔP (flipping).

2. Triplet blow-apart, which changes the combustion rate and spatial location, occurs in a discrete manner as the instantaneous pressure drop or velocity of a fuel jet of given gas evolution potential varies.

3. The reaction zone and the liquid volume of the fuel orifices form a resonant system at given levels of gas evolution potentials. The latter quantity can be considered as a measure of fuel acoustic velocity. In this particular model, the higher ΔP would be considered strictly as increased resistance.

It might be helpful to elaborate briefly on some of the considerations which underlined these three models.

a. C_d Variation

No experimental data are available to us which would confirm the hypothesis that "flipping" of a jet of high gas evolution potential occurs discretely at given levels of pressure drop. To a large extent, this hypothesis evolved from the observations on the photographs. It should be noted in passing that Northup of G. E. (Ref. Flow Stability of Small Jets: paper - ASME November 1958), found that the "flipping" characteristics or an orifice were significantly affected when it effluxed into a helium atmosphere compared to a nitrogen one.

b. Triplet Blow-Apart

It is well known from the work of other investigators that blow-apart of reactive jets can occur when sufficient time exists for the production of vapors prior to impingement. Therefore, one cannot rule out the possibility that liquid jets having such a high gas evolution potential as the ones which we are discussing could produce the same mechanism. It is not clear at the moment how the change in jet velocity would modify this particular type of blow-apart.

c. Combustion Feed System Interaction

It is, of course, possible that the combustion can couple with a fuel fluid volume to establish the right time relationship to sustain a continuous oscillation. In this case, the gas evolution potential of the fuel would establish the acoustic velocity of the fluid and the pressure drop across the orifice would be modeled as a value of resistance. We know, of course, that the complete feed system does not enter into this coupling mechanism since more or less the same frequency is obtained in test cells having widely varying configurations; however, it is possible that a specific volume within the injector, such as the injector orifices, could establish such a coupling mechanism.

Task D - The Analysis of Applicable Analogue Models

The review and analysis of this model has indicated its ability to provide correlation with test data in the following areas:

1. Simulate the LFO frequency.
2. Correlate with fuel system variations and LFO occurrence.
3. Correlate that increased chamber pressure reduced LFO incidence.

The BAC analogue model has also been shown to have the ability of simulating what the work statement defines as basic requirements of a model. These requirements include the ability of the model to simulate the following conditions and parameters.

a. Helium saturated propellants.
b. The pressure drops and volumes in various parts the injectors.
c. The pressure drops and volumes in various parts of the propellant feed lines, valve, and test stand.
d. Changes in operating conditions such as mixture ratio, chamber pressure, propellant temperatures, acoustic velocities, impingement angles, fuel and oxidizer propellant leads.
e. Combustion dynamics such as propellant stay times, combustion ignition delay.

Review of the analogue model results, conducted during the ascent engine development program, show that this model will produce LFO's when the fuel flow is reduced and that LFO's will be produced when the chamber pressure is reduced (Figure 14). These results indicate that the model is in fact capable of producing LFO's; however, additional refinements will be required in order to produce these LFO's at conditions equal to those noted in engine test.

4.0 CONCLUSIONS AND RECOMMENDATIONS

The examination of the LM development program test data confirmed that the low frequency oscillations on this program were controlled by the fuel circuit and more precisely by the pressure drop of the fuel injection orifices. Below a fuel injection orifice pressure drop of 21 psi, the oscillations were continuous when helium saturation at maximum tank pressure was maintained. At values between 21 psi to approximately 29 psi (38 psi ΔP injector) the oscillations were discontinuous with durations not exceeding 2 seconds. Above an injection orifice pressure drop of 29 psi, few oscillations were noted and these were attributed to test procedures in which unusual amounts of gas could be trapped in the fuel line.

Although the test data produced an operational limit, the mechanism producing the oscillations was not defined. Three mechanisms which might influence the oscillations were hypothesized. These mechanisms were:

1. Resonant coupling between the feed system and the combustion zone.

2. Blow apart of the fuel/ox streams amplified by a change in helium content.

3. A change in C_d at the orifice where a condition similar to "flip" may produce an oscillating mass/breakup pattern.

Examination of the Bell analogue model showed that a low frequency oscillation could be produced when programmed discontinuities as inputs were arbitrarily added. The need to input these discontinuities to produce an oscillation describes a limitation of the model which should be updated. An examination of the analogue model indicated that refinements could be made that would spontaneously produce a oscillatory condition related to the LM development experience.

The conclusion that the combustion oscillations were related to fuel injection mechanism and that the exact mechanism of producing the oscillations was unknown, led to the recommendations for further evaluation of the program.

a. Model Updating to Include Low Frequency Oscillations

The analogue model should be modified to include the limit of 21 psi pressure drop across the injection orifices. This can be accomplished in the model by increasing the "combustion frequency" and modifying the "injector" to include a coupling condition with the combustion zone. The injector modification should be examined for inclusion of either the digital injector model or the simulation of the injector by an orifice and resonant cavity rather than the currently used orifice representation.

b. Blow Apart Experimental Examination

The mechanism of blow apart as related to helium content should be examined. It is proposed that single injection element flow (photographic) tests be conducted where the helium content can be well controlled.

c. C_d Evaluation Related to a "Flip" Condition

The influence of helium content on "flip" should be examined and it is suggested that it also be done by use of photography and injectors with fuel (single) elements. The study would be directed toward determining the extent, if any, that the fuel stream oscillated with a varying content of helium.

APPENDIX I

TASK A - DATA REVIEW AND CORRELATION

A. ANALYSIS OF START "FOOTBALLS" IN TEST CELLS 3DE AND 2DW

1. Test Cell 3DE (Horizontal Sea Level Test Stand)

Review of the testing conducted during the LM stability program revealed that various configurations of injectors were tested in this facility. In order to define if injector configuration effected the occurrence of "start footballs", data from the units listed on Table I was investigated.

The test data used to evaluate was obtained from the following sources and was confined to propellant temperatures from 60 to 80°F.

Injector S/N	Test Number	Data Sources
B3-L7	3DE 972-984	Tabulated data from Cell 3DE and oscillograph records
B10A	3DE 930-946	Tabulated data from Cell 3DE and oscillograph records
E1E-13	3DE 1350-1368	Tabulated data from Cell 3DE tabulated football data
E2B-5D	3DE 988-1014	Tabulated data from Cell 3DE and oscillograph records
E2B-12F	3DE 1103-1112	Tabulated data from Cell 3DE and oscillograph records

Analysis of the tabulated test data (Tables 2-4) indicated some variance in the fuel flow data that could be due to the hand reduction of oscillograph records. In order to define more accurately fuel flow, plots of fuel feed pressure vs fuel flow rate for each unit was made, Figure I-1-I-3. A best fit line was placed through the data points and fuel flows were corrected for feed pressure. Tables 2-4 reflects corrected fuel flow rate. The data from the Tables was then plotted as functions of corrected fuel flow rate vs start football duration for each injector (Figures I-4-I-6) and a composite plot with the same parameters was made (Figure I-7) using the best fit line from each individual injector plot. Figure I-7 shows significant variation in the fuel flow required to eliminate the start "footballs".

TABLE I

INJECTOR CONFIGURATION COMPARISON

INJECTOR NUMBER	BAFFLE TYPE	FUEL MANIFOLD TYPE	FUEL MANIFOLD VOL. In^2	NO. OF TRIPLETS	NO. OF DOUBLETS	PROP LEAD	FUEL INJ. ΔP @ 4.396 lb/sec	REMARKS
B3-L7	5 Leg 1.25 In. High Uncooled	Central Disc	28.7	76	87	Fuel	43.6	
B10A	3 Leg Y 1.25 In. High Uncooled	Single Pass Torus		84	87	Oxid	37.9	
E1E-1B	3 Leg 1.25 High Prop. Cooled	Double Pass Torus	51.7	84	60	Oxid	39.0	
E2B-5D	3 Leg Uncooled 1.25 High	Double Pass Torus	51.7	78	81	Oxid	40.7	
E2B-12F	3 Leg Prop. Cooled 1.25 High	Double Pass Torus	51.7	78	81	Oxid	31.0	Barrier Orifice holes counter-sunk

TABLE 2

INJECTOR S/N	RUN NO. 3DE	P_C	FUEL $\dot{w}$	FUEL Wcorr	FUEL F.P.	PROP. TEMPS Ox/Fuel	FOOTBALL DATA DURATION	AMPLITUDE
B3-L7	972	92	4.128		172.6	70	1st .050	Data Looks Bad
							2nd .106	Data Looks Bad
	973	119	3.227		178.2	70	.220	
	974	126	4.436	4.436	165.9	70	0	
	975	110	4.459	4.401	164.4	70	0	
	976	110	4.474	4.427	165.3	70	0	
	977	109	4.005	3.955	145.6	70	0	
	978	106	3.943		161.3	70	0	Data Looks Bad
	979	-	3.942	3.955	145.6	70	-	
	980	106	3.930	3.963	145.9	70	0	
	981	116	4.471	4.482	167.8		0	
	982	112	3.938	3.975	146.5		0	
	983	102	3.627	3.600	130.6		.230	
	984	99	3.594	3.605	130.9		.250	
	3DE							
B10A	930	136	4.340	4.260	165.5	70	.090	
	931	130	4.360	4.305	168.1	70	.100	
	932	124.4	4.262	4.289	167.0	70	.116	
	933	124.3	4.352		150.6	70	.230	Bad Data
	934	-	-		-			
	935	118	4.359	4.311	168.5	70		
	936		4.089	4.089	154.5	70	.180	
	937		4.013	4.035	151.3	70	.180	
	938		4.070	4.053	152.4	70		
	939		4.288	4.301	167.8	70	.100	
	940		4.336	4.310	168.4	70		
	941		4.412	4.280	166.3	70	.114	
	942		-		168.5	70	.070	
	943		4.316	4.351	171.0	70	.094	
	944		4.293	4.328	169.6	70	.103	
	945		4.273	4.319	168.9	70	.095	
	946		4.233	4.327	170.0	70	0	

TABLE 3

INJECTOR S/N	RUN NO.	P_C	FUEL $\dot{w}$	FUEL W_{corr}	FUEL F.P.	PROP. TEMPS	FOOTBALL DATA DURATION	AMPLITUDE
	3DE							
E1E-1B	1350	107	4.192	4.035	160.5	70	45/180	
	1353	128	4.562	4.610	188.2		0	
	155	130	4.751	4.770	196.6		0	
	1356	129	-	-	-		0	
	1357	130	4.753	4.753	196.3		0	
	1358	129	4.782	4.745	194.8		0	
	1359	131	4.823	4.823	196.7		0	
	1360	131	4.800	4.800	197.0		0	
	1361	131	4.790	4.820	197.3		0	
	1362	120	4.450	4.412	178.7		0	
	1363	121	4.340	4.361	176.2		20/120	
	1364	120	4.337	4.390	177.6		0	
	1365	120	4.334	4.399	177.9		10	
	1366	113	3.991	3.971	151.6		400	
	1367	110	3.980	4.002	159.0		400	
	1368	110	3.982	3.971	157.6		460	
	3DE							
E2B-5D	988	119	4.352	4.375	167.5		0	
	989	115		4.280	164.0		0	
	990	114	4.462	4.280	164.0		0	
	991	114	4.340	4.321	165.6		0	
	992	-	4.044	3.925	149.3		1st .183	
							2nd .169	
	993	102	3.939	3.922	149.1		.410	
	994	109	3.661	3.750	141.9		.483	
	999		3.527	3.722	140.8		.553	
	1000		3.586	3.806	144.2		.560	
	1001		4.195	4.455	171.2		1st .190	
							2nd .212	
	1002		4.195	3.855	146.2		-	
	1005		4.016	4.416	169.4		.440	Data Looks Bad
	1006		4.328	4.370	167.4		0	
	1007		4.452	4.378	168.0		0	
	1008		4.389	4.378	168.0		0	
	1009		4.391	4.389	168.3		0	
	1010		4.018	3.930	149.4		1st .231	
							2nd .200	
	1011		4.027	3.958	150.5		1st .120	
							2nd .150	
	1012		5.034		204.9		0	
	1013		5.132		207.4		0	
	1014		5.083		204.6		0	

TABLE 4

INJECTOR S/N	RUN NO. 3DE	P_C	FUEL $\dot{W}$	FUEL W_{corr}	FUEL F.P.	PROP. TEMPS	FOOTBALL DATA DURATION	FOOTBALL DATA AMPLITUDE
E2B-12F	1103		4.428	4.372	168.2	70	.170/160	
	1104		4.383	4.285	157.5	70		Data Looks Bad
	1105		4.285	4.285	165.0	70	.170/.200	
	1106		4.276	4.279	164.7	70	.170/.160	
	1107		4.361	4.385	167.9	70	.590	
	1108		4.030	3.915	151.4	70	.650	
	1109		3.935	3.985	153.9	70	.620	
	1110		3.912	3.995	154.3	70	.546	
	1111		3.992	3.980	153.6	70	.123	
	1112		4.721	4.835	185.7	70	0	

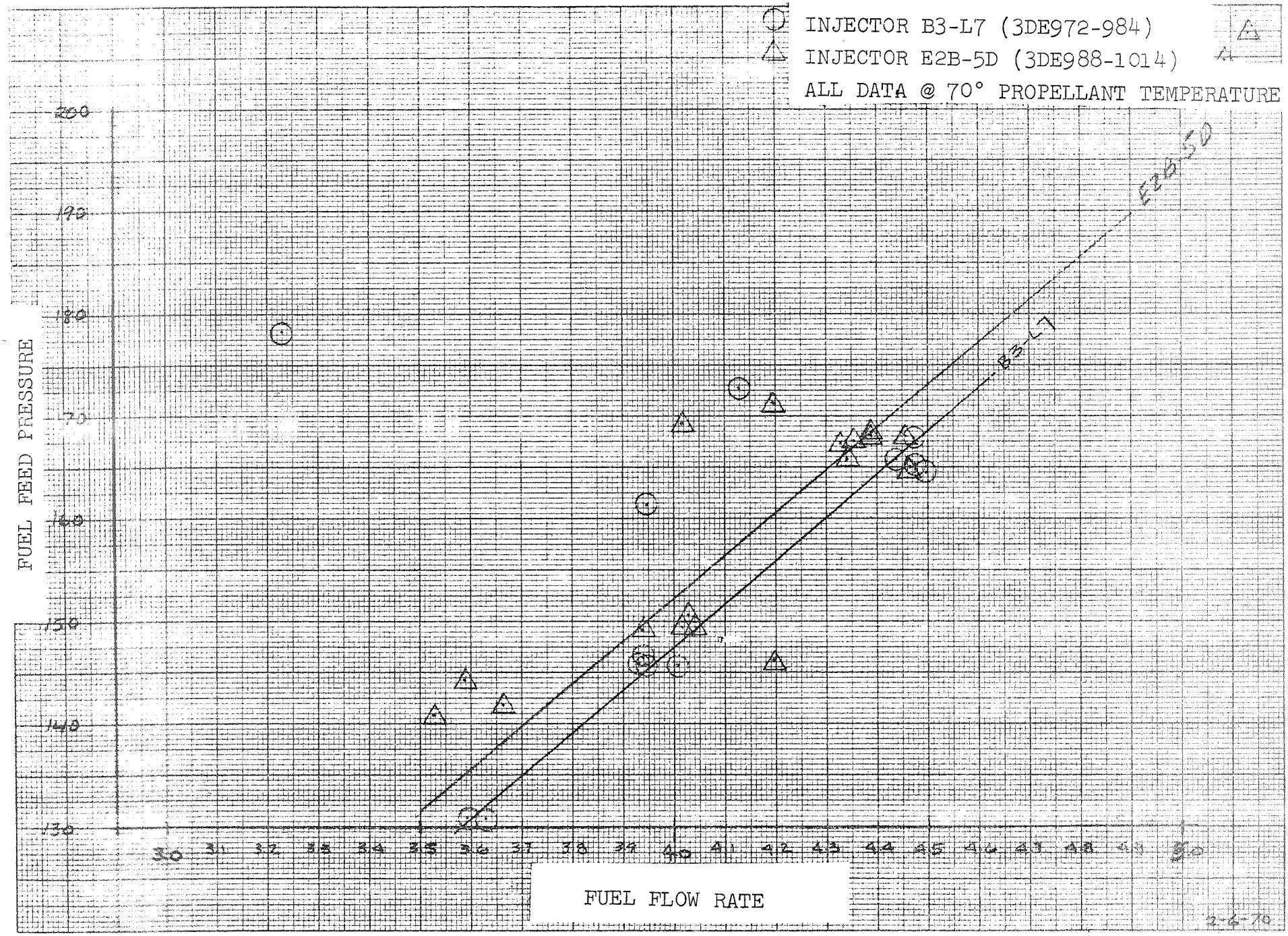
INJECTOR B3-L7 (3DE972-984)
INJECTOR E2B-5D (3DE988-1014)
ALL DATA @ 70° PROPELLANT TEMPERATURE
FUEL FEED PRESSURE
FUEL FLOW RATE
E2B-5D
B3-L7
200
190
180
170
160
150
140
130
30
31
32
33
34
35
36
37
38
39
40
41
42
43
44
45
46
47
48
49
50
2-6-70

FIGURE I-1

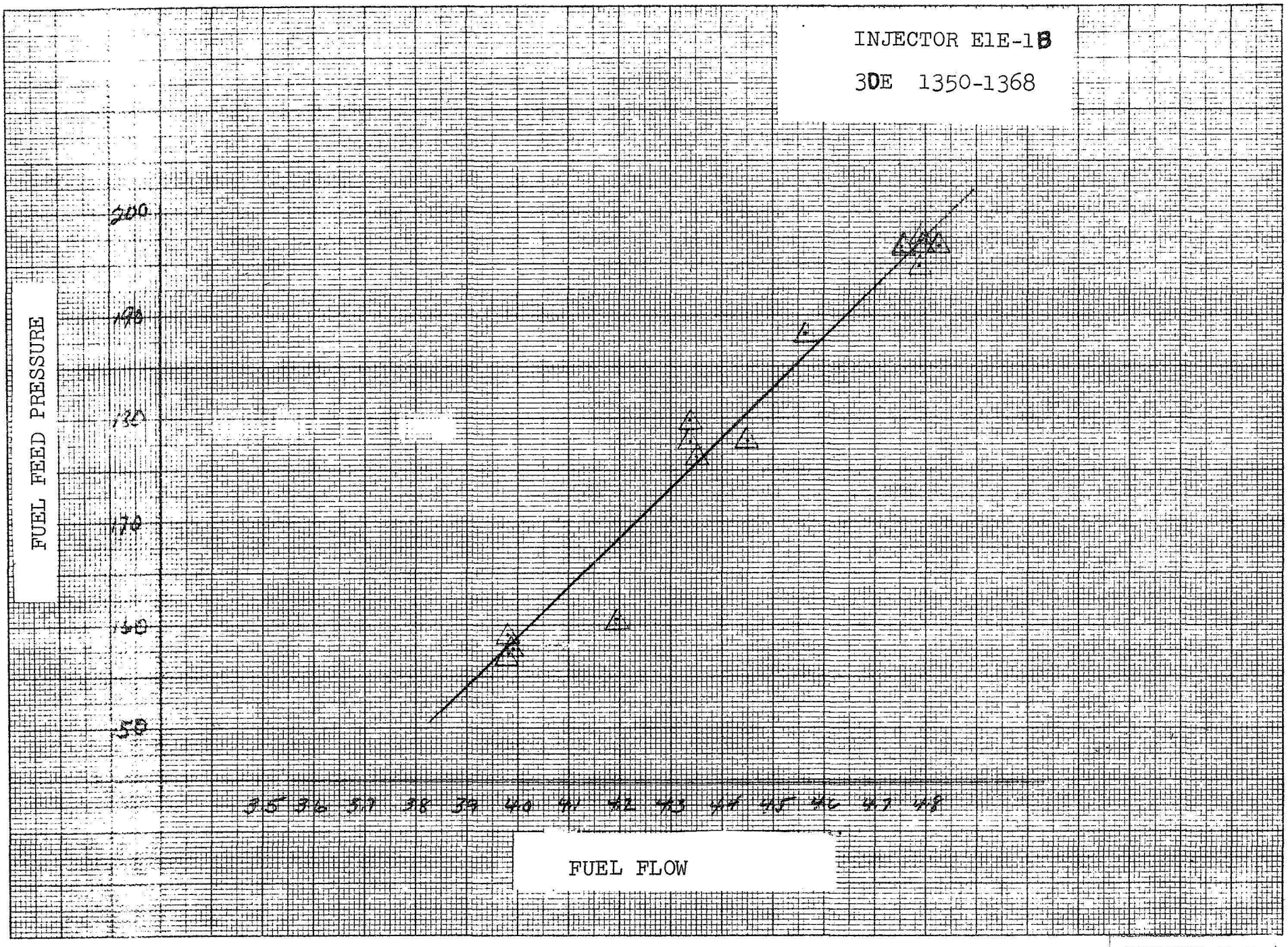

FIGURE I-2

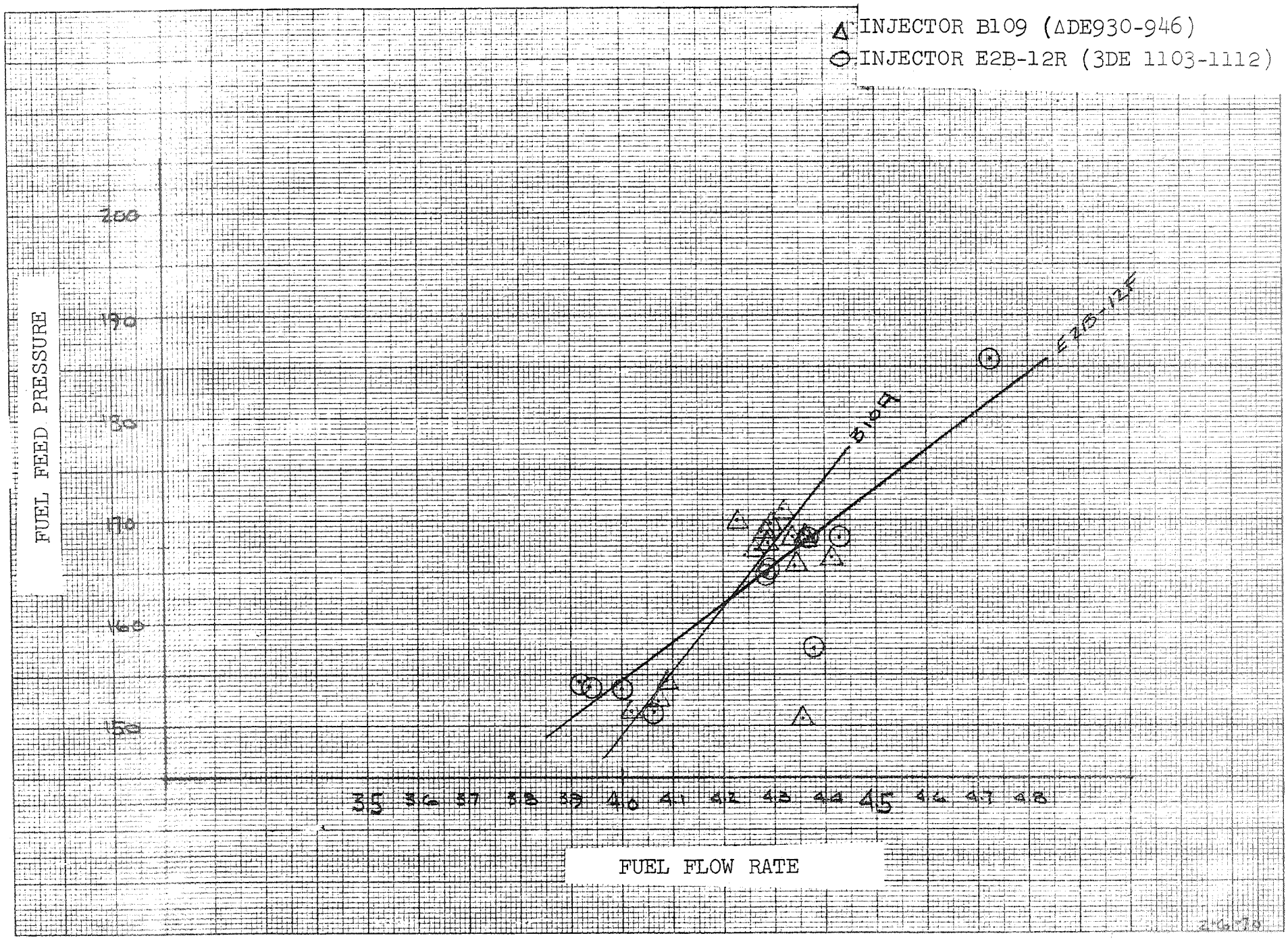

FIGURE I-3

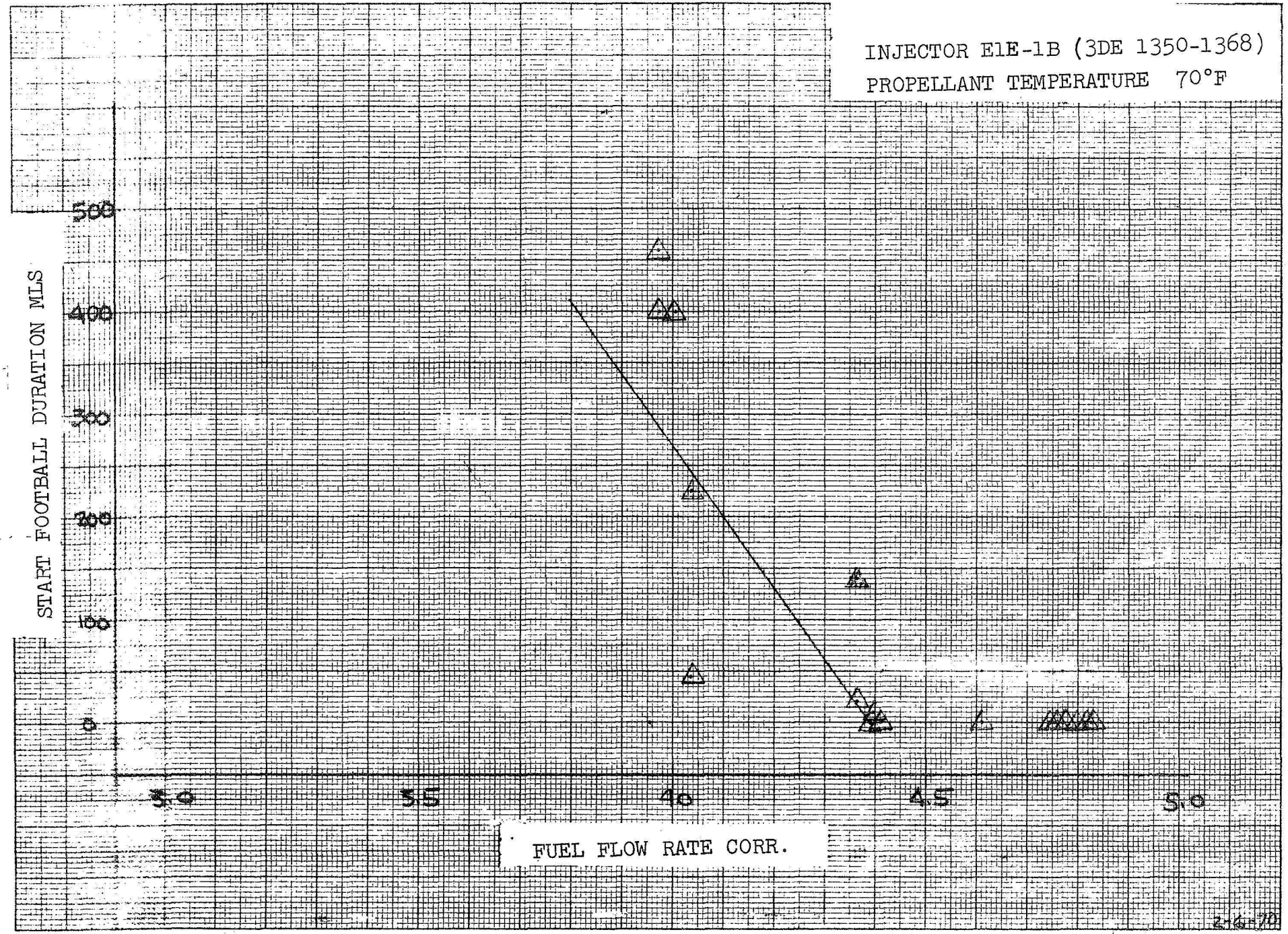

FIGURE I-4

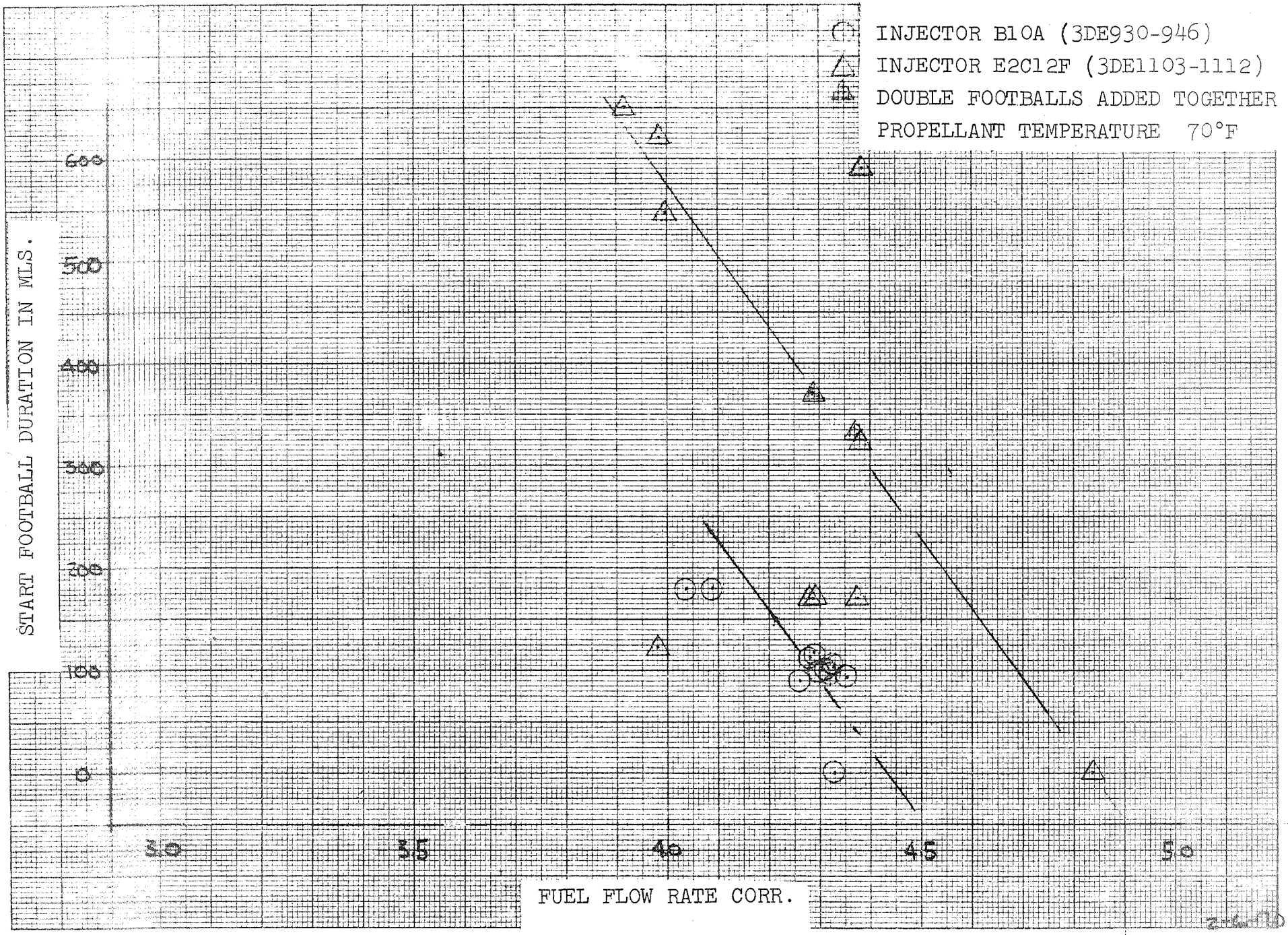

FIGURE I-5

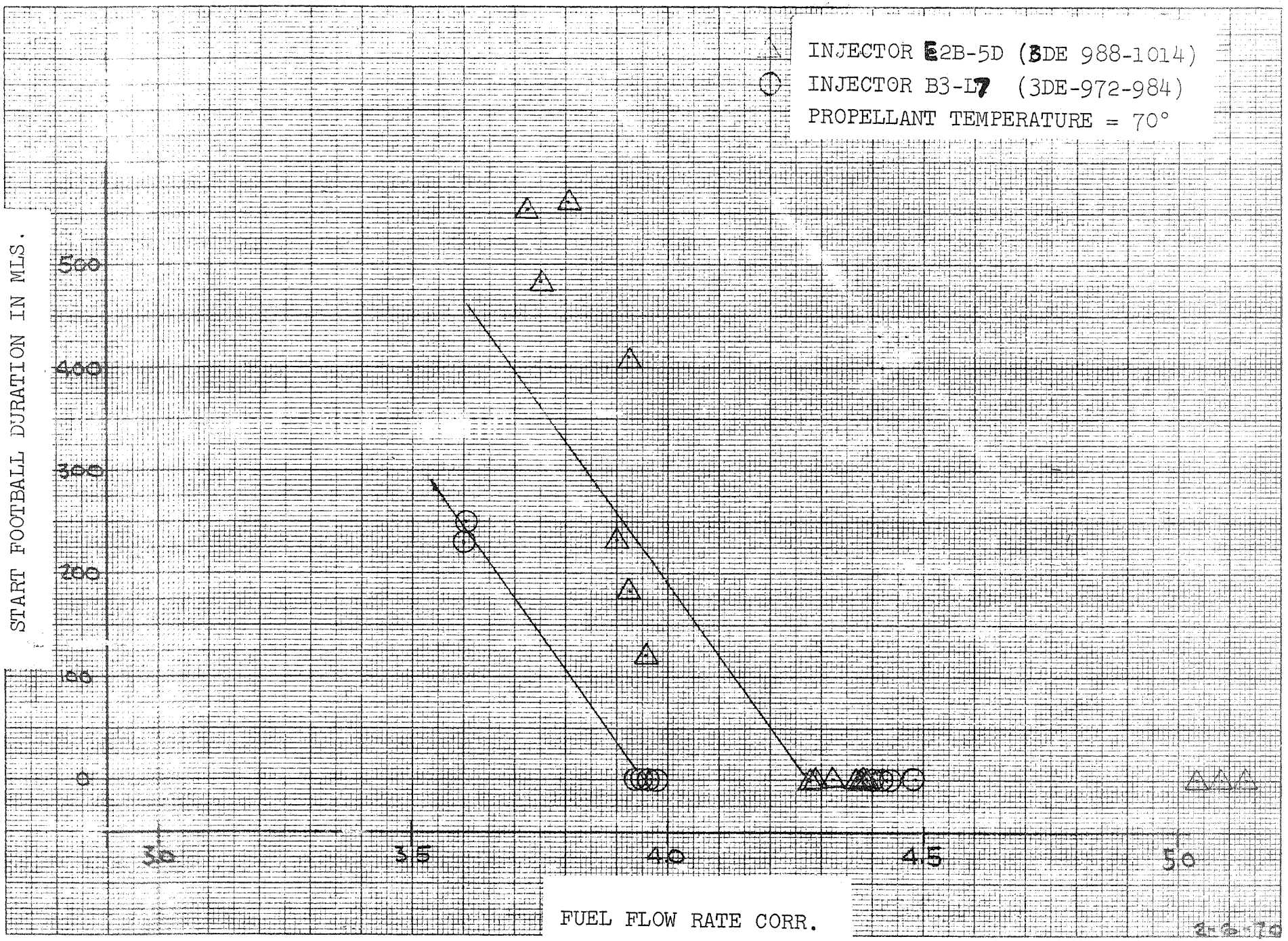

FIGURE I-6

In order to define if the variation in the configuration of the injectors or the injector pressure drop was the cause of the football "break point" difference, the pressure drop was calculated for each injector at the football "breakpoint". The following is a tabulation of corrected fuel injector pressure drops.

B3-L7	36.0	
B10A	38.4	Fuel injector ΔP at which footballs start
E1E-1B	38.5	
E2B-5D	38.5	
E2B-12F	37.5	
Average	37.8	

B. TEST CELL 2DW (Vertical Test Stand)

Review of the testing conducted in this test cell indicated that of the data available only the E2C type injector could be examined for start footballs in test cell 2DW. The E2C injectors examined, incorporated a three leg propellant cooled Y baffle, had a double pass peripheral torus fuel manifold with 51.7 cubic inches of volume. The injector design incorporated 84 primary triplets and 81 barrier doublets. This injector has an oxidizer lead. The fuel pressure drops at rated flow (4.396 lb/sec*) were as follows:

E2C-38 L	27.1 psi
E2C-38 O	27.1 psi
E2C-40 B	28.5 psi
E2C-58	28.5 psi

The test data used to evaluate these units was obtained from the following sources and was confined to propellant temperatures of 60-80°F.

Injector S/N	Test Number	Data Sources
E2C-38 L	2DW 434-448	Tabulated data from cell 2DW and oscillograph records
E2C-38 O	2DW 500-516	"
E2C-40B	2DW 591-608	Tabulated dated from test Cell 2DW and tabulated football data
E2C-58	2DW 709-748	Tabulated data from test cell 2DW and tabulated football data

TABLE 5

E2C-380 2DW 70°F

RUN NO.	FFP	$\dot{W}_f$	$\dot{W}_{fc}$	FOOTBALL DURATION
500	--			
501	--			
502	--			
503	--			
504	150.5	4.056	4.021	.280
505	185.6	4.726	4.742	0
506	186.4	4.853	4.756	.050
507	186.8	4.764	4.764	0
508	186.8	4.772	4.764	0
509	--			
510	--			
511	169.7	4.446	4.420	.203
512	169.8	4.403	4.422	.198
513	169.7	4.420	4.420	.210
514	170.0	4.421	4.425	.167
515	170.4	4.435	4.435	.148
516	168.9	4.427	4.423	.165
E2C-38L				
434	--			
435	--			
436	--			
437	170.4	4.529	4.432	.128
438	169.3	4.520	4.407	.128
439	152.2	4.178	4.057	.242
440	--			
441	191.0	4.886	4.750	0
442	167.4	4.288	4.371	.130
443	167.8	4.346	4.380	.150
444	167.4	4.271	4.371	.165
445	148.4	4.190	3.979	.298
446	145.3	3.846	3.918	.332
447	146.1	3.842	3.932	.320
448	167.1	4.313	4.379	.173

TABLE 6

E2C-40B

RUN NO.	P_C	FFP	$\dot{W}_{f\ corr}$	START FOOTBALL DURATION
591	--	191.4	4.935	0
592	136	188.8	4.880	0
593	137	191.0	4.928	0
594	132	182.2	4.748	N/A
595	132	183.4	4.760	80
596	109	146.8	4.008	380
597	110	146.5	4.001	330
598	112	147.1	4.010	320
599	110	145.3	3.924	360
600	121	165.3	4.395	240
601	120	165.2	4.395	240
602	107	160.2	4.282	260
603	120	165.5	4.396	240
604	117	167.3	4.465	250
605	129	180.7	4.714	130
606	130	181.0	4.715	160
607	130	183.1	4.761	120
608	107	146.5	4.001	430
E2C-58				
709		160.8	4.356	200
710		161.5	4.370	160
711		161.8	4.372	190
712		161.8	4.372	200
713		177.4	4.708	-
714		179.5	4.748	-
715		176.4	4.685	-
716		178.1	4.716	No Data
717		178.3	4.718	-
718		145.2	4.025	340
719		146.4	4.050	270
720		146.4	4.050	250
721		146.1	4.048	260
722		182.8	4.816	-
723		183.5	4.832	No Data
724		182.2	4.805	-
725		181.9	4.798	-
726		180.5	4.770	-

TABLE 7

E2C-58

RUN NO.	FFP	$\dot{W}_f$	$\dot{W}_{f_{corr}}$	START FOOTBALL DURATION
727	148.5		4.108	280
728	148.2		4.100	310
729	146.8		4.056	270
730	147.8		4.080	280
739	166.1		4.470	140
740	165.5		4.455	250
741	166.6		4.492	170
742	164.5		4.436	150
743	161.8		4.378	180
744	162.5		4.392	200
745	163.5		4.414	180
746	-			No Data
747	163.1		4.402	160
748	181.8		4.800	0

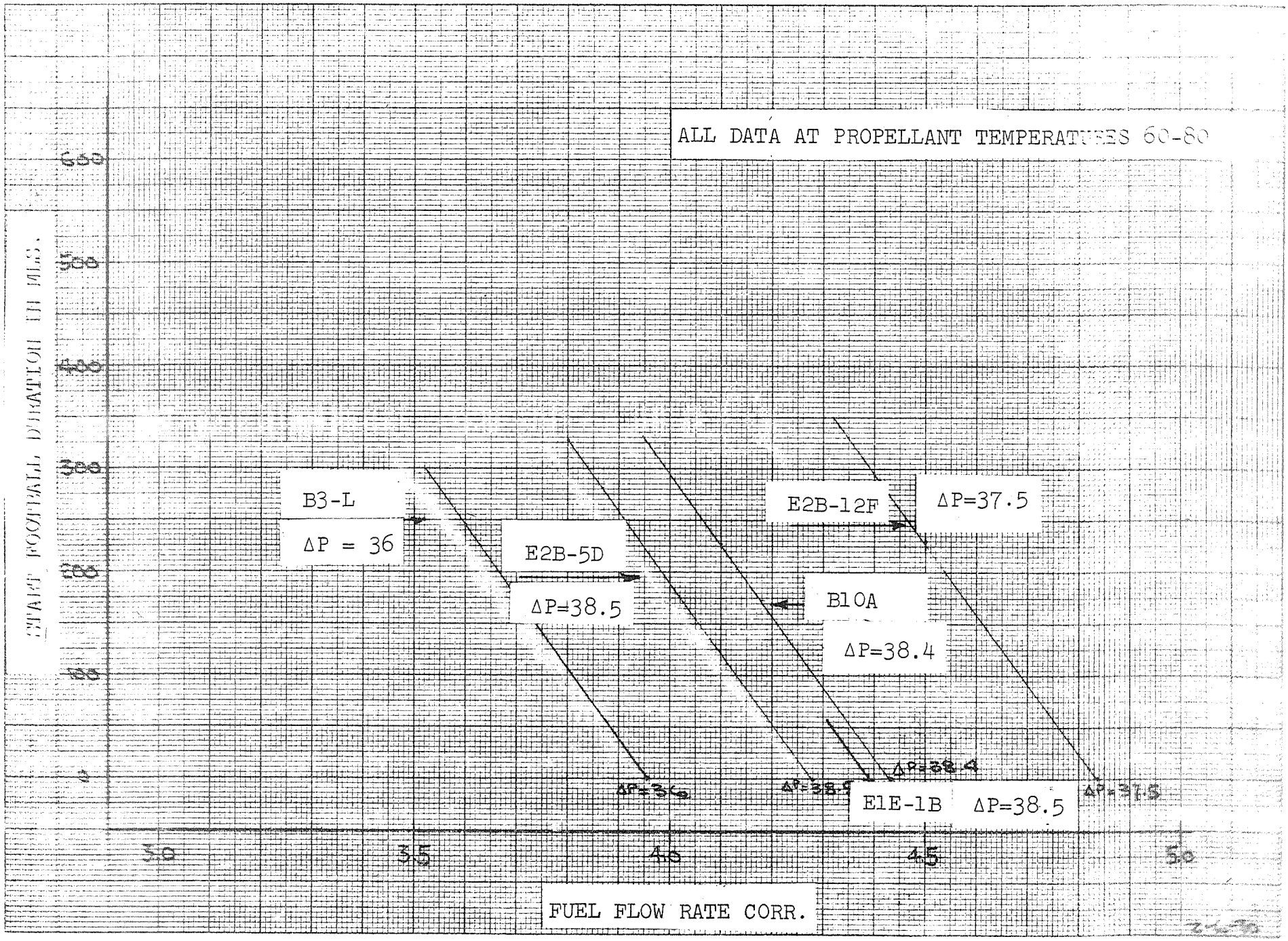

FIGURE I-

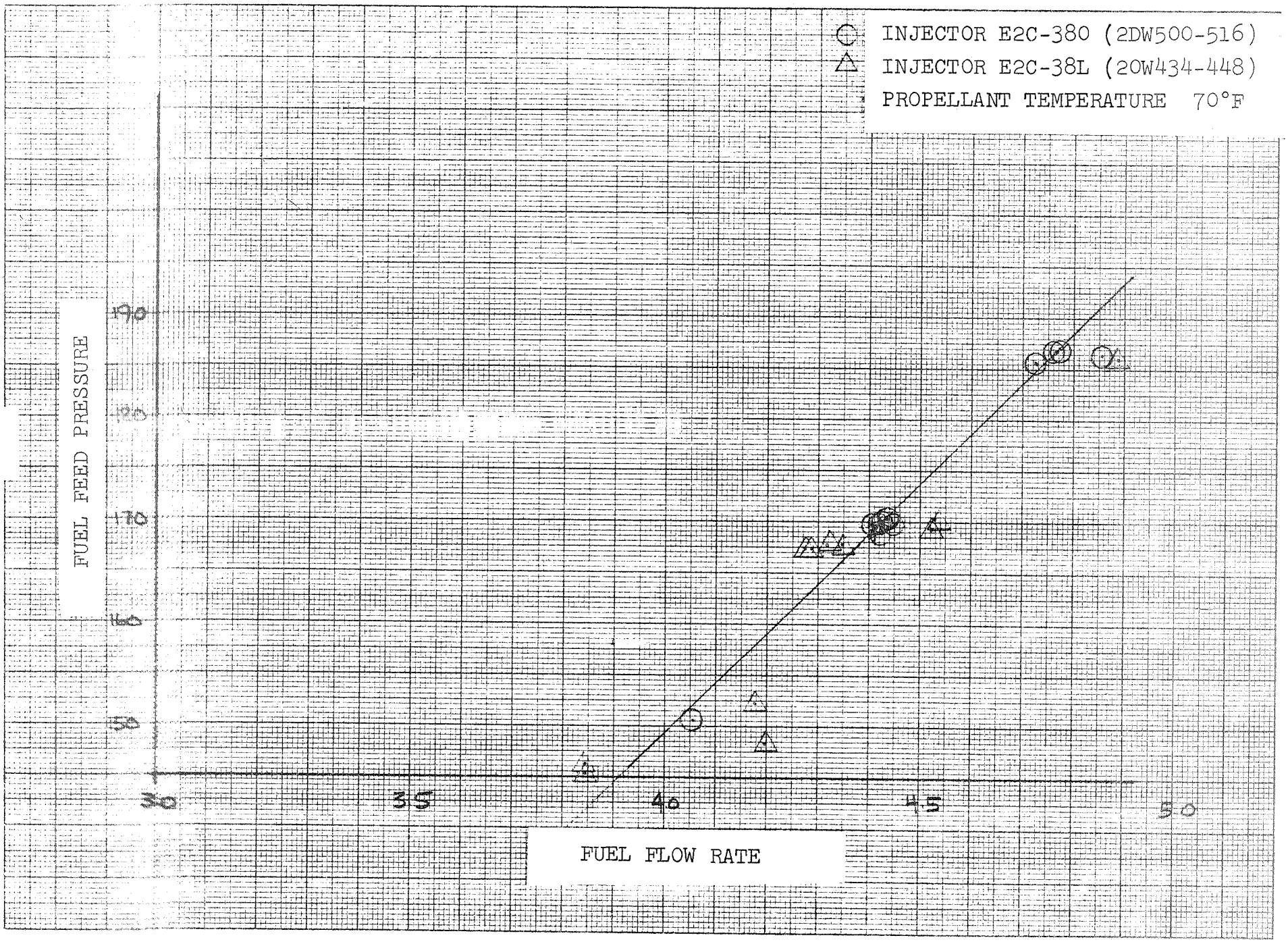
INJECTOR E2C-380 (2DW500-516)
INJECTOR E2C-38L (20W434-448)
PROPELLANT TEMPERATURE 70°F
FUEL FEED PRESSURE
190
180
170
160
50
30
35
40
45
50
FUEL FLOW RATE

FIGURE I-8

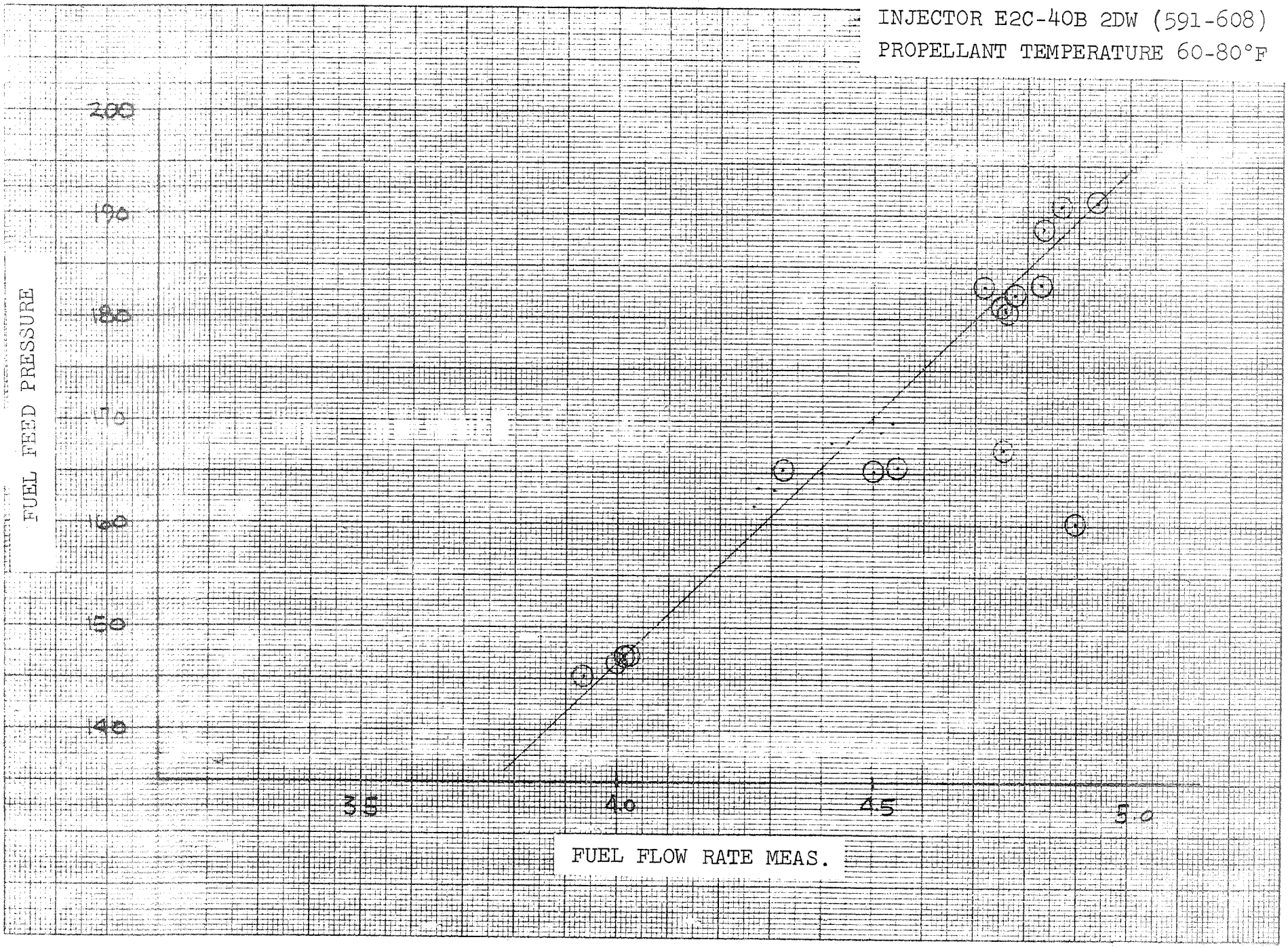

FIGURE I-9

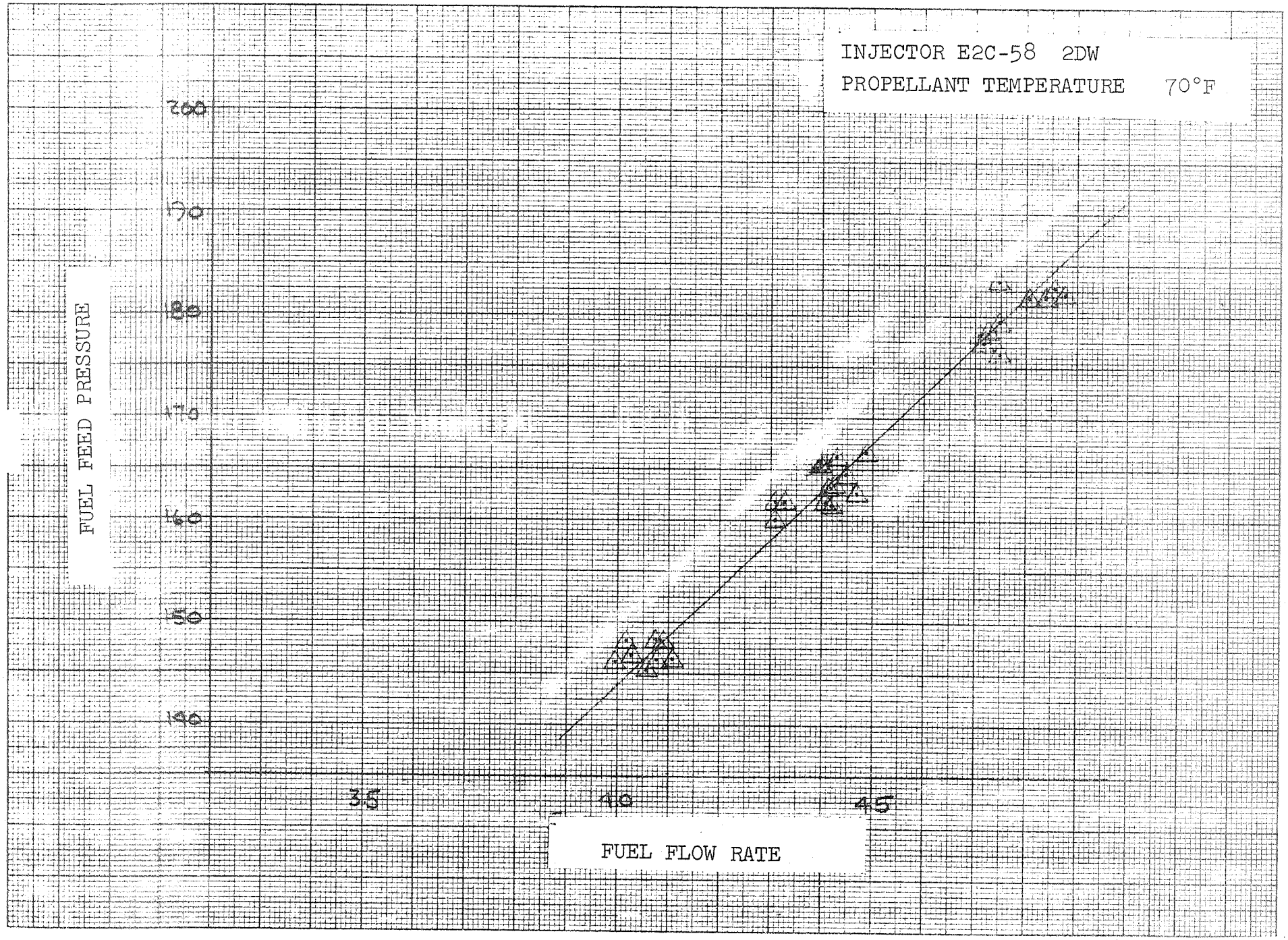

FIGURE I-10

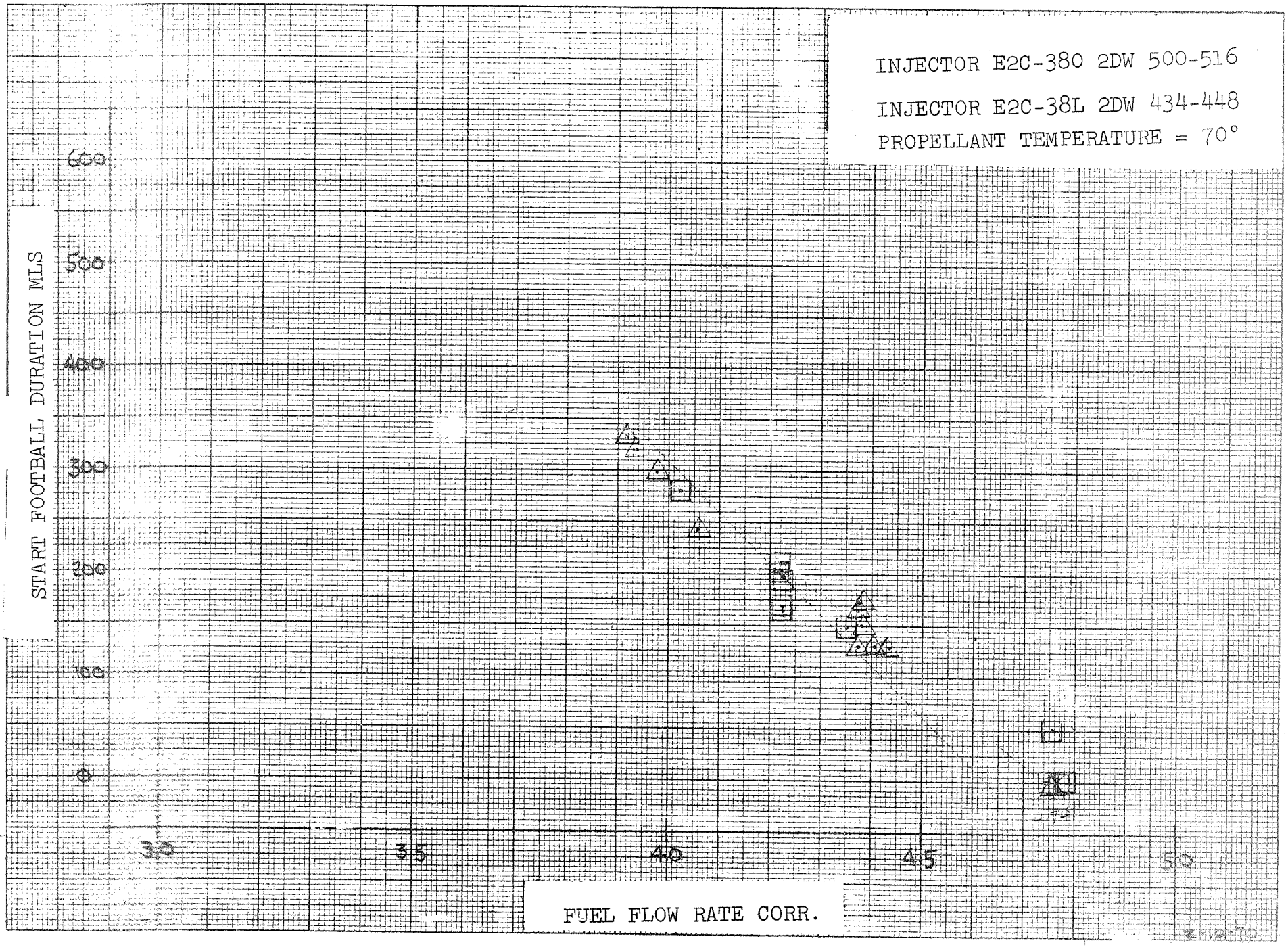

FIGURE I-11

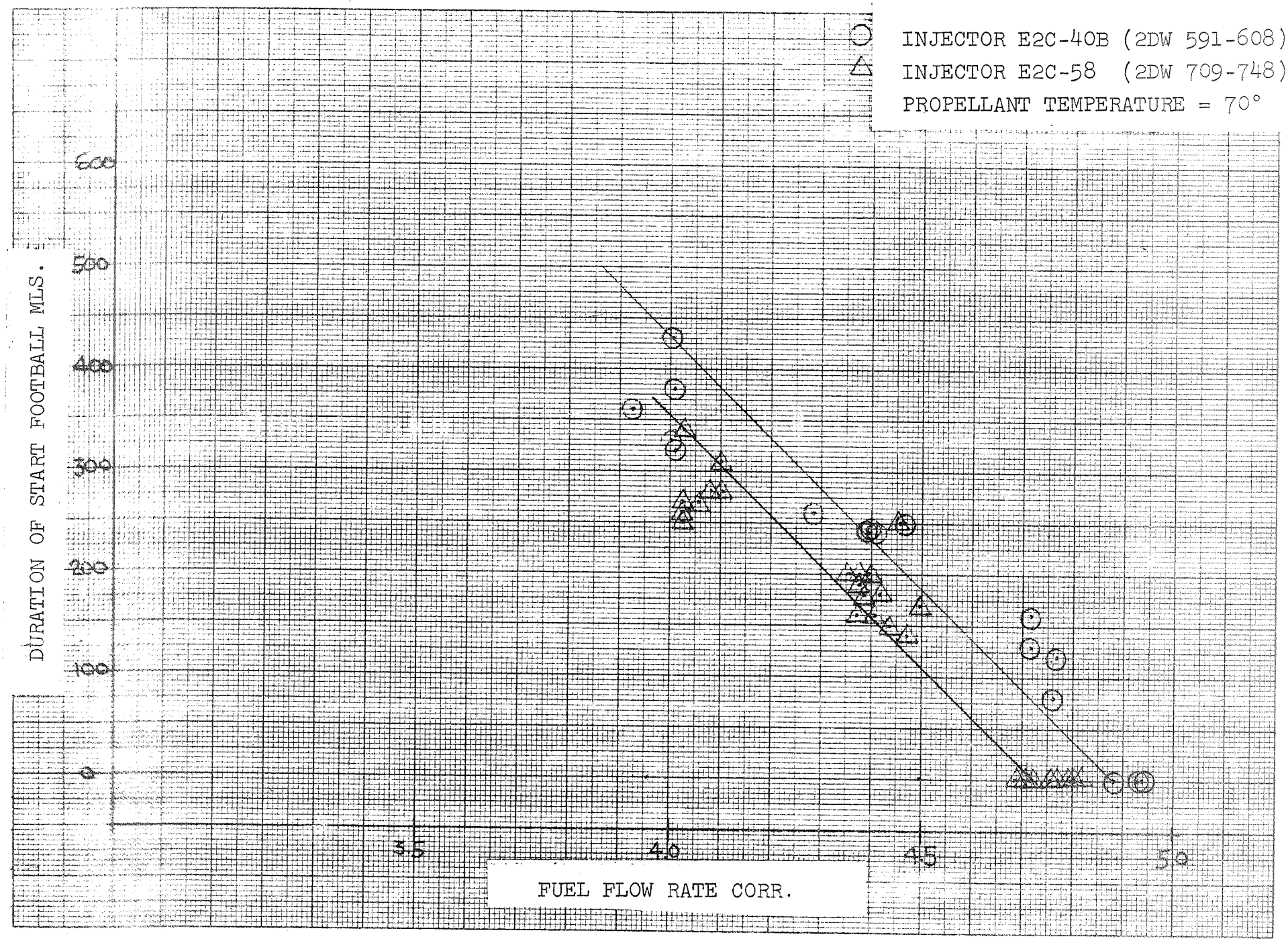

FIGURE I-12

The same method of correcting fuel flow rate was used for the 2DW evaluation as was previously described for cell 3DE. Figures I-8 thru I-10 show the data plots used to obtain corrected fuel flow. The tabulated test data, including corrected fuel flow, is presented in Tables 5 through 7. This data was then re-examined by plotting fuel flow rate (corrected) vs start football duration (Figure I-11 thru I-12). It is interesting to note the E2C-38 data obtained on test series conducted at different times show almost perfect agreement (Figure I-11). To compare this data with that of 3DE, the injector pressure drops were again calculated at the "football breakpoint". These drops are as follows:

E2C-38L	31.6	Fuel injector ΔP at which footballs start
E2C-38O	31.5	
E2C-40B	35.1	
E2C-58	32.9	
Average	32.8	

1. Analysis of Start Footballs in Test Cells 1BN (Altitude) 2BE and 3DW (Sea Level)

In order to determine the critical injector pressure drop in all test cells utilized during the LM Ascent Engine development testing, an analysis has been conducted on injectors tested in test cells 1BN, 2BE and 3DW. This analysis was conducted in the same manner as described in the first monthly progress report (i.e. all data at 70°F and fuel flow corrected for fuel feed pressure, saturation pressure of 50 psi. A word of caution must be inserted about the exactness of the 50 psi saturation level. Most tests were conditioned to a desired temperature level at 50 psi helium. The amount of helium absorption was effected by the conditioning time required to obtain this desired temperature. Therefore, the amount of helium absorption could vary from run to run. This may explain why a few of the tests with 50 psi saturation did not produce footballs at values less than $C\Delta P$.

The injectors analyzed in these three test cells were oxidizer lead injectors, incorporating double pass toroidal manifold and propellant cooled baffles.

a) Test Cell 1BN

A data survey in test cell 1BN indicated that only one injector (E2C-60) was tested in a series that was applicable for this analysis. This injector was tested with propellant conditioning at 50 psi and propellant flow variations adequate to determine the critical pressure drop. The test data used for this analysis is as follows:

Injector S/N	Run No. 1BN	$\dot{W}_f$ Test	FFP Test	$\dot{W}_{f\ corr}$ for FFP	Football Duration
E2C-60	426	5.153	202.0	5.153	0
	427	4.695	190.3	4.870	0
	428	4.316	181.3	4.638	0
	429	4.706	181.9	4.650	0
	430	3.943	164.2	4.160	0.110
	431	3.982	154.5	4.030	0.140
	432	4.339	171.5	4.360	0
	433	4.238	159.3	4.040	0.130
	434	3.661	146.6	3.680	0.060

All tests with propellant temperatures from 60-80°F. Figure I-13 is a plot of fuel feed pressure vs fuel flow rate test. Figure I-14 is a plot of fuel flow rate corrected vs start football duration from this figure we see that the critical fuel flow rate is 4.360 #/sec which is equivalent to a fuel injector pressure drop with this injector of 27.4.

b) Test Cell 2BE

In test cell 2BE data from injectors E2C-38 and E2C-60 was analyzed to define critical injector ΔP as before all data was with propellant temperatures from 60-80°F. The data analyzed is as follows:

Injector S/N	Test No.	$\dot{W}_f$ Test	FFP Test	$\dot{W}_f$ Corr	Football Duration Sec.
E2C-38	2BE-2427	4.174	150.0	3.992	.540
	2428	4.871	185.7	4.725	.116
	2429	4.837	185.7	4.725	0
	2430	4.024	148.5	3.960	.580
	2431	3.825	160.0	4.198	.536
	2432	4.759	183.6	4.680	.113
	2433	4.572	178.3	4.572	.349
	2434	4.020	154.0	4.073	.560
	2435	3.929	155.4	3.999	.600
	2436	4.738	190.6	4.822	0
	2437	--	--	--	--
	2438	4.766	191.0	4.831	.090

Injector S/N	Test No.	$\dot{W}_f$ Test	FFP Test	$\dot{W}_f$ Corr	Football Duration, Sec.
E2C-60	2636	4.401	163.3	4.200	0
	2637	3.798	150.7	3.932	.520
	2638	4.463	175.5	4.463	0
	2639	4.780	182.5	4.590	.058
	2640	4.131	158.0	4.090	0
	2641	4.991	200.4	4.960	0
	2642	4.148	168.1	4.296	.304
	2643	5.392	210.8	5.392	0
	2644	4.626	190.4	4.760	.030

Figure I-15 shows fuel feed pressure vs fuel flow rate test, from this figure fuel flow rate corrected is defined. Figure I-16 is a plot of fuel flow rate corrected vs start football duration. From this figure we see that the average critical pressure drop is 33.6 for test cell 2BE.

c) Test Cell 3DW

In test cell 3DW injector E2B-22 was used to determine critical pressure drop. The data used for this analysis is as follows:

Injector S/N	Run No. 3DW	FFP Test	$\dot{W}_f$ Test	$\dot{W}_f$ Corr	Football Duration
E2B-22A	722	166.0	4.300	4.395	.350
	723	164.5	4.347	4.360	.350
	724	166.0	4.390	4.395	.330
	725	166.0	4.436	4.395	.330
	726	166.8	4.359	4.415	.330
	727				
	728	152.5	4.163	4.095	.400
	729	151.6	4.156	4.075	.400
	730				
	731	151.2	4.118	4.065	.430
	732	187.9	4.876	4.876	
	733	187.9	4.838	4.876	
	734	185.6	4.818	4.829	
	735	185.6	4.854	4.829	
	741	166.3	4.446		.310
	742	167.6	4.414		.320
	743				
	744	187.3	4.916	4.865	

Injector S/N	Run No. 3DW	FFP Test	$\dot{W}_f$ Test	$\dot{W}_f$ Corr	Football Duration
E2B-22F	759	164.8	4.769	4.365	.310
	760	163.4	4.346	4.338	.300
	761	164.4	4.332	4.355	.280
	762	147.1	3.975	3.975	.480
	763	145.7	4.125	3.945	.490
	764	145.4	4.063	3.935	.590
	765	144.8	4.063	3.925	.540
	766	184.1	4.698	4.790	.090
	767	183.5	4.757	4.780	.110
	768	184.4	4.806	4.800	.140
	769	184.1	4.678	4.791	.120
	770	165.5	4.348	4.386	.330
	771	164.2	4.371	4.355	.320

Figures I-17 & I-18 are plots of fuel feed pressure vs fuel flow rate test and fuel flow rate corrected vs start football duration respectively. From Figure 6 we see that the critical pressure drop for this injector in test cell 3DW is 33.8 psi.

A review of the analysis for critical pressure drop by test cell shows the following:

Test Cell	Critical Pressure Drop
2DW	32.8
2BE	33.6
3DE	37.8
3DW	33.8
1BN	27.4

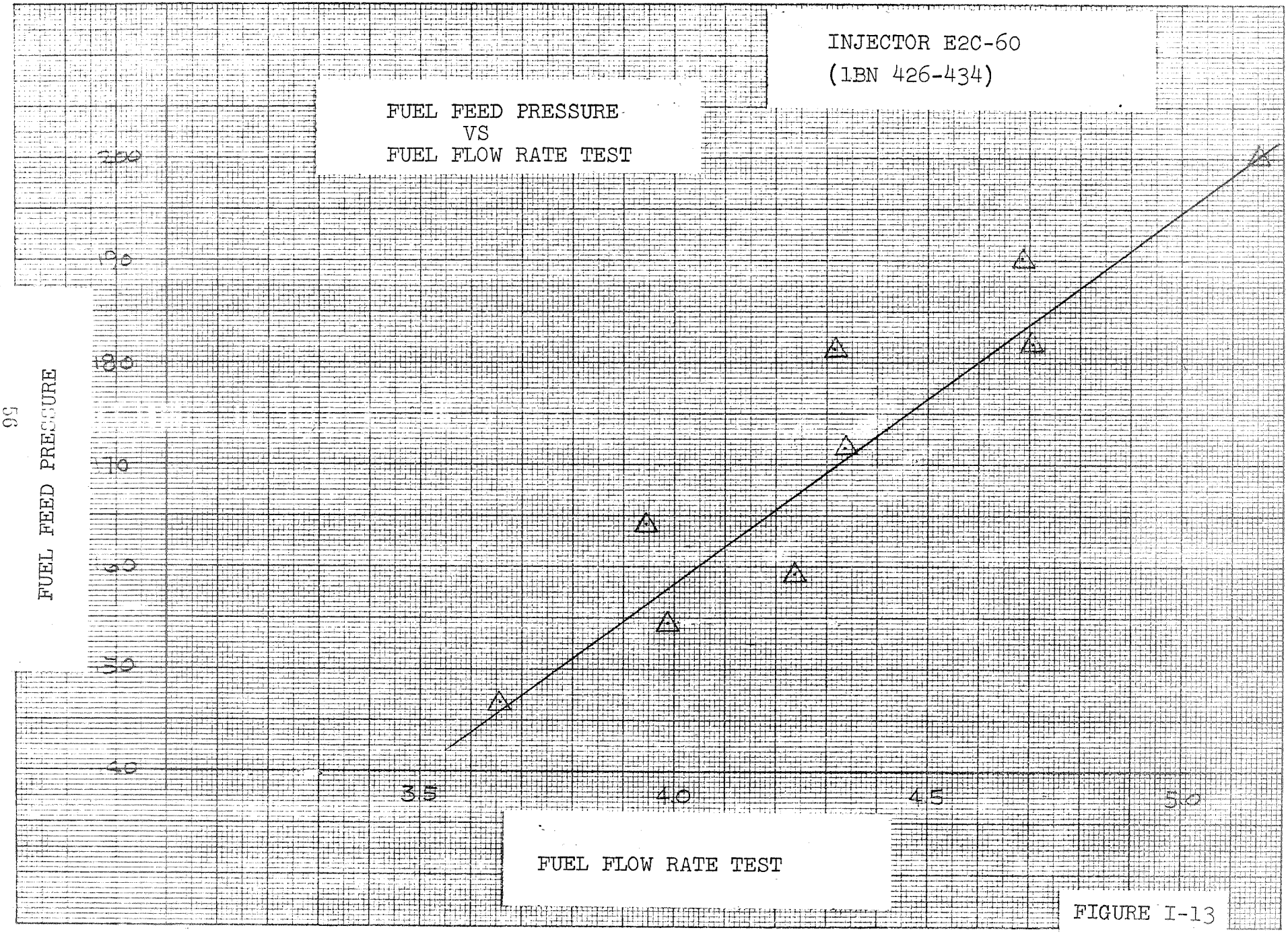

FIGURE I-13

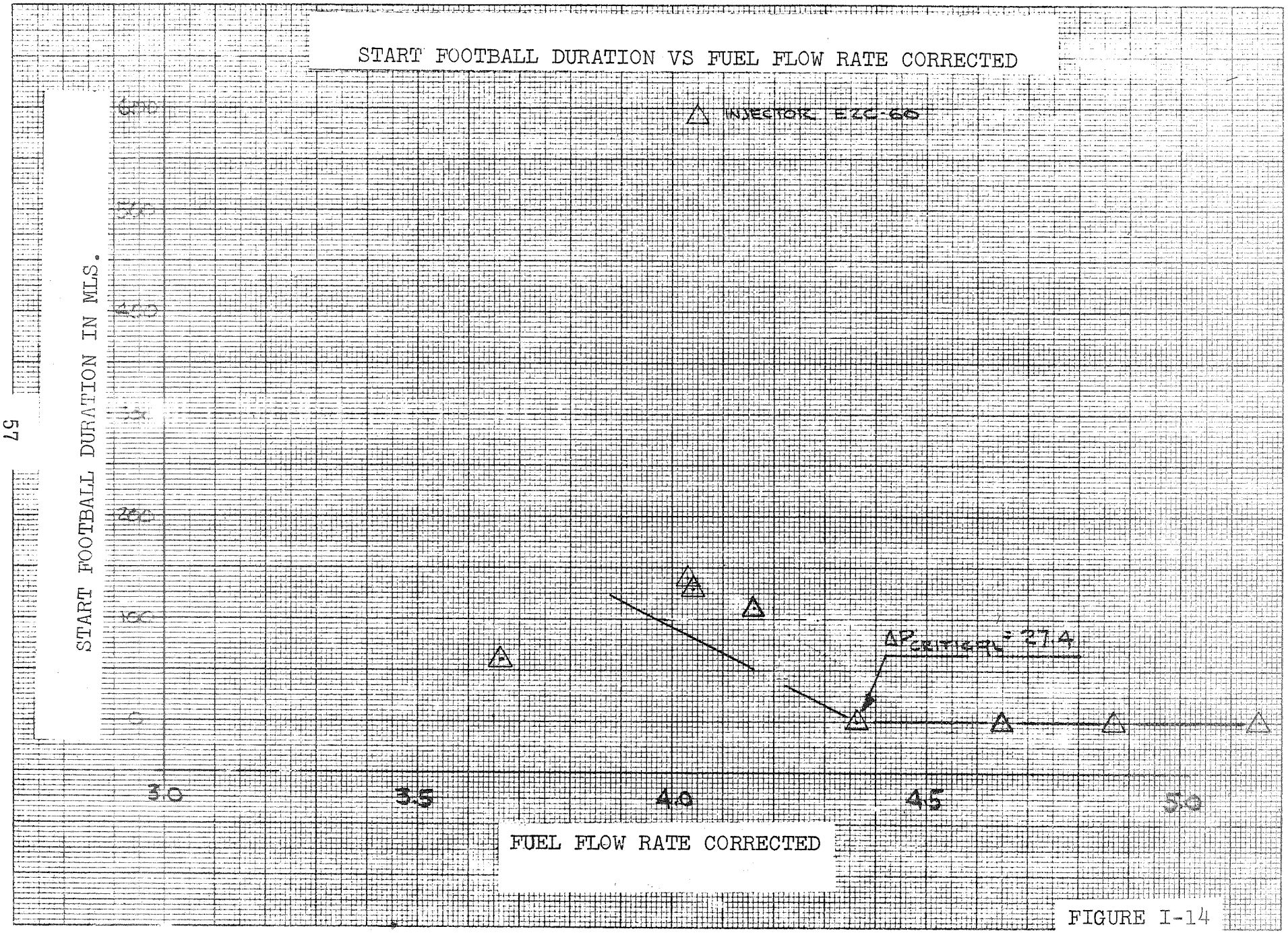

FIGURE I-14

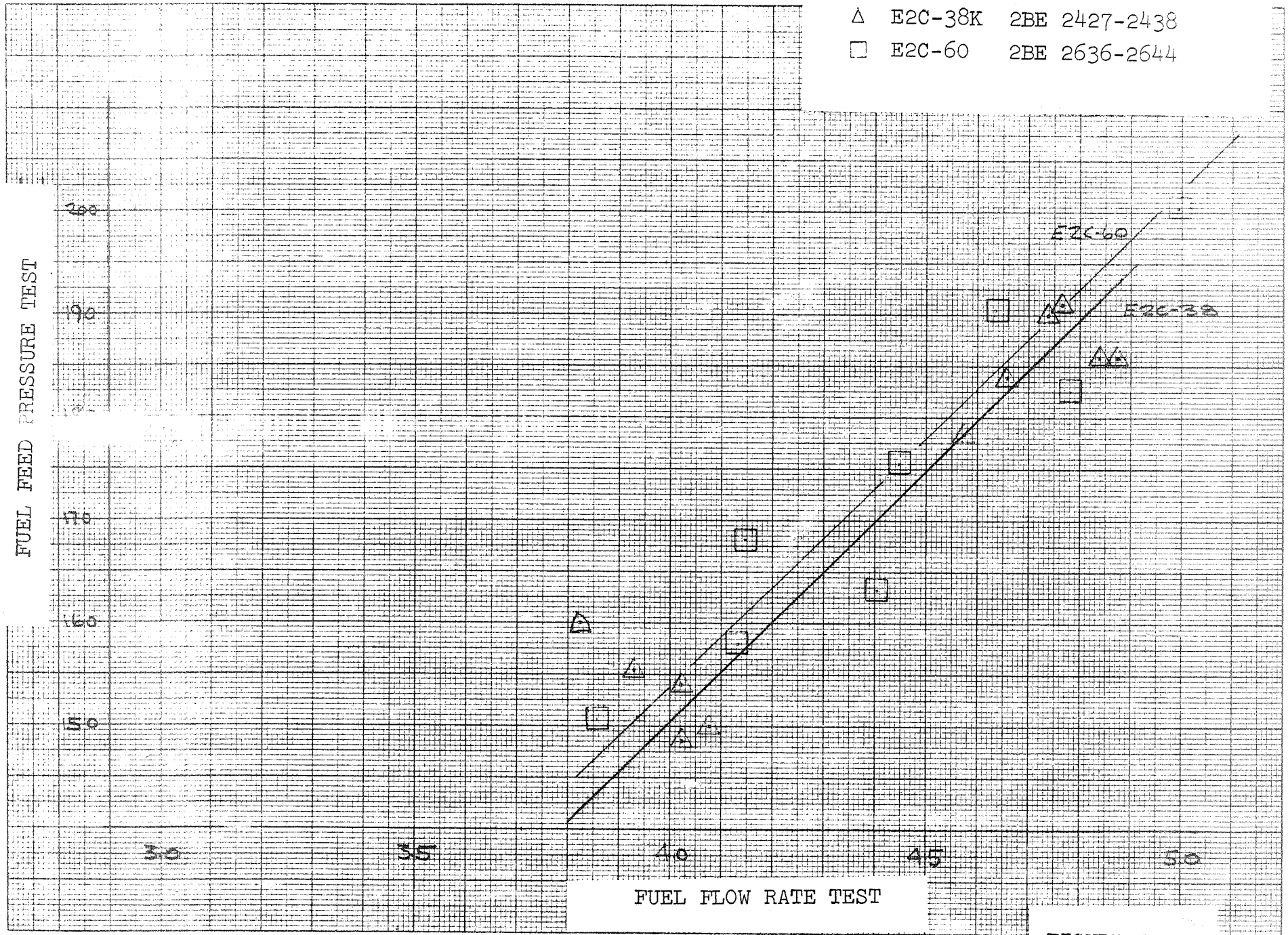
△ E2C-38K 2BE 2427-2438
□ E2C-60 2BE 2636-2644
E2C-60
E2C-38
FUEL FEED PRESSURE TEST
60
70
80
90
100
35
40
45
50
FUEL FLOW RATE TEST

FIGURE I-15

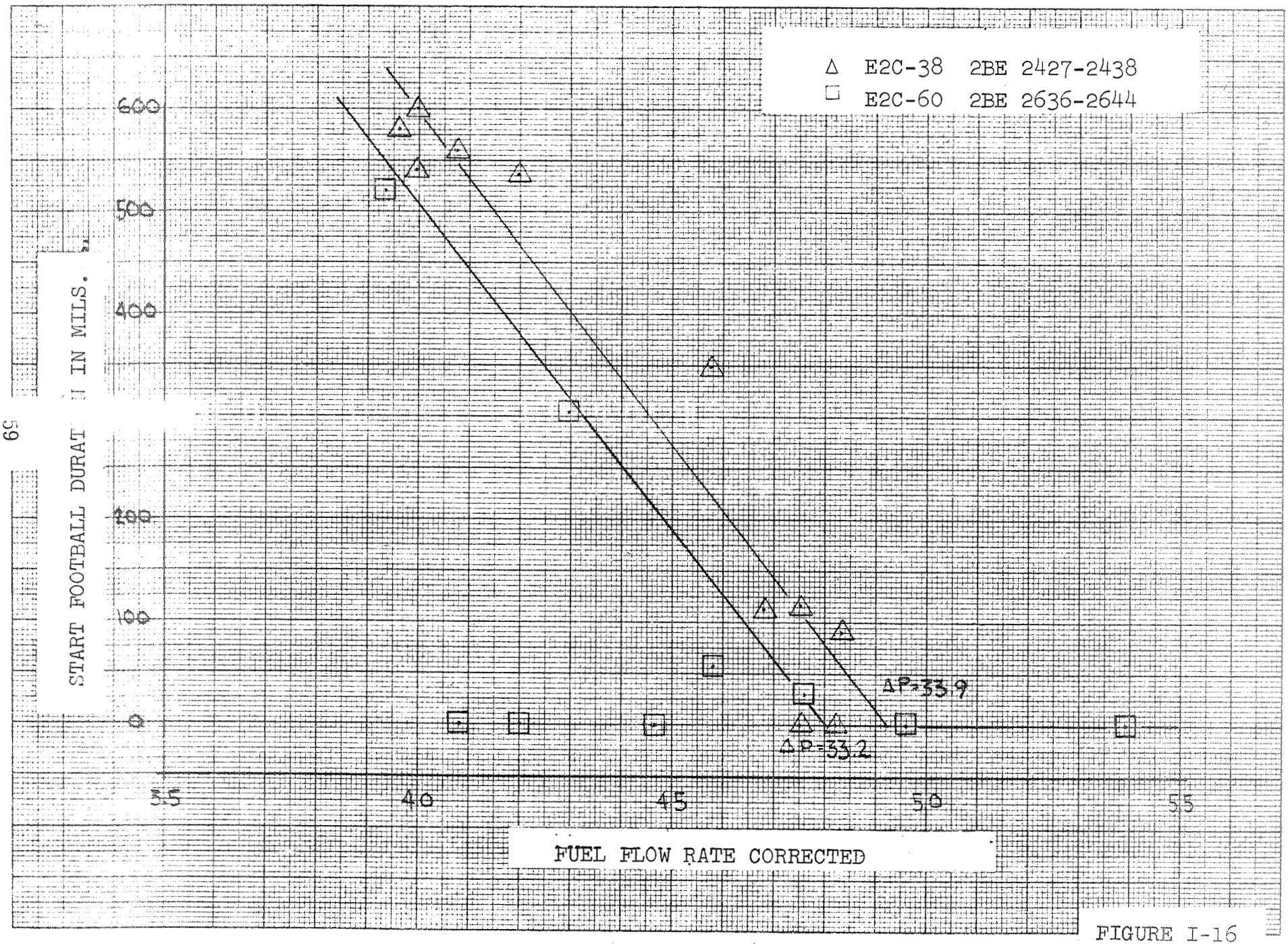

FIGURE I-16

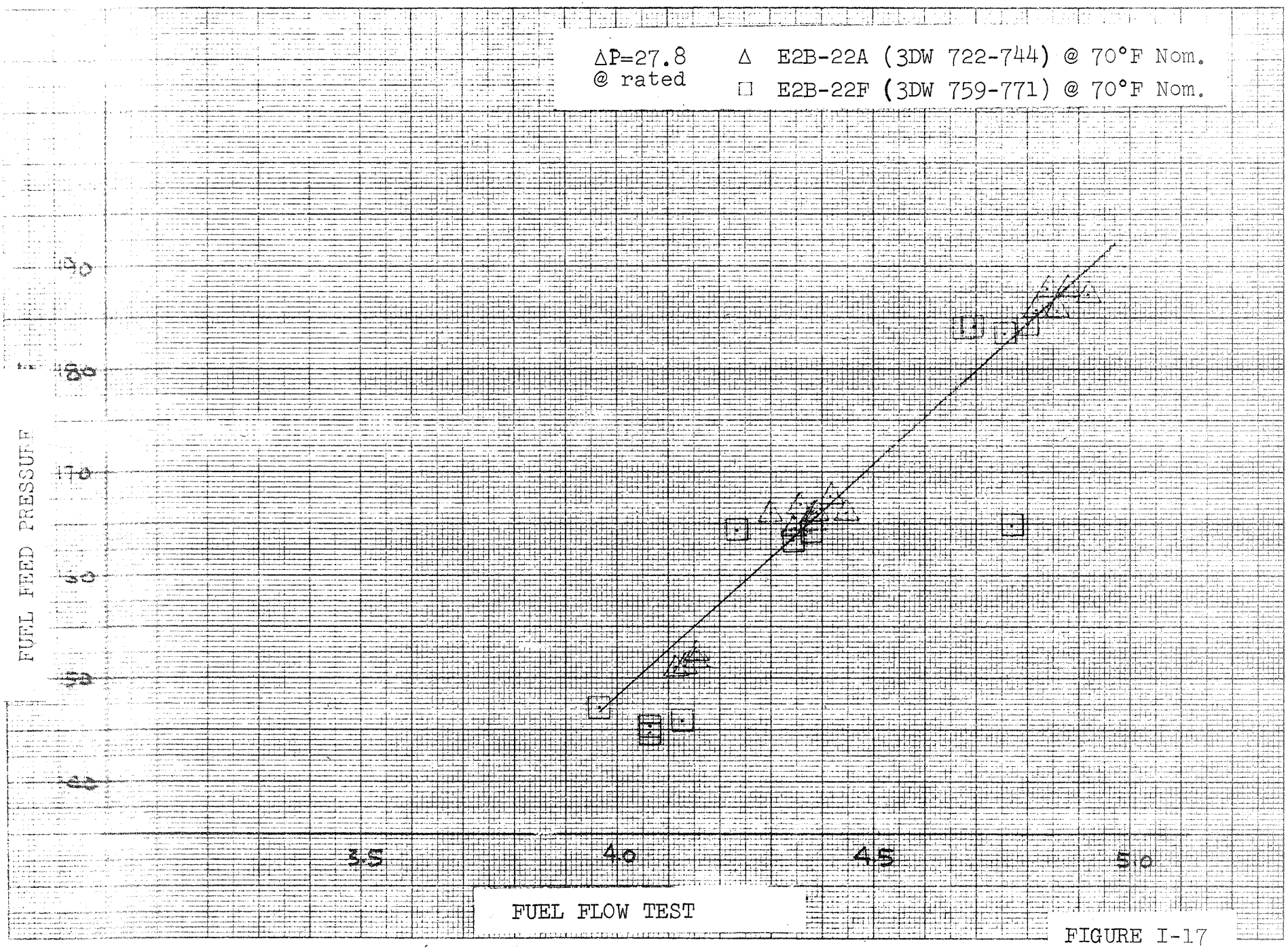
ΔP=27.8
@ rated
Δ E2B-22A (3DW 722-744) @ 70°F Nom.
□ E2B-22F (3DW 759-771) @ 70°F Nom.
FUEL FEED PRESSURE
80
60
40
35
40
45
50
FUEL FLOW TEST

FIGURE I-17

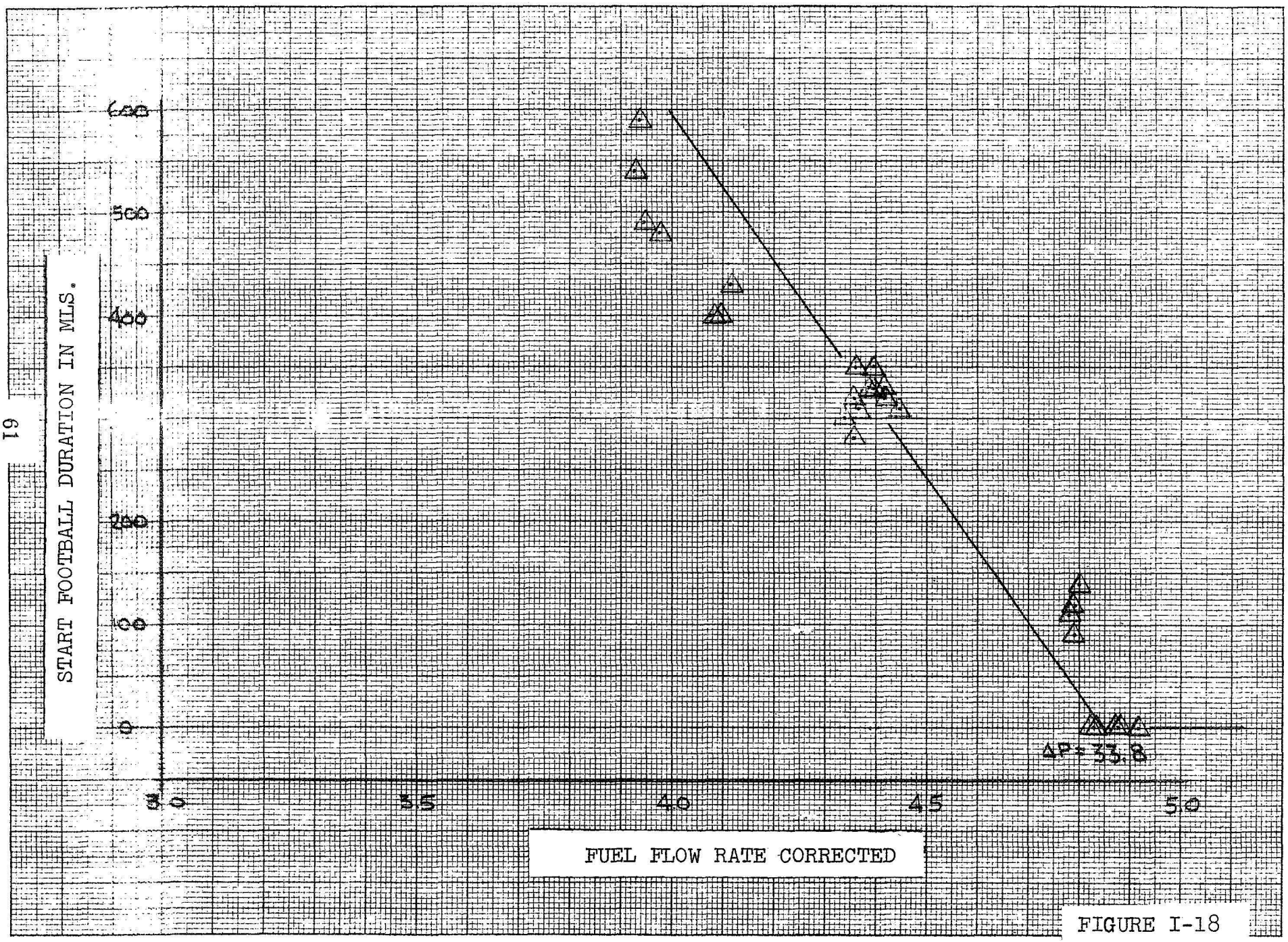

FIGURE I-18

C. ANALYSIS OF HELIUM SATURATION TYPE AND THE EFFECT ON POST START FOOTBALLS

During the LFO testing in test cell 2DW at Bell Test Center, various procedures for saturating the propellants were used. Review of these procedures (Figures I-19 thru I-22) indicate that various amounts of H_e in solution could be achieved, depending on the procedure used. In some cases, the procedure could produce supersaturated propellants at test conditions.

In order to determine if the type of saturation affected the post start football on the LM injector, the data were reviewed to find a single injector that had been tested using the four types of saturation. It was determined that injector E2CA-113HF was the only source of data. The data used for this comparison is tabulated in Table 8 and was confined to tests at 70°F. For the purpose of this analysis, fuel flowrate was plotted vs. football amplitude. Figure I-23 is a plot of all data available on this unit and shows that there is an effect with saturation type. Figure I-24 shows the trends from Figure I-23 without the data points.

From this analysis the following hypotheses have been made about the saturation types.

1. Saturation Type IIA

This type saturates at pressure levels higher than run levels, then vents the tank pressure to run conditions. This approach conceivably allows the gas to come out of solution and be distributed throughout the entire feed system. This would create a supersaturated condition. As can be seen from Figure I-18 footballs, were created on all tests using this type of saturation and there is no amplitude trend with flow changes.

2. Type III

This type saturates the propellant at 140 psia. This pressure is lower than any run pressures used in this test series. Therefore, the higher run pressure could create a condition that would permit absorption of any gas that might come out of solution due to pressure drops in the propellant feed system. Figure I-24 shows that no footballs were noted.

3. Saturation Types I and IIB are similar. This is due to the fact that there is no rapid venting prior to the engine testing. Therefore, the system can operate without LFO's until it reaches its own "Breakpoint". Figure I-24 shows that Types I and IIB show similar trends. It should be noted that the breakpoint is at a higher flowrate for Type IIB than it is for Type I. It could be hypothesized that this effect is due to more gas being available with Type IIB saturation because of the higher saturation levels.

INJECTOR S/N E2CA-113 HF TEST CELL 2DW

Test No.	W_t Lb/ Sec	P_c PSIA	Mixture Ratio O/F	Start Football Dur. Sec	Start Football Ampl. P-P PSI	Subsequent Footballs No.	Subsequent Footballs Dur. Sec	Subsequent Footballs Avg. Ampl. P-P PSI	Total Dur. of Footballs (Incl.1st) Sec	Termination of Last Football Sec	Type of Saturation	Helium Saturation Level - % Oxid $X10^{-3}$	Helium Saturation Level - % Fuel $X10^{-3}$
906	4.251	121	1.748	0.915	70	None		--	0.915	1.115	T-1	Lost	2.0
913	3.859	107	1.641	14.8	112	Continuous		45	14.8	14.8	T-1	20.0	2.0
914	3.885	112	1.766	15.0	32	Continuous		32	15.0	15.0	T-1	11.2	1.95
915	4.243	123	1.760	0.110	19	None		--	0.110	0.260	T-1		
916	4.284	120	1.678	0.791	18	None		--	0.791	0.864	T-1		
917	4.811	128	1.542	None	--	--		--	--	--	T-1		
918	4.447	131	1.811	None	--	--		--	--	--	T-1		
922	3.928	111	1.701	1.089	31	None		--	1.089	1.089	T-III	18.3	2.3
923	3.889	110	1.707	15.0	23	Continuous		17	15.0	15.0	No Rec. T.P.Held 1.5 Hrs.		
924	4.342	119	1.641	0.120	59	None		--	0.120	0.200			
925	3.986	110	1.653	0.240	74	None		--	0.240	0.292	III	19.8	1.69
926	3.928	109	1.691	0.862	87	None		--	0.862	0.901	III	15.9	1.78
927	3.912	112	1.777	0.296	89	1	0.358	30	0.654	0.718	III	16.0	1.59
928	3.946	113	1.802	1.896	87	Intermittent		20		15.0	II-A	22.2	2.19
929	3.934	111	1.740	1.139	77	None		--	1.139	1.937	III	23.9	1.53
930	4.214	108	1.487	2.122	89	Intermittent		26		15.0	II-A		2.37
931	3.861	110	1.762	0.900	71	None		--	0.900	0.920	III	15.8	1.75
932											II	28.0	2.12
933	3.973	106	1.600	15.1	76	Continuous		26	15.1	15.1	II-A		2.48
934	4.096	112	1.648	14.8	51	Continuous		29	15.4	15.4	II-A	29.0	2.45
935	4.086	112	1.658	15.3	74	Continuous		28	15.3	15.3	II-A	22.5	2.24
936	4.153	113	1.615	1.610	78	Intermittent		22			II-A	34.1	2.20
937	4.120	112	1.619	14.8	81	Continuous		18	14.8	14.8	II-A	27.1	1.94

NOTE: All times taken from P_c overshoot.

TABLE 8

INJECTOR S/N E2CA-113 HF TEST CELL 2DW (Continued)

Test No.	W_t Lb/ Sec	P_c PSIA	Mixture Ratio O/F	Start Football Dur. Sec	Start Football Ampl. P-P PSI	Subsequent Footballs No.	Subsequent Footballs Dur. Sec	Subsequent Footballs Avg. Ampl. P-P PSI	Total Dur. of Footballs (Incl.1st) Sec	Termination of Last Football Sec	Type of Saturation	Helium Saturation Level - % Oxid $X10^{-3}$	Helium Saturation Level - % Fuel $X10^{-3}$
938	4.069	111	1.655	15.2	74	Continuous		24	15.2	15.2	II-A	27.4	2.03
939	4.037	112	1.692	14.6	66	Continuous		20	14.6	14.6	II-A	28.9	1.98
940	3.889	111	1.789	14.6	58	Continuous		20	14.6	14.6	II-A	32.1	2.34
941	4.107	112	1.620	15.3	68	Continuous		20	15.3	15.3	II-A	33.1	2.42
942	4.044	113	1.696	14.6	73	Continuous		25	14.6	14.6	II-A	24.2	3.16
948	4.208	114	1.584	None		Intermittent		11			II-B	27.5	1.41
949	3.999	108	1.616	None		Intermittent		23			II-B		1.39
950	4.378	121	1.653	None		None					II-B	21.7	1.36
951	4.389	120	1.633	None		None					II-B		1.51
952	4.747	132	1.664	None		None					II-B	10.0	1.65
953	[illegible]	[illegible]	1.623	None		Intermittent		13			II-B	24.1	1.37
954	4.055	112	1.663	None		Intermittent		16			II-B		1.58
955	4.085	112	1.650	None		Intermittent		16			II-B		1.49
956	4.101	113	1.651	None		None						19.7	2.00
957	4.103	112	1.629	None		Intermittent		10		15.3			

TABLE 8 (Continued)

TYPE I PROPELLANT He SATURATION

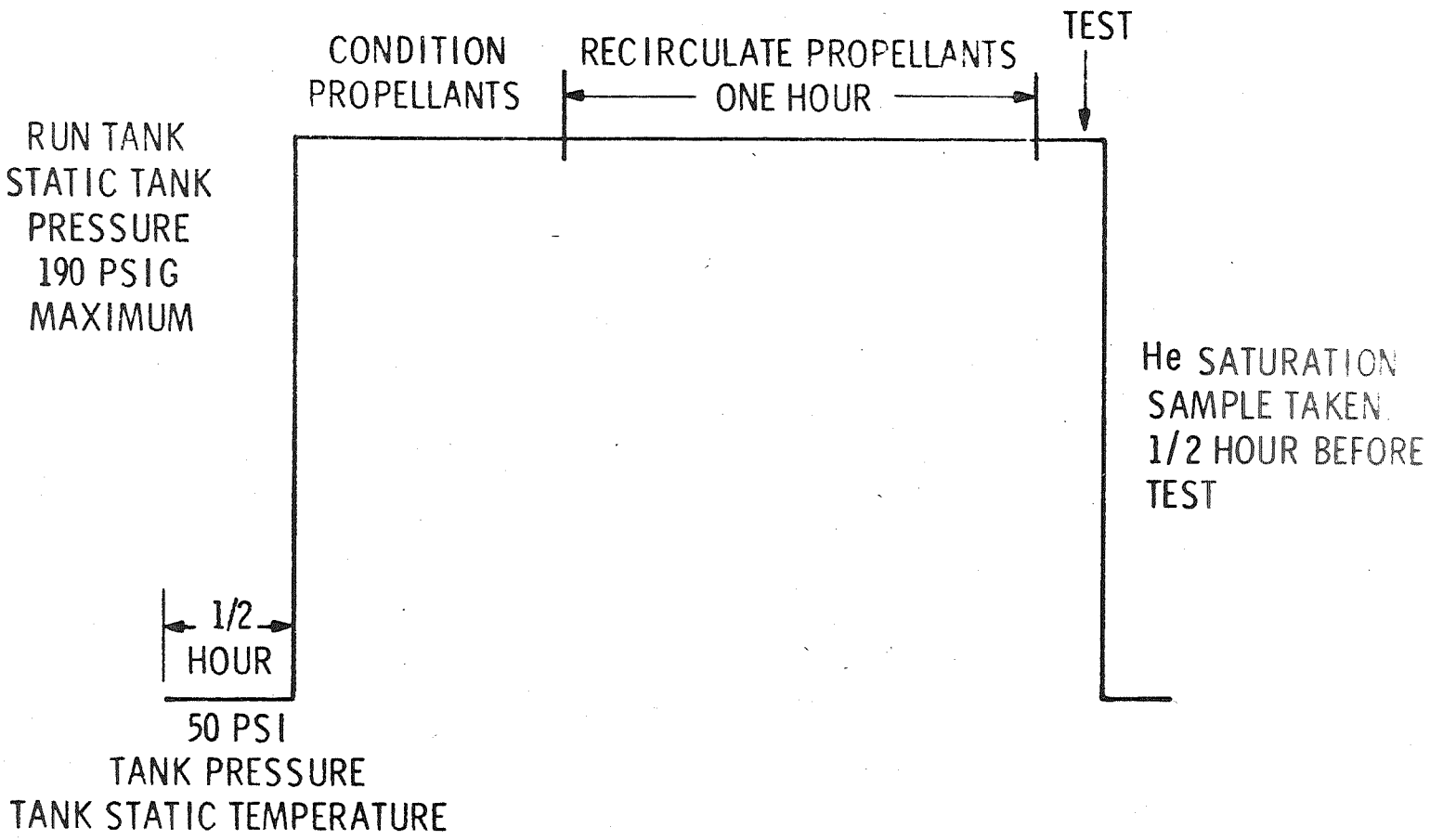

FIGURE I-19

TYPE IIA PROPELLANT He SATURATION

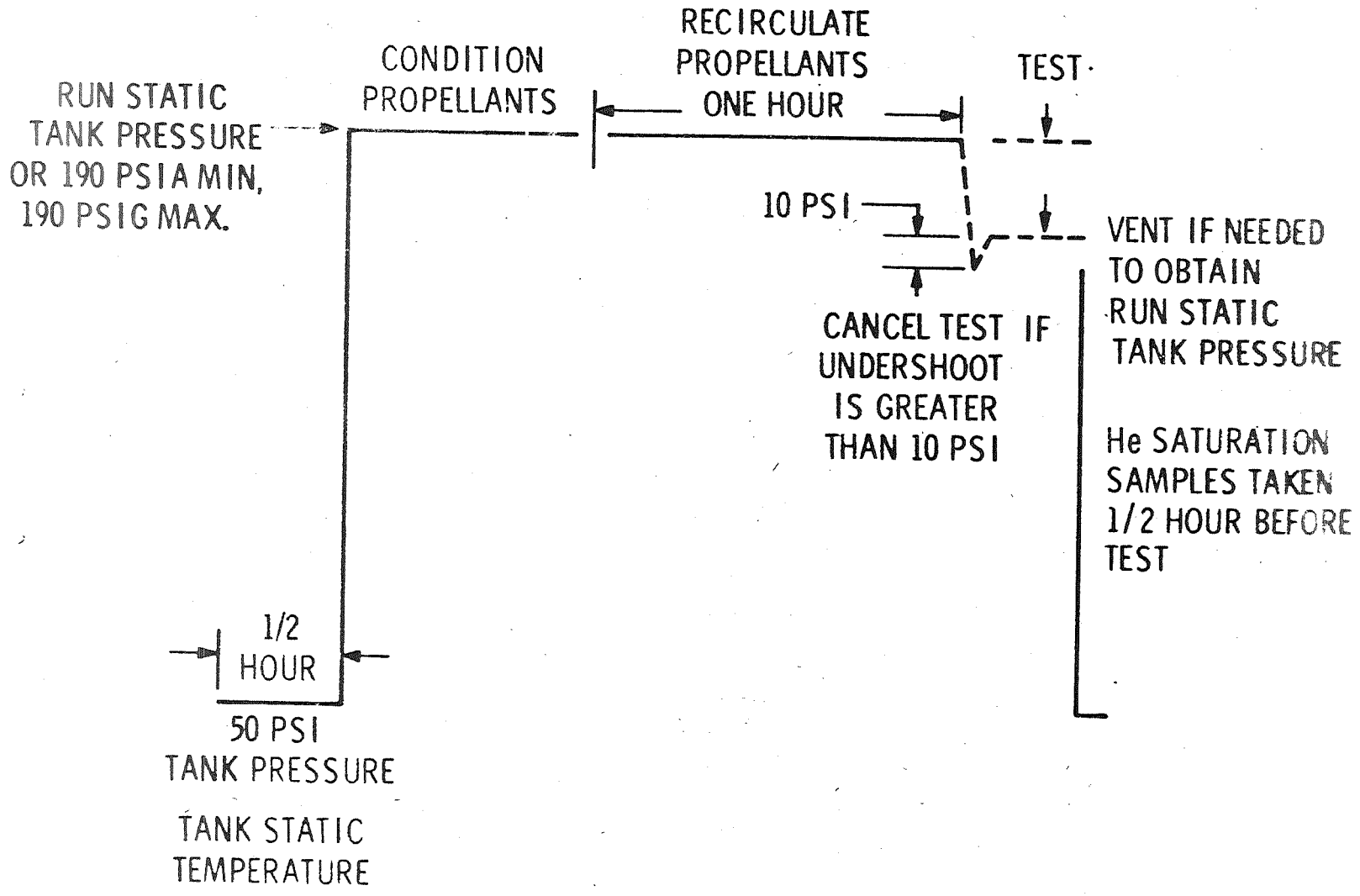

FIGURE I-20

TYPE II-B PROPELLANT He SATURATION

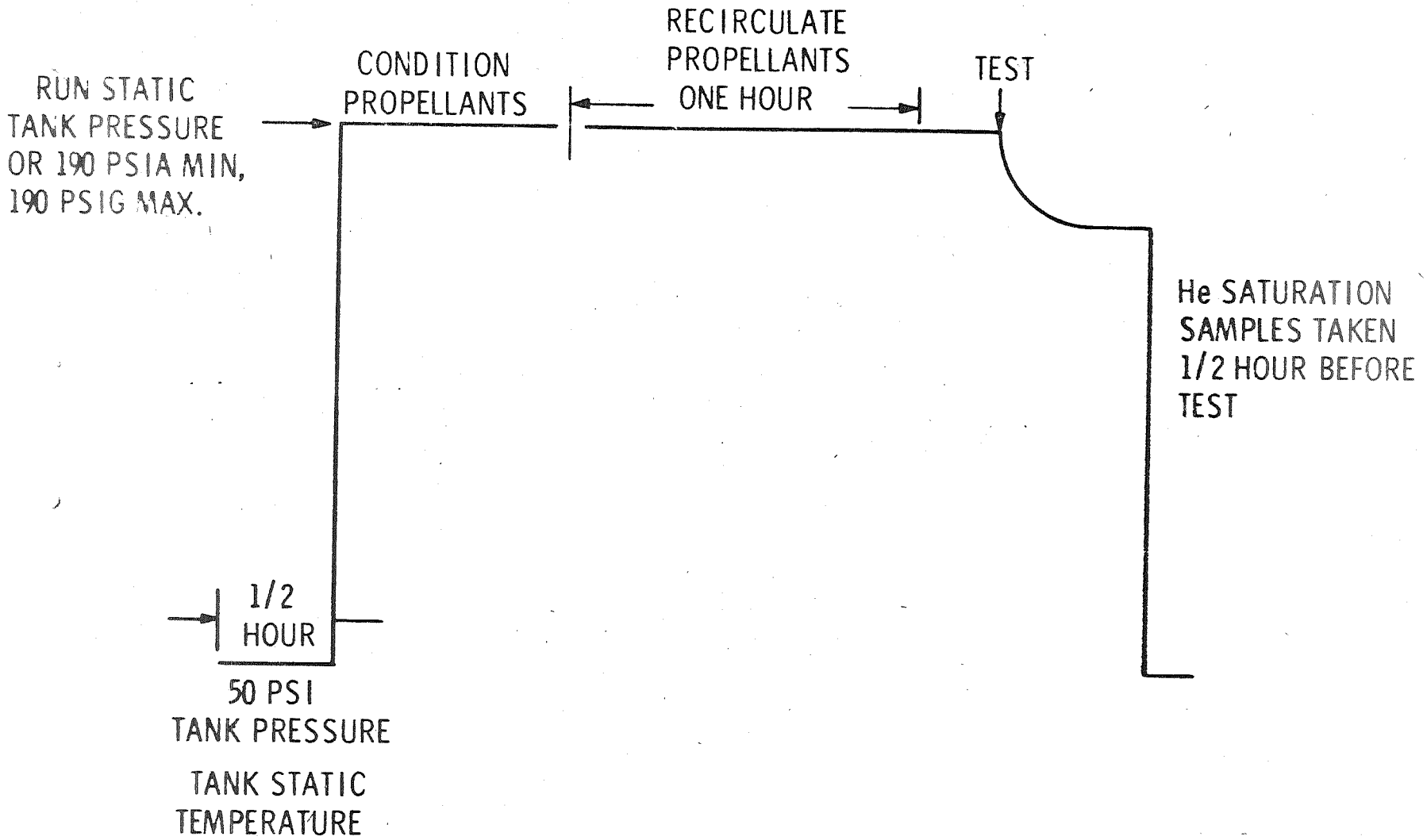

FIGURE I-21

TYPE III PROPELLANT He SATURATION

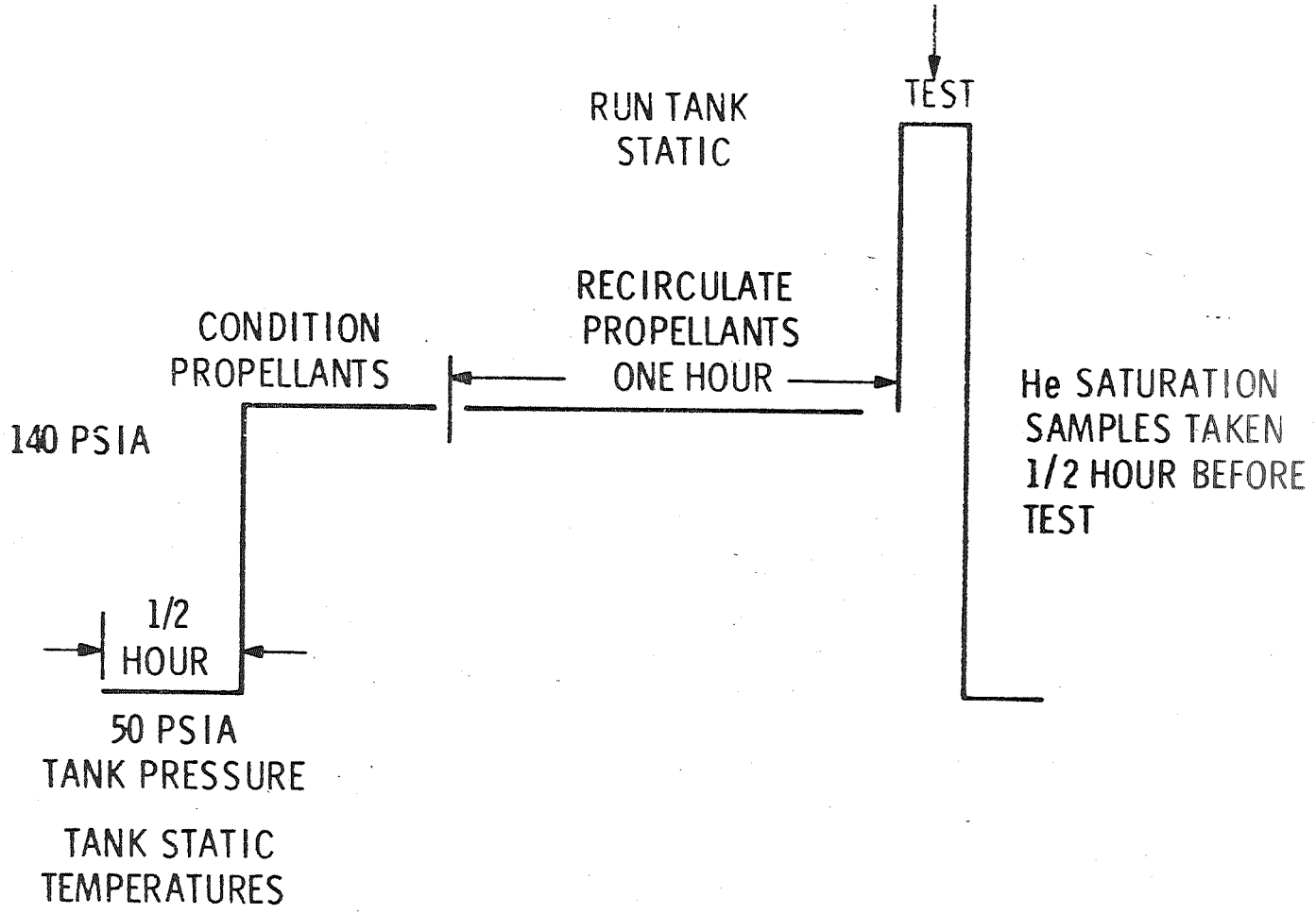

FIGURE I-22

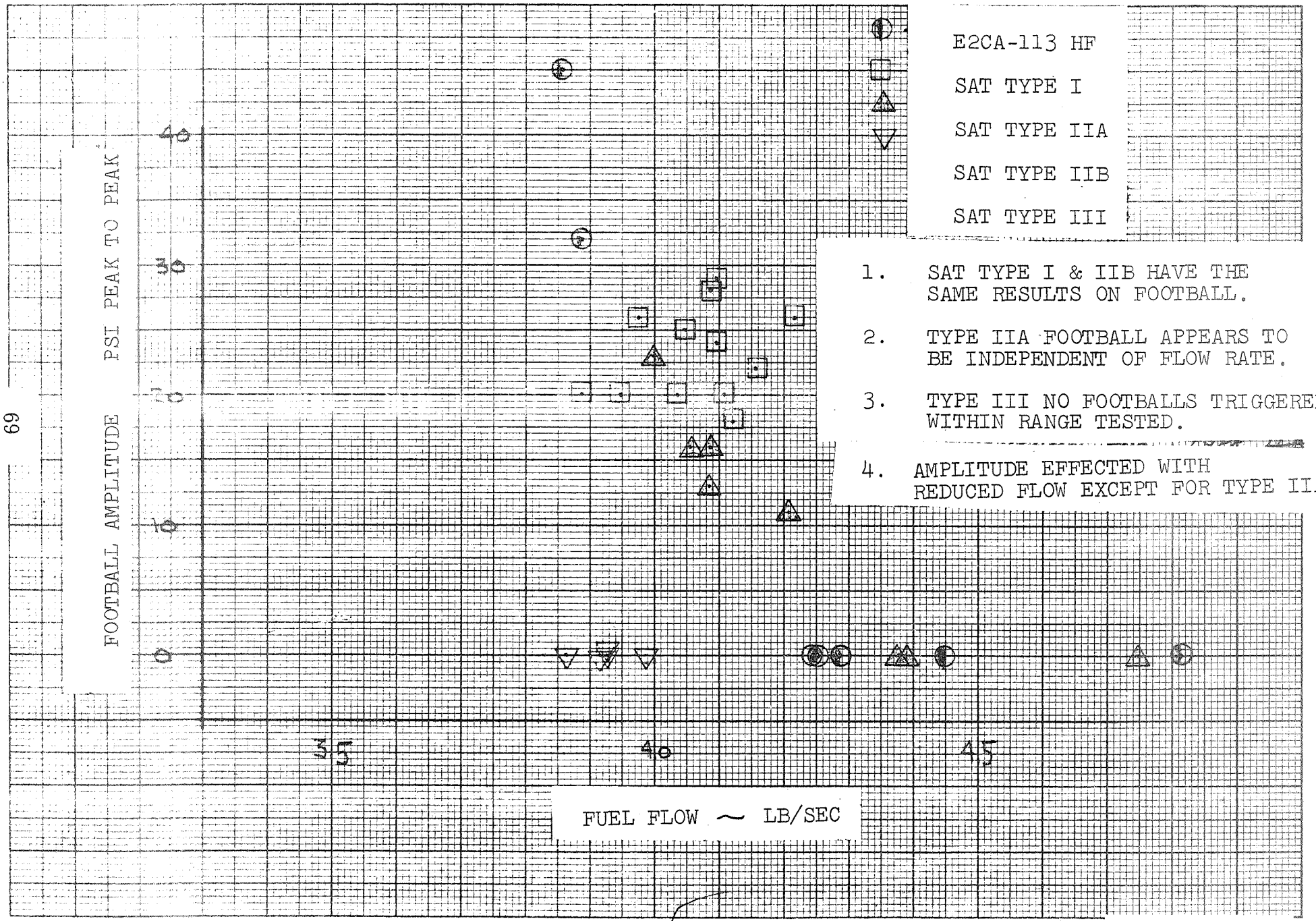

FIGURE I-23

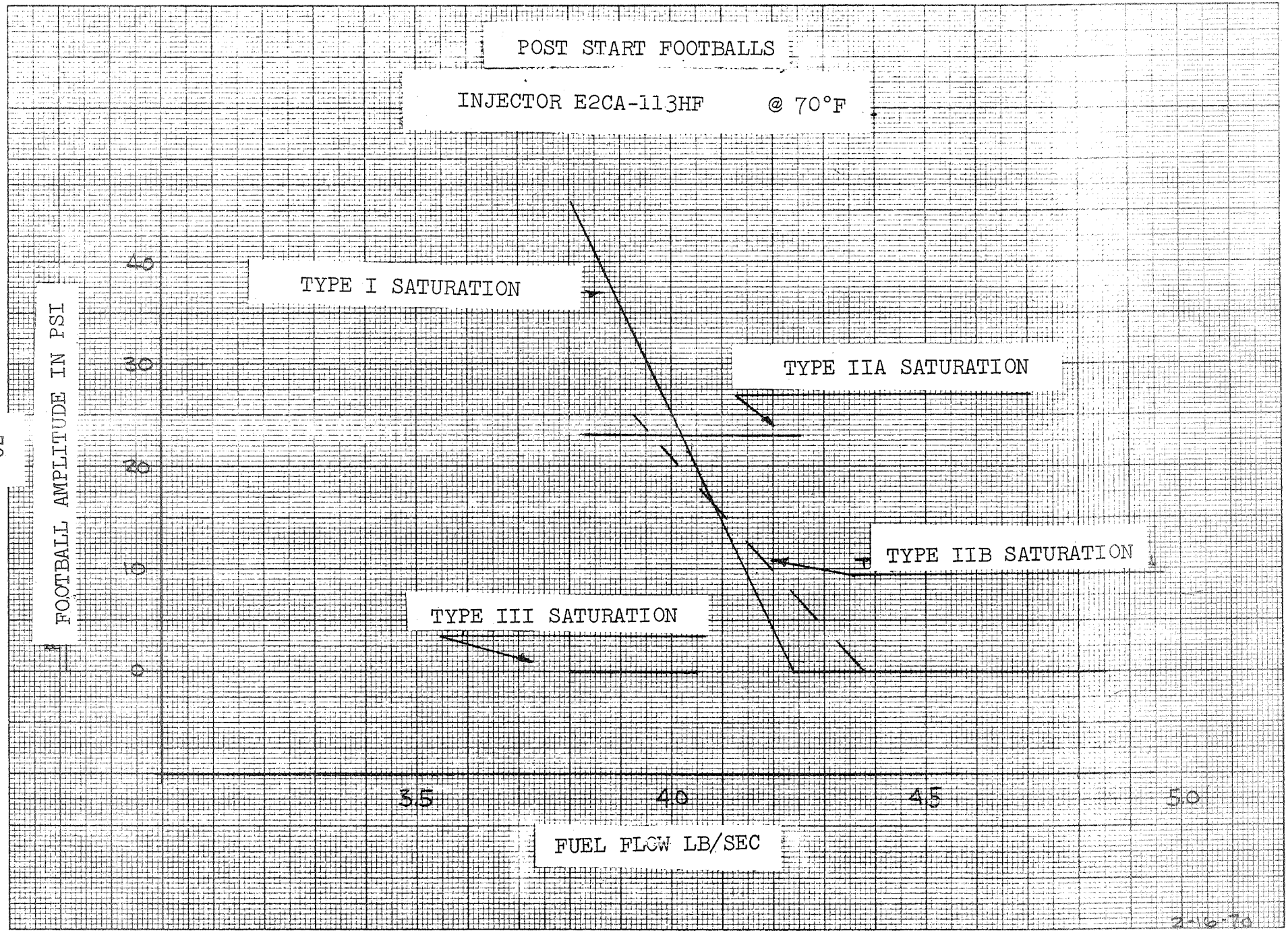

FIGURE I-24

TENTATIVE CONCLUSIONS

1. The method of helium saturation is an important variable.

2. The pressure difference between saturation and test feed pressure is an important variable.

3. At conditions of constant saturation level injector pressure drop appears to be an important variable.

a) Analysis of Test Cell Configuration and its Effect on Critical Injector Pressure Drop

In order to determine if the variation in critical pressure drop was a function of the test cell configuration the variations in the test cell and the start transient hydraulics were examined. The test cell diagrams (1BN, 2DW, 3DE and 3DW) are shown in Figures I-25 thru I-29. As can be seen from these figures the variations in the test cell geometry are substantial. In order to define the effects of line length and volume, plots were made of these parameters vs critical pressure drop (Figure I-30). This figure would indicate that the variation in critical pressure drop is not a function of physical variations in volume or length. In order to determine the effects of system pressure drop, plots were made of the start transient fuel feed pressure decay and the steady state pressure drop from tank to engine interface (Figure I-31). This figure would indicate that the start football breakpoint is not a function of system pressure drop. Figure I-32 shows plots of fuel overflow and fuel feed pressure recovery time during the start transient. This figure would indicate a correlation with both parameters when compared to injector critical pressure drop. This data would indicate that the fuel velocity during the start transient is an important parameter with respect to start footballs. It is also interesting to note that in a fixed system the flow velocity increases as supply pressure increases, this observation agrees with the reduction and elimination of start footballs with increased chamber pressure.

b) Analysis of the Effect of Increased Saturation Pressure on Start Footballs

In order to define if the pressure at which the propellant is saturated has an effect on the start football duration or the injector critical pressure drop the following analysis was conducted.

1) Test Cell 2DW

During the engine development testing in Cell 2DW variations in propellant conditioning pressure were made. Initially, all propellant conditioning was conducted at 50 psi. The start football analysis discussed in the first monthly progress report utilized only tests during which the propellant conditioning was conducted at 50 psi. This data revealed that the critical injector pressure drop for start footballs was 32.8 psi. In an attempt to define the critical pressure drop for injectors when the propellants are saturated at 190 psi data from testing with injectors E2C-113, E2CE-147 and E2CE-141 was plotted against fuel flow rate. This data is plotted in Figure I-33. Due to the lack of data at fuel flow rate above 4.8 pounds per second, the data had to be extrapolated in order to predict the critical injector pressure drop. This drop is projected to be 40 psi for saturation pressure of 190 psi as compared to 32.8 psi for saturation pressure of 50 psi. It is also interesting to note that the football duration is significantly increased at saturation pressures of 190 psi and continues until the engine shutdown at reduced flow rates.

2) Test Cell 1BN

In order to collaborate the results noted in Cell 2DW, test results in cell 1BN were examined. As previously discussed in this report, the injector critical pressure drop has been defined at 27.4 psi for saturation pressures of 50 psi. Additional data has been examined from tests on injector E2CE-133 with saturation pressures of 140 psi. This data is plotted in Figure I-34 and again when compared to the 50 psi saturation data shows an increase in critical pressure drop; again the increased duration football is noted with increased saturation pressure.

1BN
MAIN LINE FEED SYSTEM
FUEL
ALTITUDE CHAMBER WALL
INLINE FILTER
CIRCULATION RETURN
116"
47"
22.5"
141"
72"
33"
23"
28"
1/2" LINE (4)
BIPROP INLET
CIRCULATION RETURN
TANK FILTER
4"
FUEL SYSTEM
15"
0"
8"
8"
1.5" LINES FROM TANK TO STAND ANNIN
1.25" LINES FROM STAND ANNIN TO BIPROP
*NOTE: TROMBONE LINES - 0.5"

FIGURE I-25

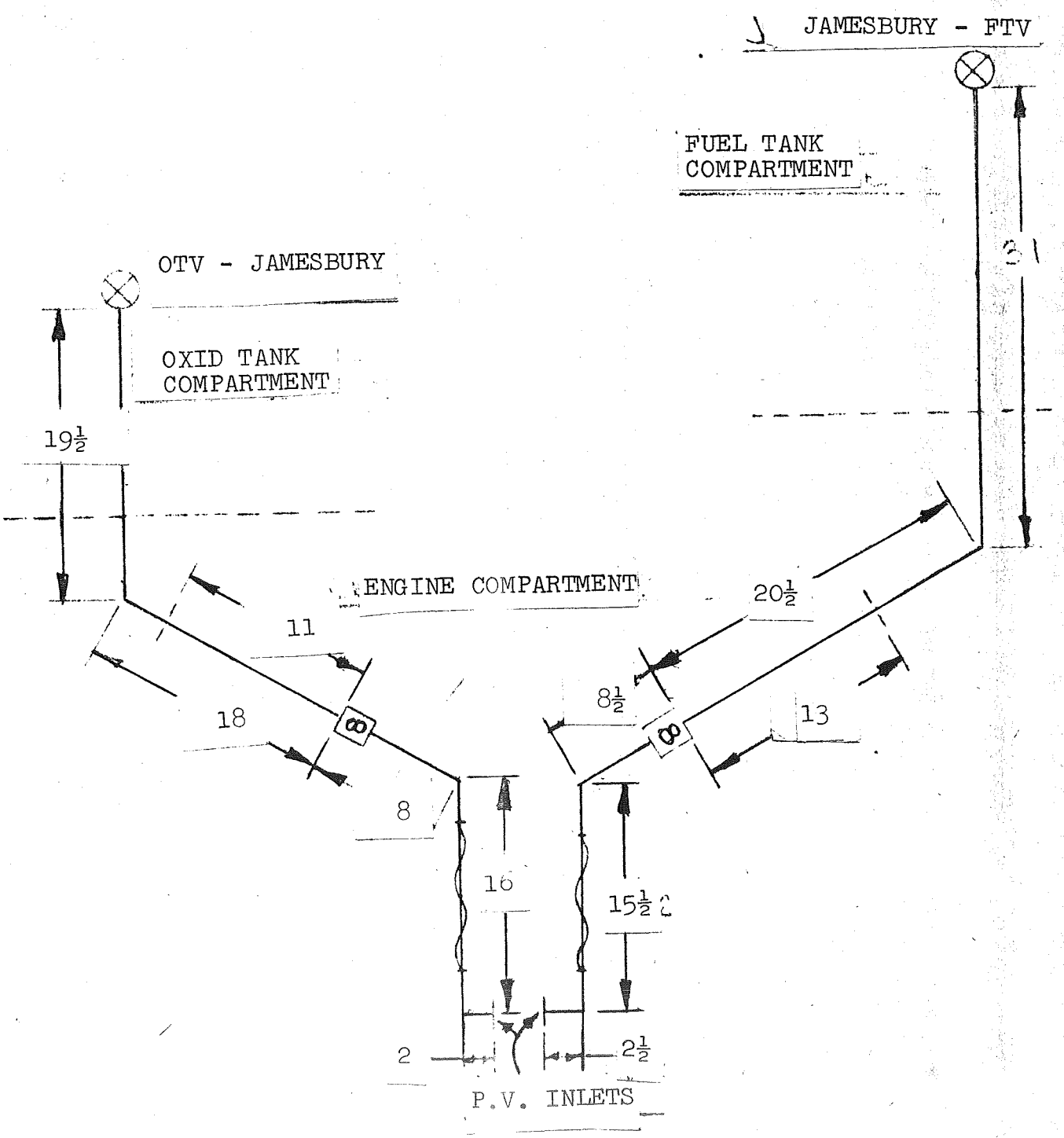
2DW - 1-1/4"
FEED LINE LENGTHS
JAMESBURY - FTV
FUEL TANK
COMPARTMENT
OTV - JAMESBURY
OXID TANK
COMPARTMENT
19½
ENGINE COMPARTMENT
11
18
8
8
20½
8½
13
8
16
15½
2
2½
P.V. INLETS

FIGURE I-26

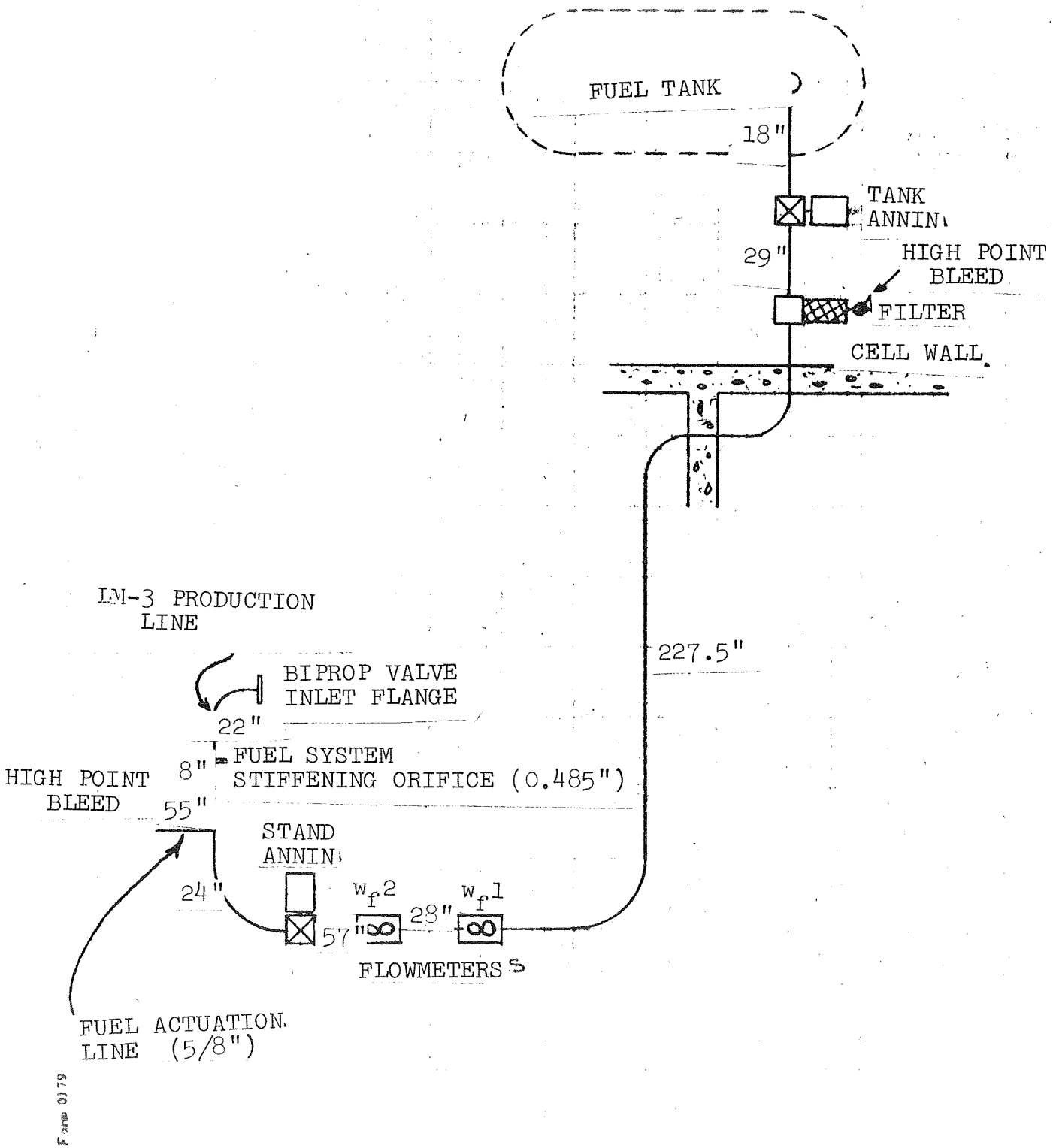
2BE
1.5" MAIN FUEL FEED
LINE (FROM SOURCE TANK
TO BIPROP VALVE INLET)
FUEL TANK
18"
TANK
ANNIN
29"
HIGH POINT
BLEED
FILTER
CELL WALL
LM-3 PRODUCTION
LINE
227.5"
BIPROP VALVE
INLET FLANGE
22"
FUEL SYSTEM
STIFFENING ORIFICE (0.485")
HIGH POINT
BLEED
8"
55"
STAND
ANNIN
24"
$w_f 2$
$w_f 1$
28"
57"
FLOWMETERS
FUEL ACTUATION
LINE (5/8")

FIGURE I-27

3DE FUEL FEED SYSTEM

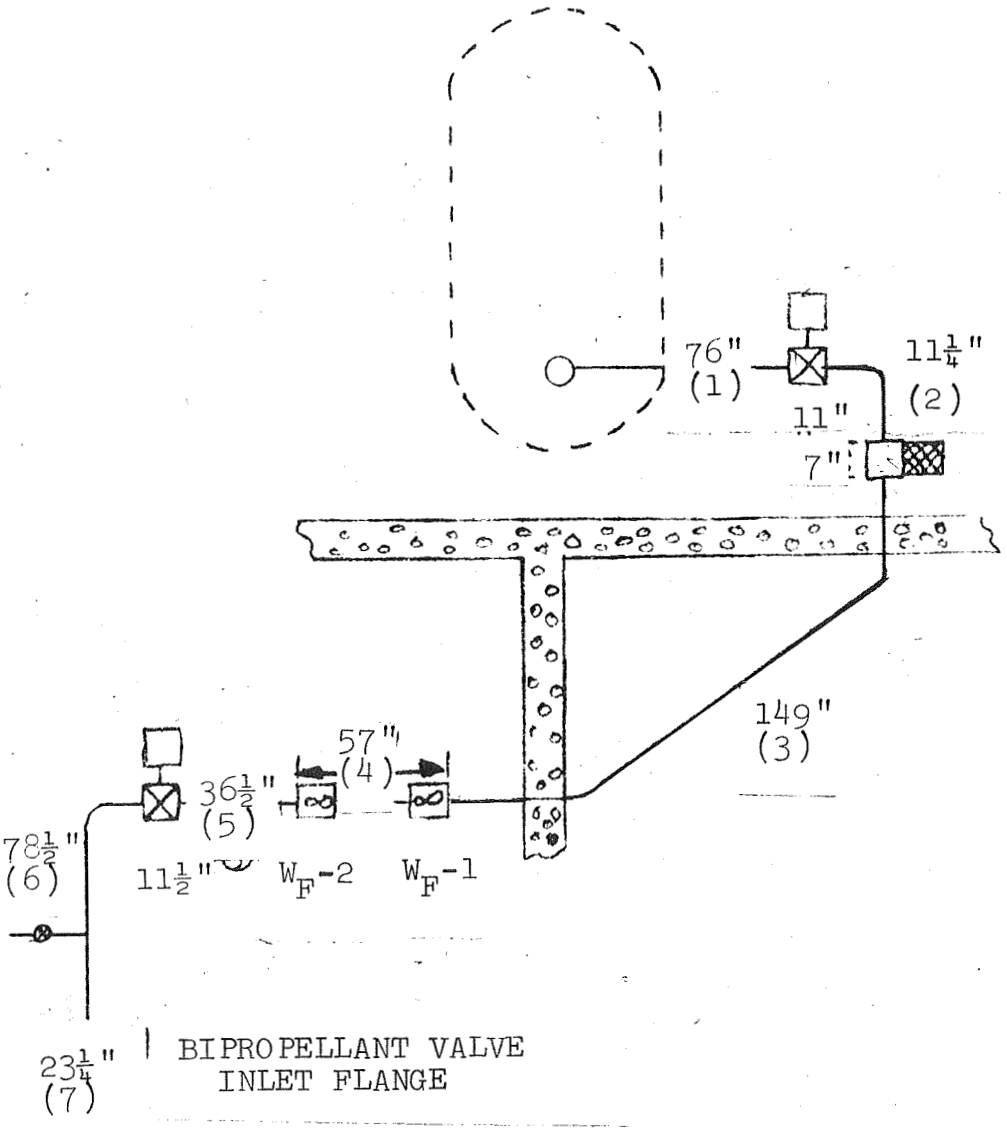

(1)	TANK TO TANK ANNIN	2½" LINE
(2)	TANK ANNIN TO FILTER	1½" LINE
(3)	FILTER TO W_F-1	1½" LINE
(4)	W_F-1 TO W_F-2	1½" LINE
(5)	W_F-2 TO STAND ANNIN	1½" LINE
(6)	STAND ANNIN TO HI-PT.	1¼" LINE
(7)	HI-PT. TO BIPROP INLET	1¼" LINE

FIGURE I-28

CELL 3DW FEED SYSTEM

NOTE:

a. Line size from tank outlets to stand annins are 1-1/2" 0.065" wall

b. Line size stand annins to bipropellant valve 1-1/4" 0.049 wall

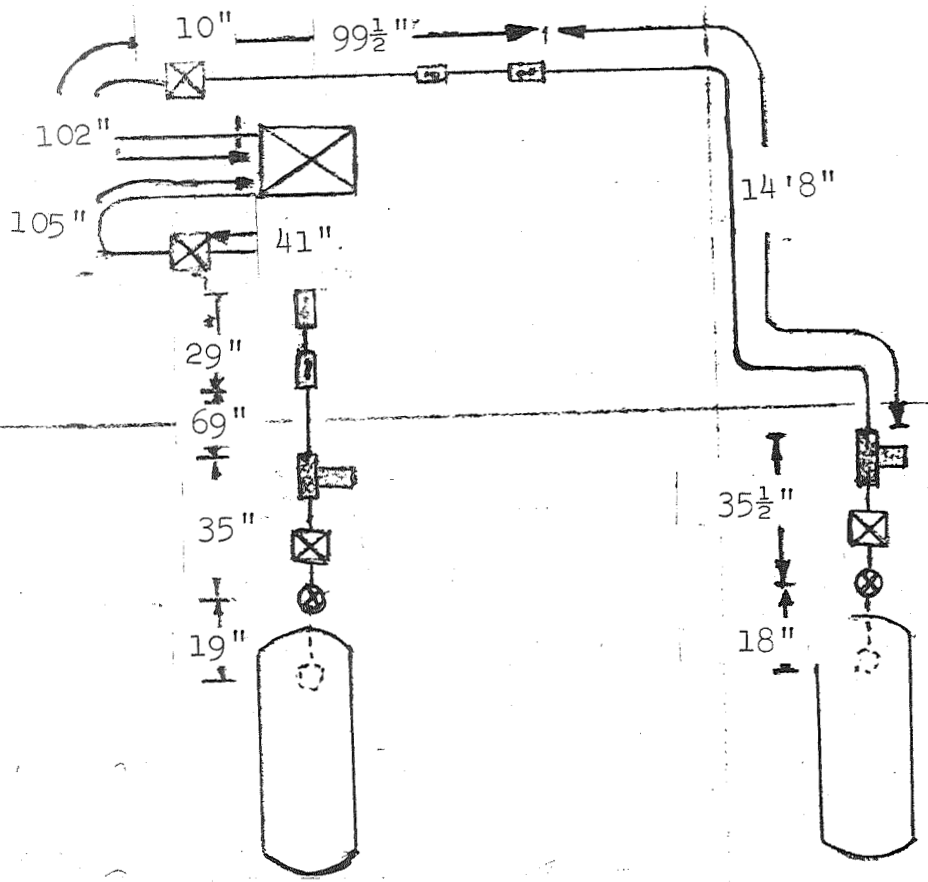

FIGURE I-29

FIGURE I-30

FIGURE I-31

FFP RECOVERY TIME @ RATED
$\dot{W}_{TRANSIENT}/\dot{W}_{STEADY\ STATE}$ (@ RATED)
INJECTOR FUEL $\Delta P_{CRITICAL}$
FFP RECOVERY TIME
CELL
$\Delta P_{CRIT.}$
RECOVERY TIME
3DW 33.8 0.332
3DE 37.6 0.330
2BE 33.6 0.510
2DW 32.8 0.300
1BN 27.4 0.249
CELL
$\Delta P_{CRIT.}$
$\dot{W}_T/\dot{W}_{SS}$
3DW 33.8 184.0
3DE 37.6 173.8
2BE 33.6 163.1
2DW 32.8 190.0
1BN 27.4 216.5

FIGURE I-32

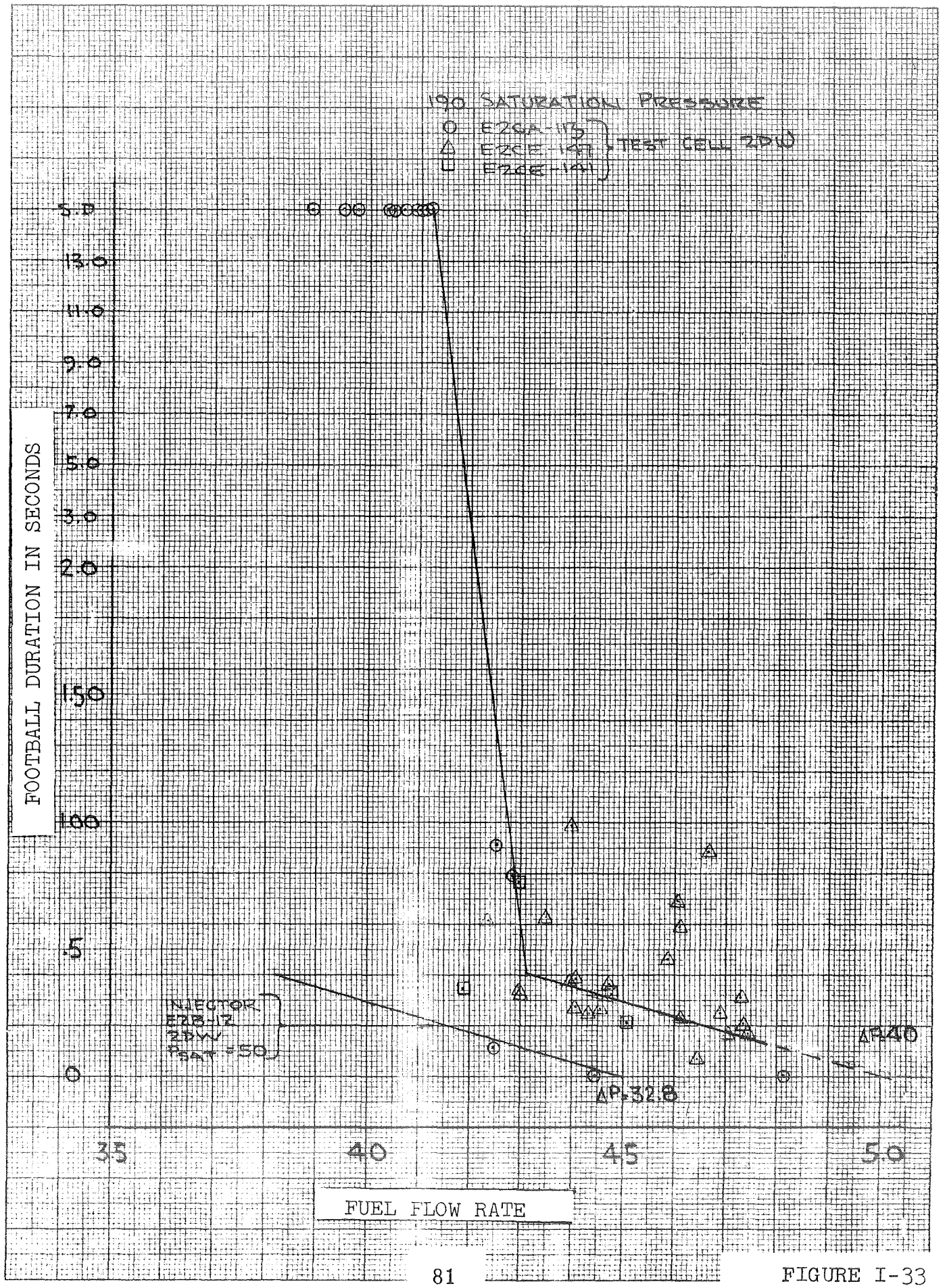

FIGURE I-33

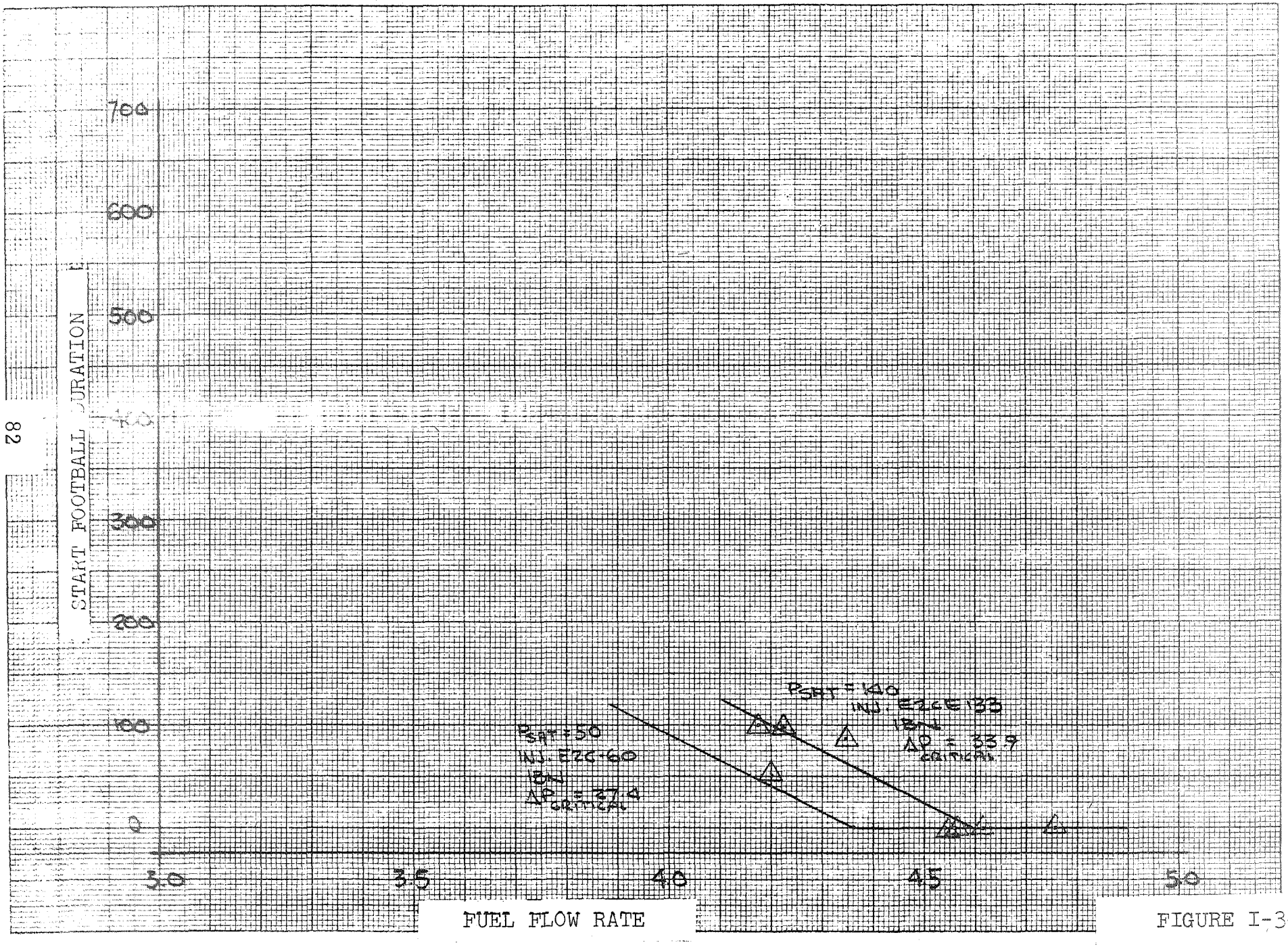

FIGURE I-34

D. REVIEW AND ANALYSIS OF FIRE TEST DATA IN TEST CELL 2DW WITH INJECTOR E2B-12

During May and June of 1967, an extensive test program, Table 9, was conducted with injector E2B-12 in test cell 2DW at Bell Test Center. The objective of the test program was to determine the operating parameters required to eliminate footballs. Review of this data has revealed the following information:

1. Post Start Footballs

During this test program there were no post start or sustained footballs noted. Figure I-35 is a plot of fuel flowrate vs. post start football duration. From this figure we can see that no post start footballs were ever noted even at fuel flowrates as low as 3.68 lb/sec of fuel (equivalent to injector $\Delta P=19.9$). However, it should be noted that the maximum pressure and temperature used to saturate the propellants was 80 psi and 100°F. The H_e in solution at this pressure and temperature is still less than the propellant is capable of absorbing at the feed pressure required for the 3.68 lb/sec fire test (FFP = 143.8) and 70°F temperatures. Thus, a dependency of saturation level or condition on critical pressure drop is clearly apparent.

2. Start Footballs

Following the first few fire tests, start footballs were noted on all runs at nominal and low pressure. These footballs were noted even with many changes to the test cell and engine hardware. These changes were as follows:

a. Orifices removed from feed system (20 psi at rated)

b. Orifices removed from engine (16 psi at rated)

c. Large throated thrust chamber

Figure I-36 is a plot of fuel flowrate vs. start football duration. The data plotted shows that the above noted changes had no effect on the football "breakpoint" or the duration. It is interesting to note that the injector pressure drop at the "breakpoint" fuel flow is equal to 29.9 psi which is approximately the same as noted in A (32.8). The lower breakpoint may be due to the reduced saturation level.

3. Helium Injection

During this test series, several tests were conducted with H_e being injected into the oxidizer and fuel feed systems. For the tests analyzed the H_e injection pressure was constant.

a. H_e Injection into Fuel Feed Line

Figure I-37 is a plot of fuel feed pressure vs. football duration. This plot shows that H_e injected into the fuel feed system will create a football and that the duration of the football appears to be dependent on the feed pressure. Footballs created by injecting H_e were very repeatable at the low feed pressure, however, as the feed pressure increased the duration of the football decreased. It is very possible that as the feed pressure increases both the H_e quantity injected decreases and more helium goes into solution. Figure I-38 which is a plot of fuel flow and fuel feed pressure vs. run time shows that at approximately 4.0 seconds the flow and pressure were disturbed. This is the time that the H_e was injected.

b. H_e Injected into Oxidizer Feed Line

Figure I-39 is a plot of oxidizer feed pressure vs. football duration. As can be seen no footballs were noted during H_e injection. Figure 24 is a plot of oxidizer flow and feed pressure is run time. The H_e was injected into the oxidizer at approximately 7.0 seconds. The perturbations noted on Run 124 at 4.0 seconds are due to H_e being injected into the fuel.

c. Tentative

1. The saturation level of the propellant appears to be the prime factor in producing post start footballs.

2. Start footballs are a function of injector pressure drop.

3. The fuel side of the injector is sensitive with respect to producing footballs.

4. H_e content in the oxidizer within the range tested has no significant effect on footballs.

5. The absolute value of chamber pressure.

GAS ENTRAPMENT TESTING FOR LOW FREQUENCY OSCILLATIONS

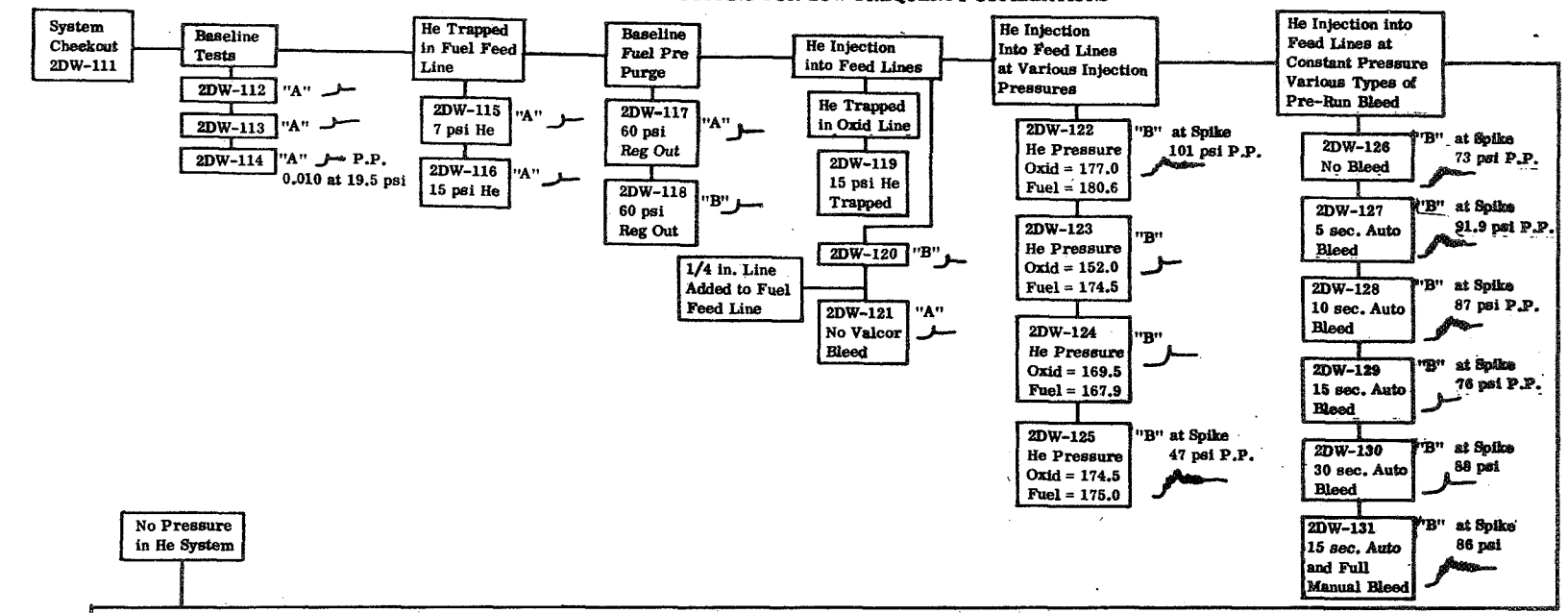

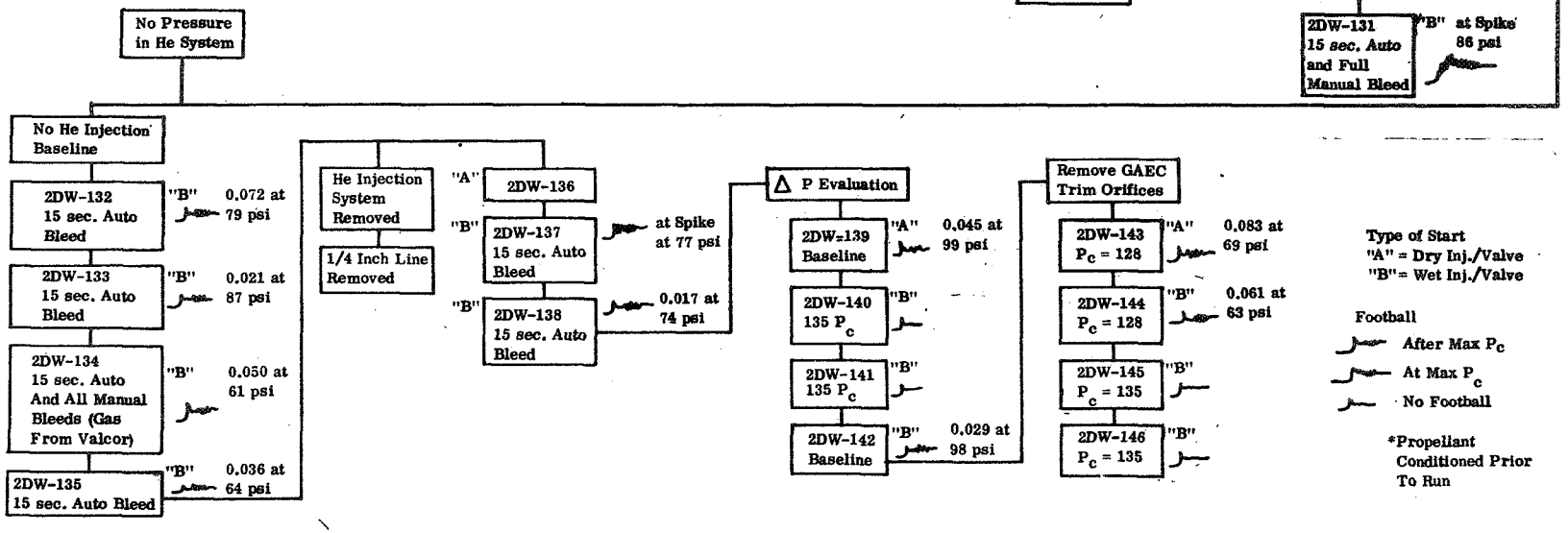

BAC 0345 Rev. 1248

Injector E2B-12/Valve 12 "Football Testing"

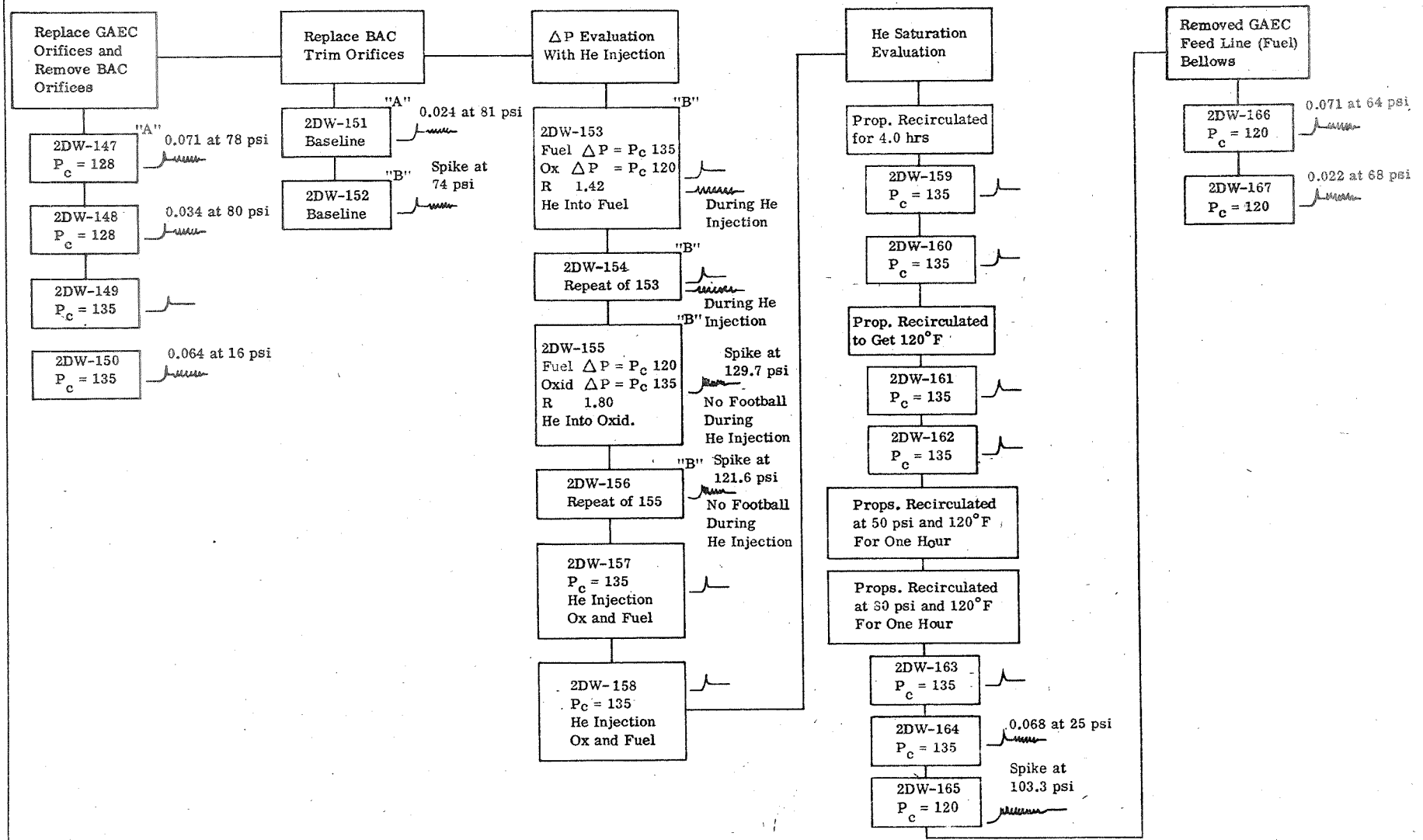

TABLE 9 (continued)

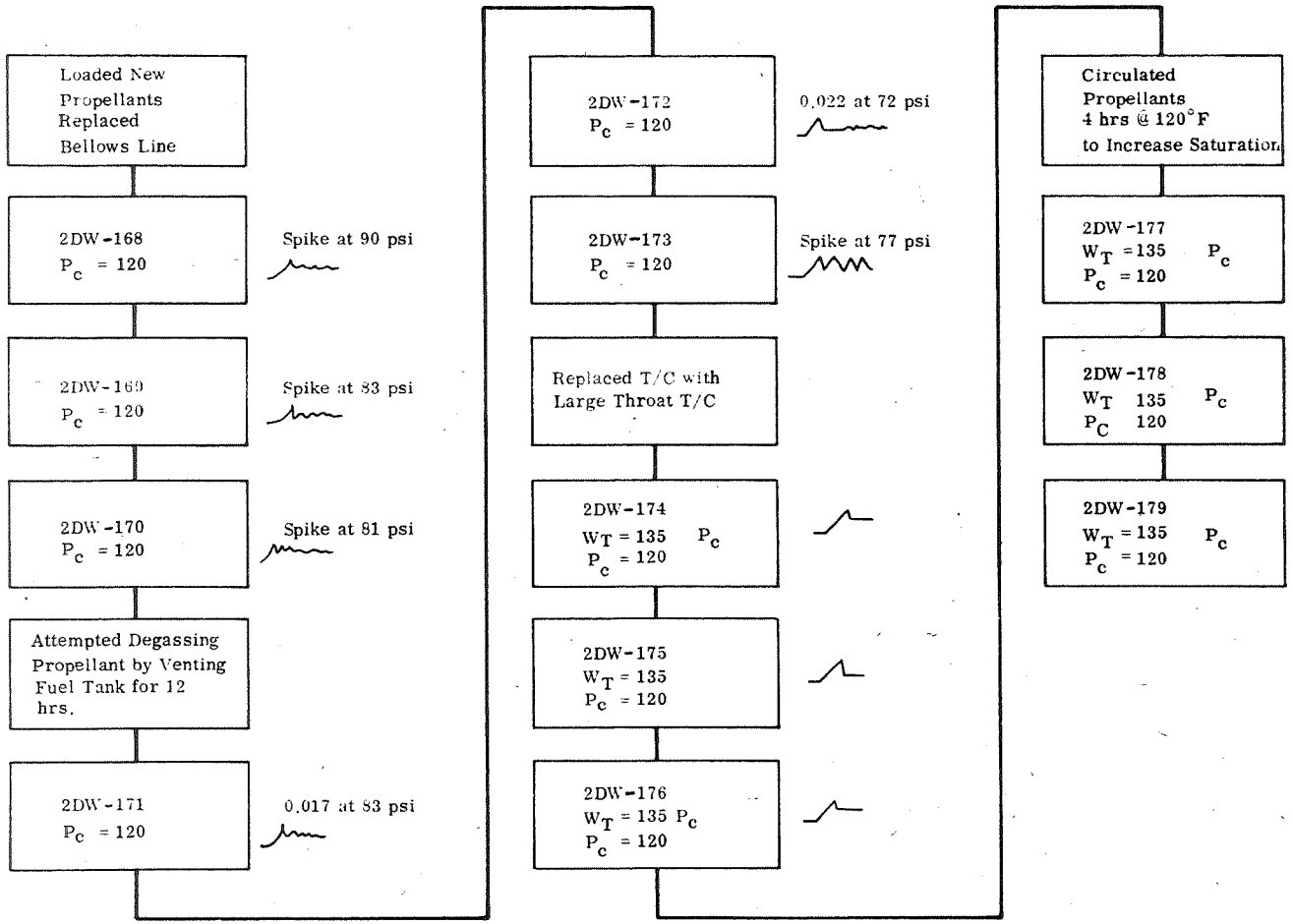

TABLE 9 (continued)

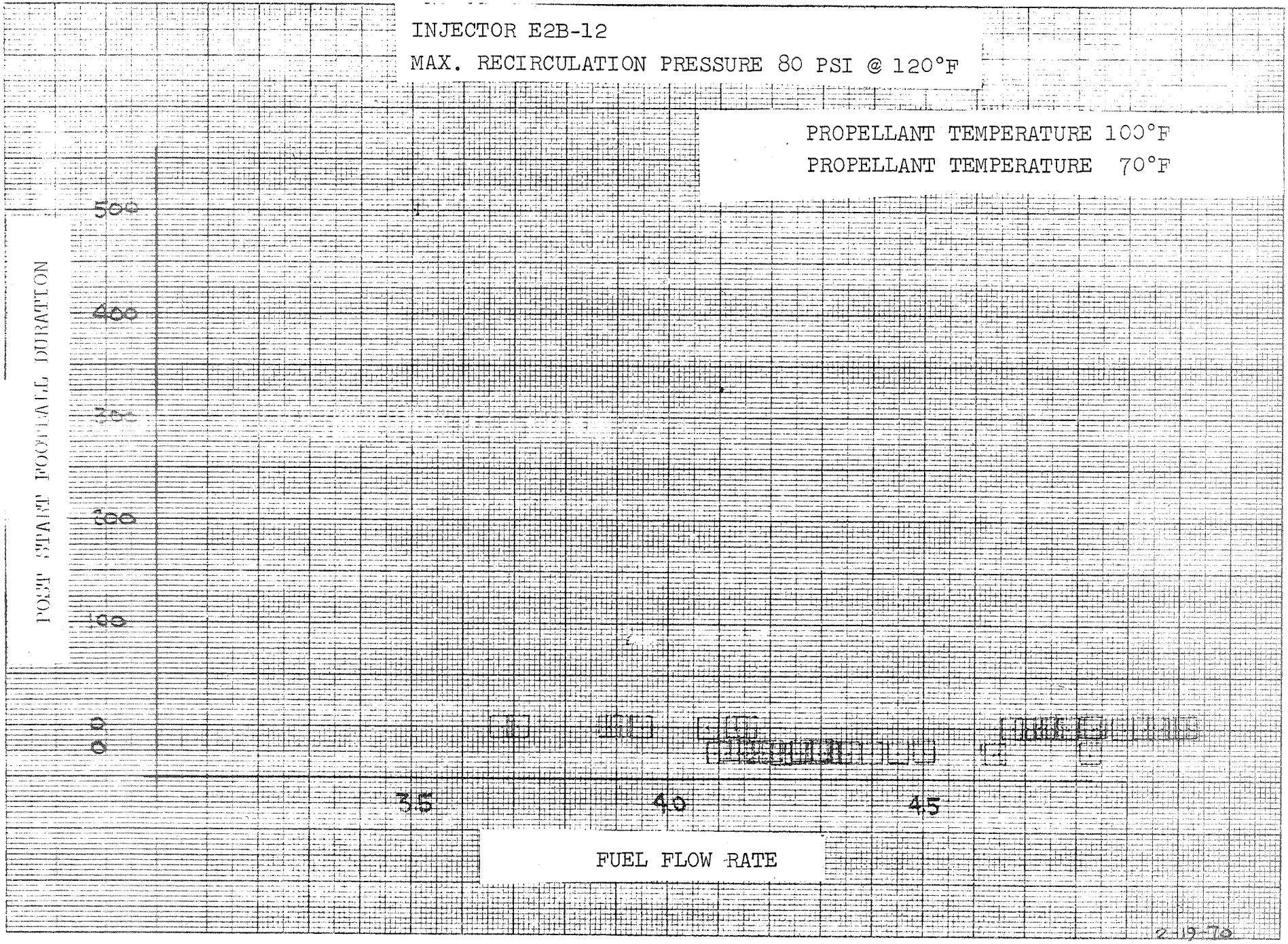
INJECTOR E2B-12
MAX. RECIRCULATION PRESSURE 80 PSI @ 120°F
PROPELLANT TEMPERATURE 100°F
PROPELLANT TEMPERATURE 70°F
POST SPLIT POST TAIL DURATION
500
400
300
200
100
0
35
40
45
FUEL FLOW RATE
2-19-70

FIGURE I-35

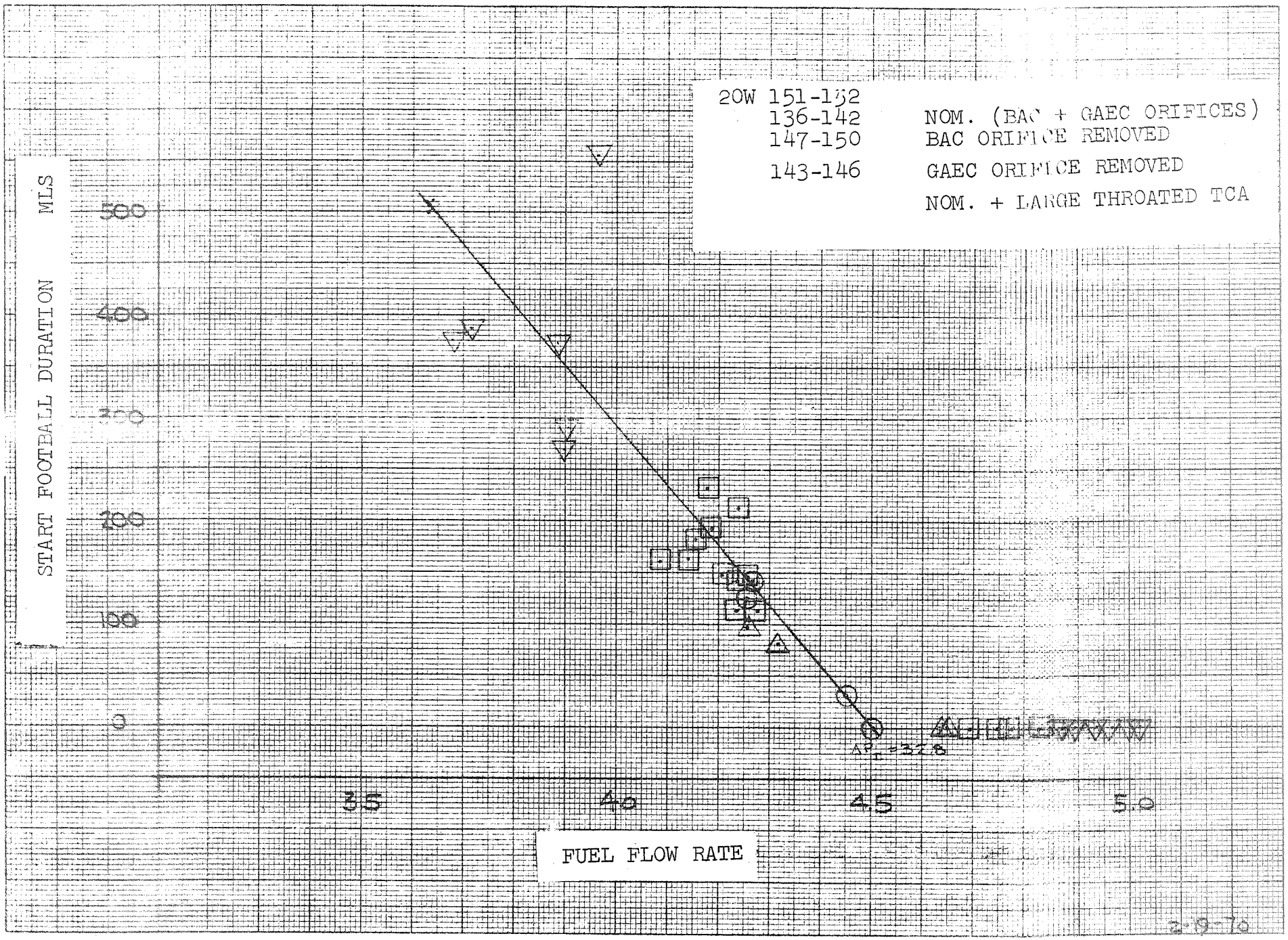

FIGURE I-36

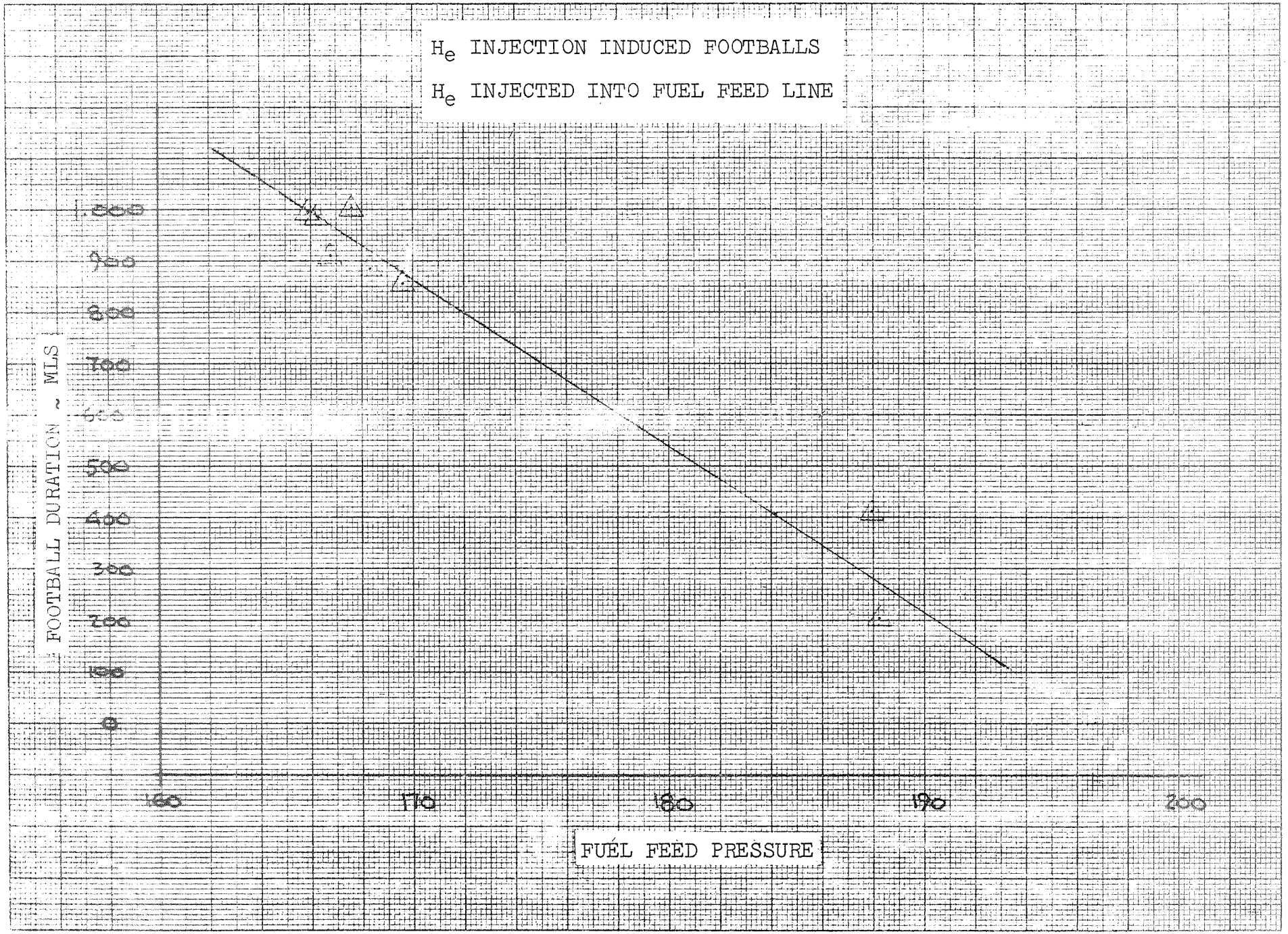

FIGURE I-37

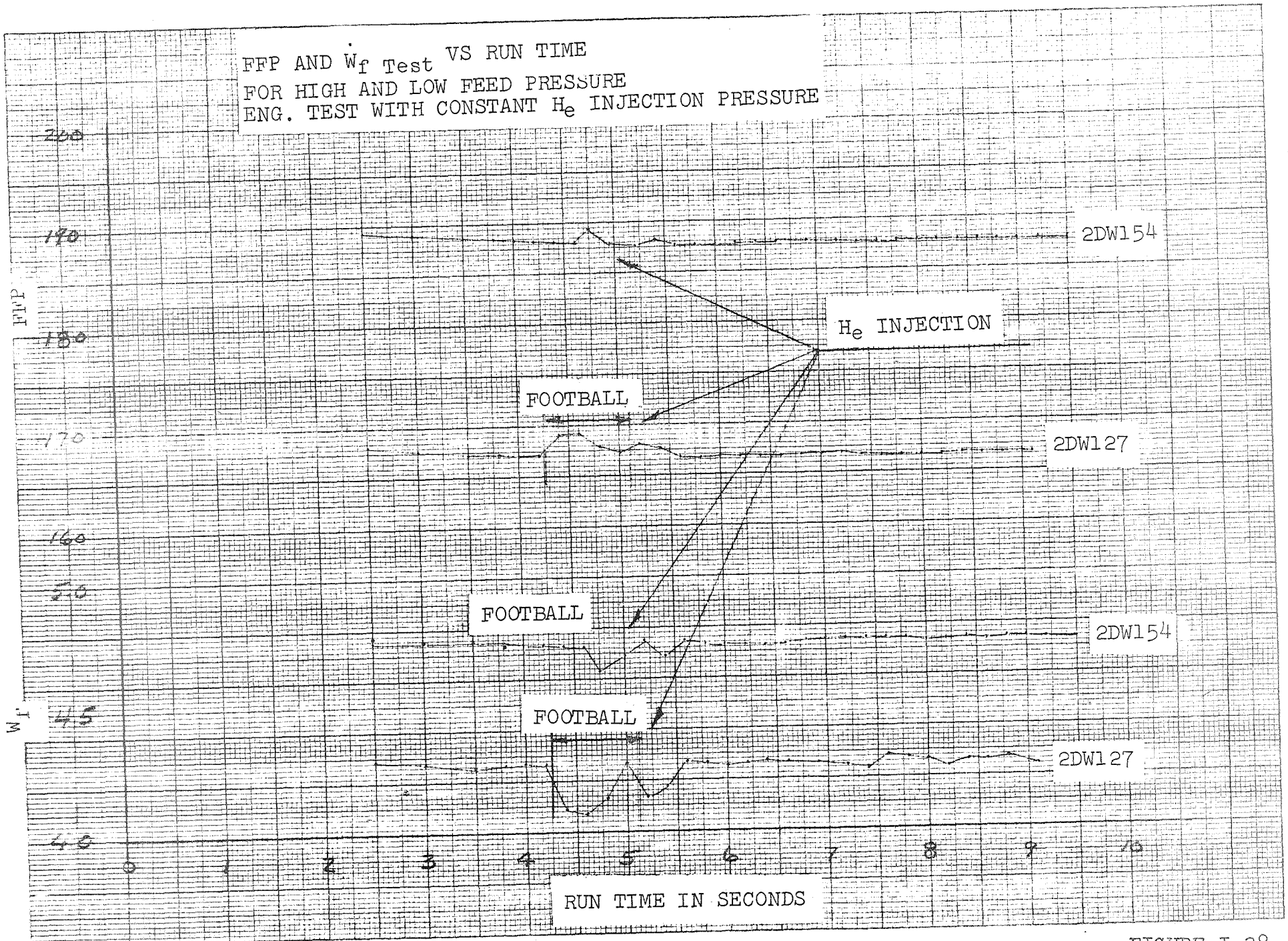

FIGURE I-38

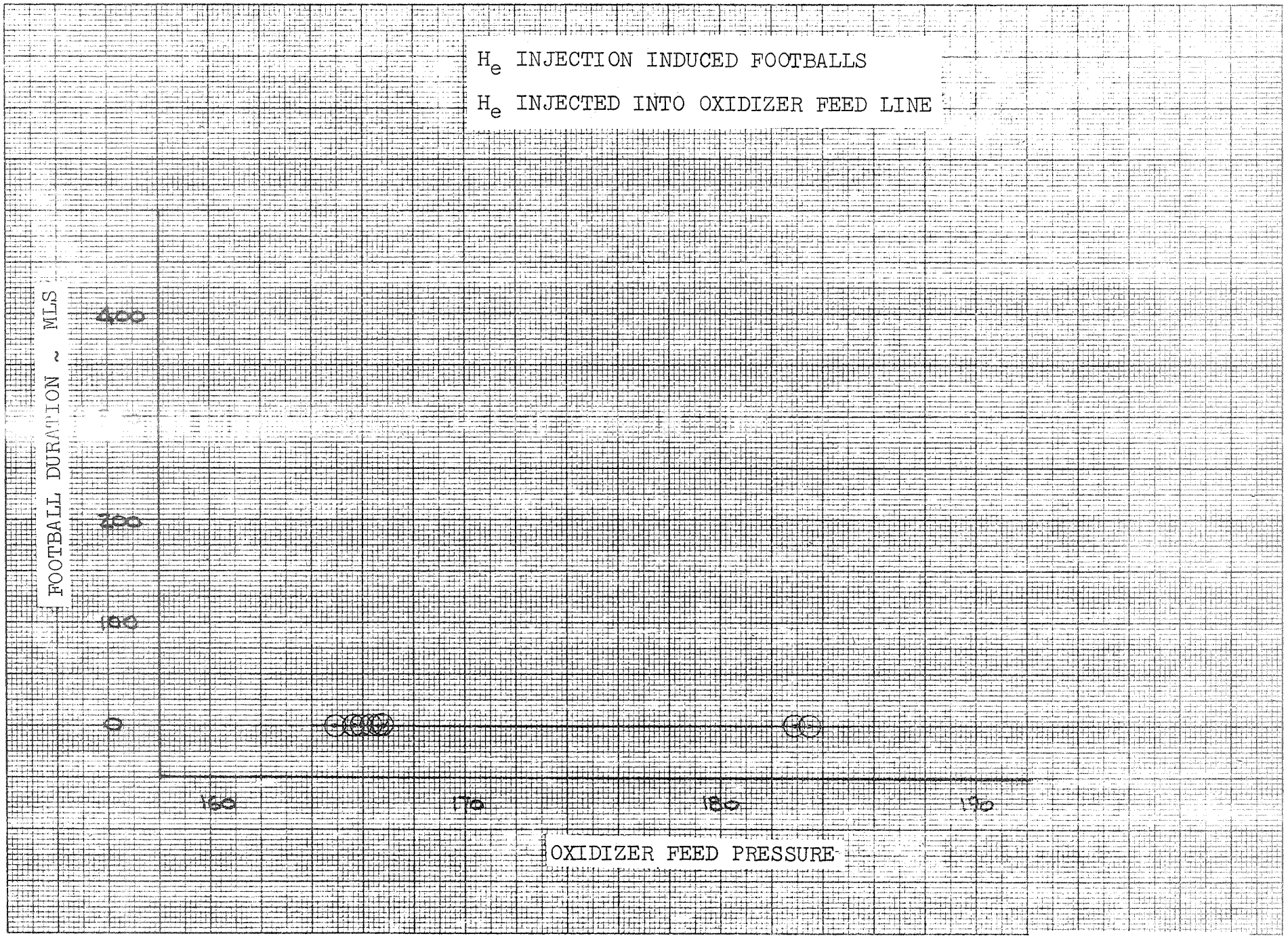

FIGURE I-39

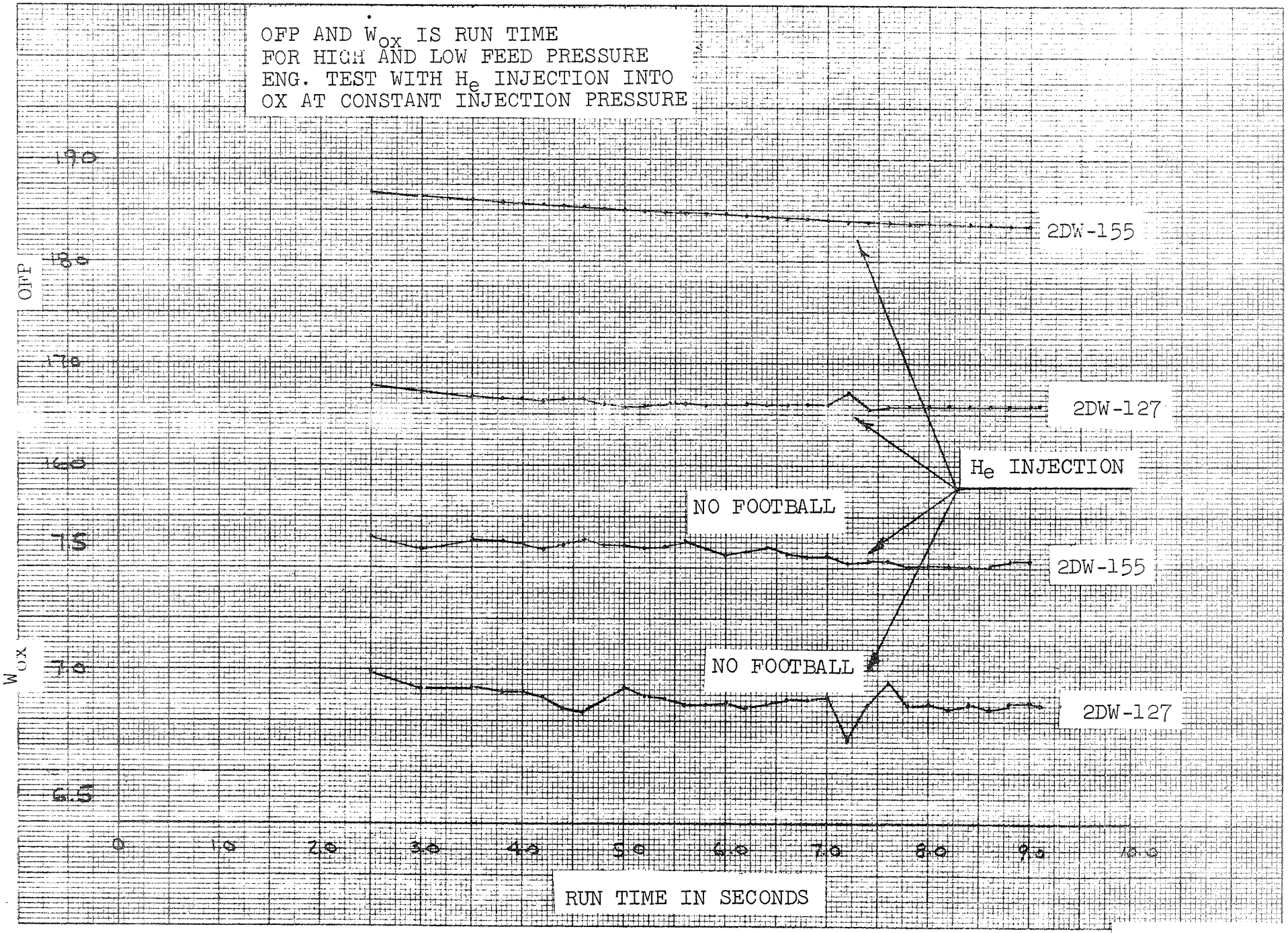

FIGURE I-40

APPENDIX II

TASK B - REVIEW AND ANALYSIS OF PHOTOGRAPHIC STUDIES

TASK B - REVIEW AND ANALYSIS OF PHOTOGRAPHIC STUDIES

The review and analysis of the photographic work conducted during the BAC-LM program has been conducted. This review was conducted on three specific tests; these tests were conducted with a single primary injector element consisting of two-fuel-on-one oxidizer orifice. Purpose of tests were:

1) Baseline - Impinging oxidizer and fuel jets with no helium in the propellant (Figure II-1).

2) Nominal 0.1 percent by weight of helium - Impinging oxidizer and fuel jets with helium injected into the fuel feed line upstream of the injector (Figure II-2).

3) Nominal 0.2 percent by weight of helium - Impinging oxidizer and fuel jets with helium injected into the fuel feed line upstream of the injector (Figure II-3).

It should be noted that the amount of helium injected into the fuel for tests 2 and 3 represents approximately 100 and 200 times respectively the amount of helium present in propellants saturated at 190 psi and 70°F.

The review conducted examined the film frame by frame, (the frames reviewed are shown in Figures II-1 thru II-3 in total 44 frames were examined for each case) for variations with respect to the baseline in the following areas:

1) Liquid Jets

   a) Pulsing or oscillation of the fuel jets
   b) Breakup or two phase flow
   c) Expansion and contraction of the jet

2) Impingement

   a) Variations in impingement point
   b) Blowapart
   c) Oscillations

3) Fan (post impingement area)

a) Pulsing or oscillation

b) Combustion retarding

Analysis of the films revealed the following:

1) Liquid Jets

a) With no helium injection, the liquid jets were relatively steady and non-pulsing. There was very little expansion or contraction of the jet.

b) With 0.1 percent helium, the liquid jets pulses and undergoes rapid local expansions and contractions (diameter changes). The jet itself on the average is smaller in diameter than the jet with no helium.

c) With 0.2 percent helium the liquid jets is steady and non-pulsing. However, the jet diameter is smaller than with 0.1 percent helium.

2) Impingement

a) With no helium injection, the impingement point has some variation. In order to define the mean and the amount of variation, a plot (Figure II-4) was made of the intersection of right side fuel jet with the oxidizer jet. The measurement was made from the injector face to the lower edge of the fuel jet. The mean reduced "impingement" point measured on the photographs for no helium injection was 0.120.

b) With 0.1 percent helium injection, the impingement variation (Figure II-5) is much greater than with no helium. The mean impingement point was calculated to be 0.152 which is about 25 percent higher than with no helium.

In order to determine if the impingement variation noted in Figures II-4 and II-5 contained any predominant frequency components an autocorrelation* function analysis was conducted on the data. Figures II-6 and II-7 show plots of this function. These plots would tend to indicate that the triplet with no helium injection oscillates in a random manner with no predominant frequency. However, the plots of 0.1 and 0.2 percent may indicate that a predominant frequency exists in this data. It should be noted that the data sample is too small to derive at any definite conclusions.

*The autocorrelation function is a Fourier transformation of the power density spectrum and thus defines the distribution of power in a signal according to the frequencies present.

3) Fan (Post Impingement)

a) With no helium injection the fan is very uniform. The breakup (appearance of light areas) and the combustion process appears to be very steady.

b) With 0.1 percent helium inspection the fan width is reduced and the breakup oscillates at approximately 100 cps.

Figure II-8 is a plot showing this oscillation in fan breakup.

c) With 0.2 percent helium the fan width is significantly increased over both no helium and 0.1 percent. Also the combustion process (appearance of light regions) appears to be retarded. This is conceivable due to a lack of rapid fan break-up.

In order to obtain a better definition of any predominate frequency that may be contained in the impingement of the no-helium and 0.1 percent helium cases additional frames of film were examined. For this analysis 200 frames, or approximately 0.5 seconds, were examined. The purpose of this analysis was to determine whether any predominant frequencies were apparent and how they might be related to the 1000 cps observed in the reaction zone luminosity. This might provide some insight as to whether the fuel jets themselves or the combustion are the driving force in maintaining periodic oscillatory low frequency oscillations.

A Fourier analysis of the axial impingement point variations vs time was made and the results are shown in Figure II-9. Although the noise background within the 0.1% helium spectrum precludes an unequivocal conclusion, it does appear that there is a significant difference between the no-helium and the 0.1% spectra. It also appears that a 400 cycle frequency and its harmonics are present.

Figure II-10 is a comparison of the frequency content of the impingement variation of a liquid jet with 0.1 percent helium compared to the frequency content of chamber pressure during a typical LFO. It is interesting to note the same frequencies are present.

CONCLUSION

Helium injection has a significant effect on the operation of the triplet element examined. This effect is noted in the liquid jet, the impingement point and the fan breakup. The effect noted in the impingement of the liquid jet would appear to have the same frequency content as a typical LFO.

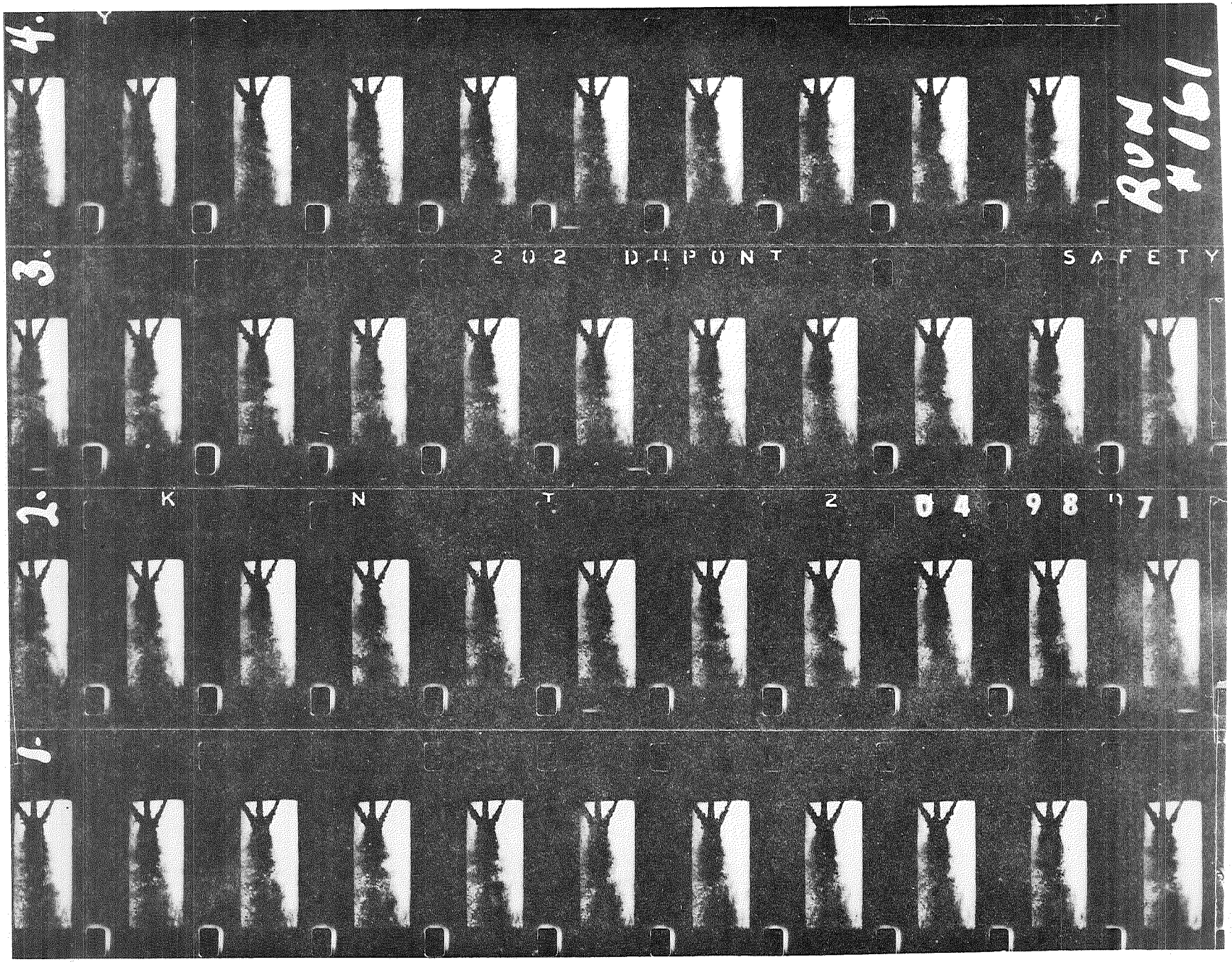

Figure II-1. E2C Tripled at Nominal Firing Conditions - 5400 Frames/sec - One Microsecond Exposure each Frame - Time Sequence Top to Bottom from Left to Right

R416

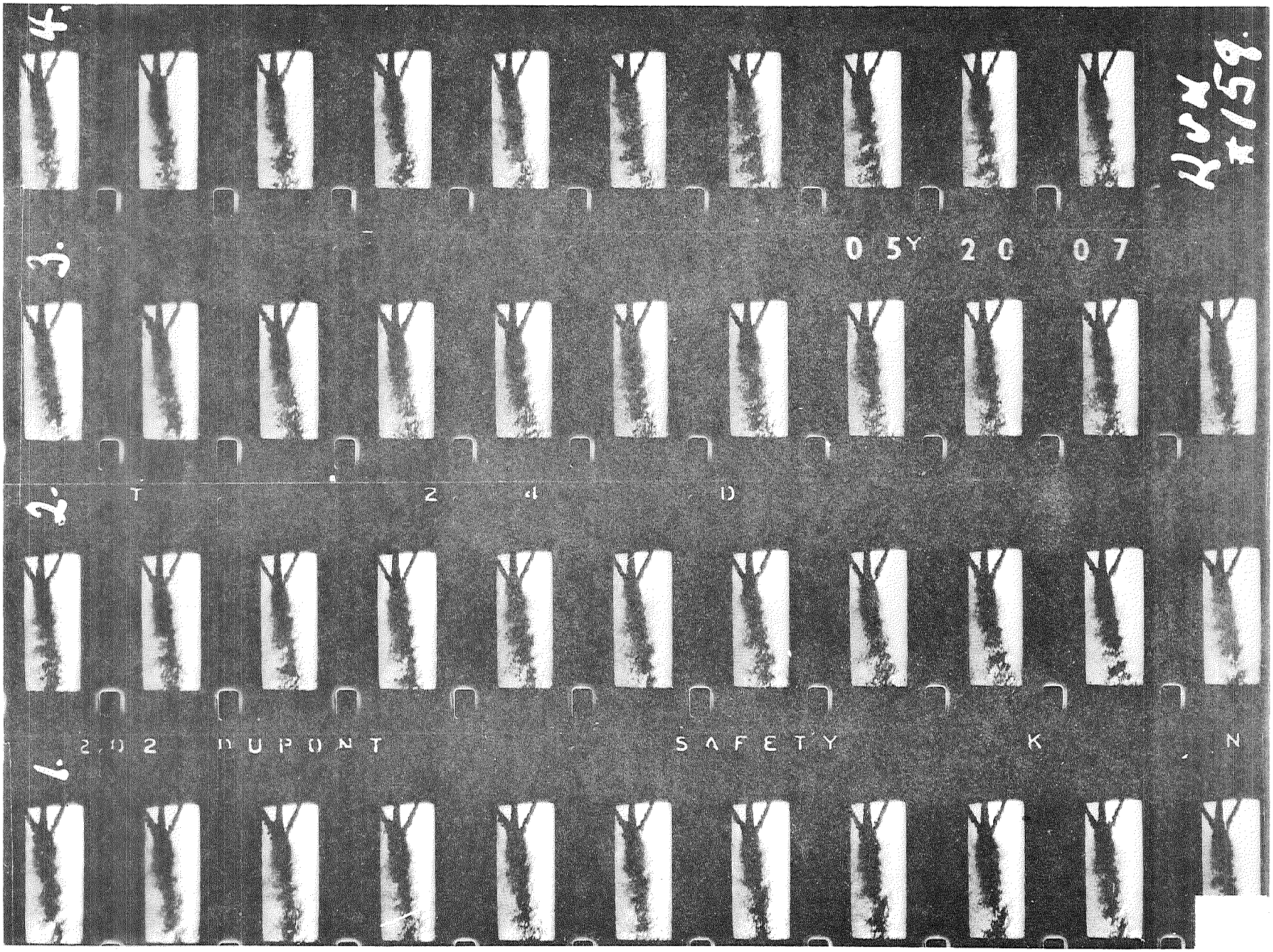

R417

Figure II-2. Same as Previous Figure Except Helium Injected into Fuel; 0.1 Percent Ratio of Weight Flow of Helium to Fuel Flow

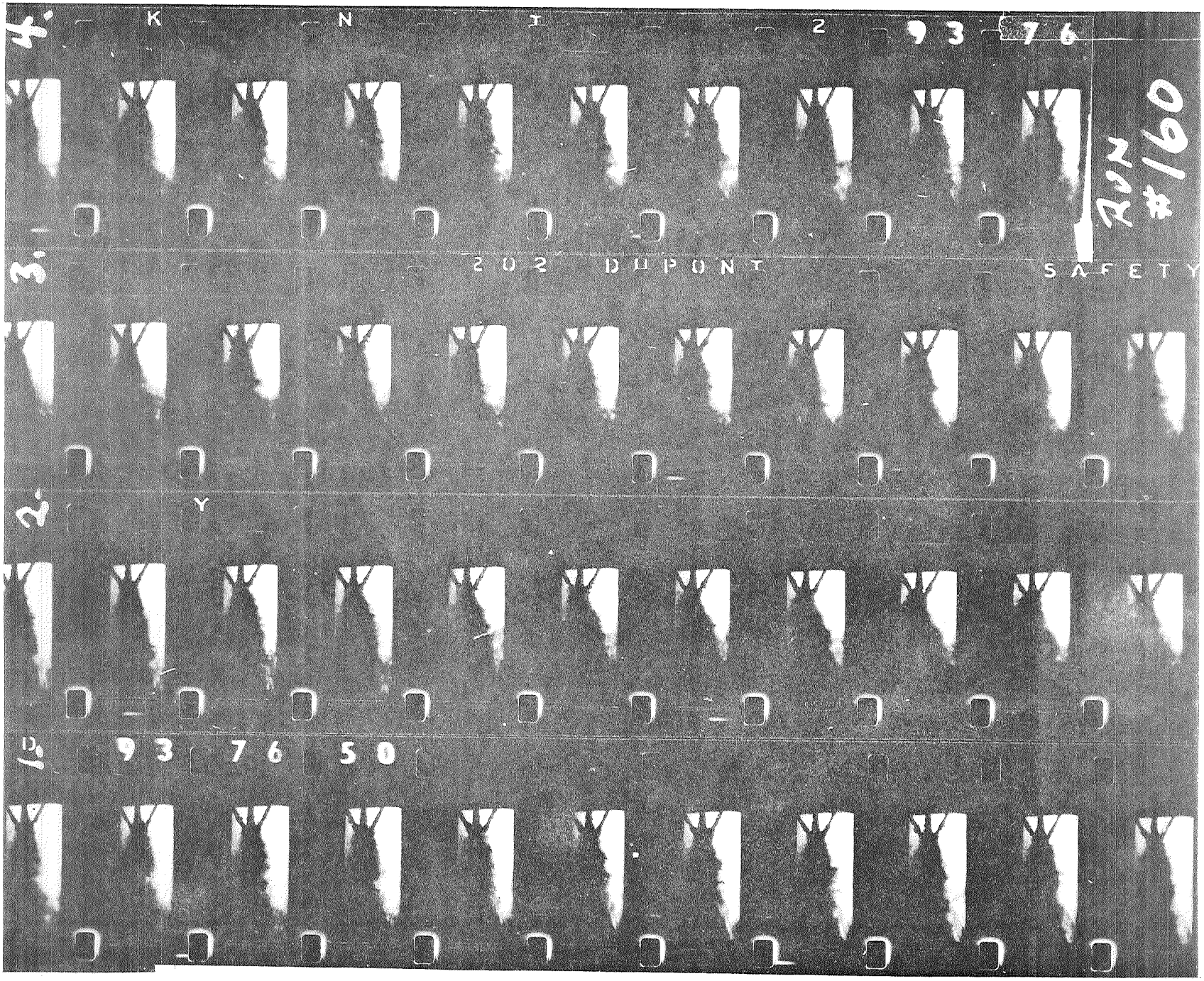

Figure II-3. Same as Previous Figure Except Helium Injector Injector Ratio is 0.2 Percent

R418

FIGURE II-4

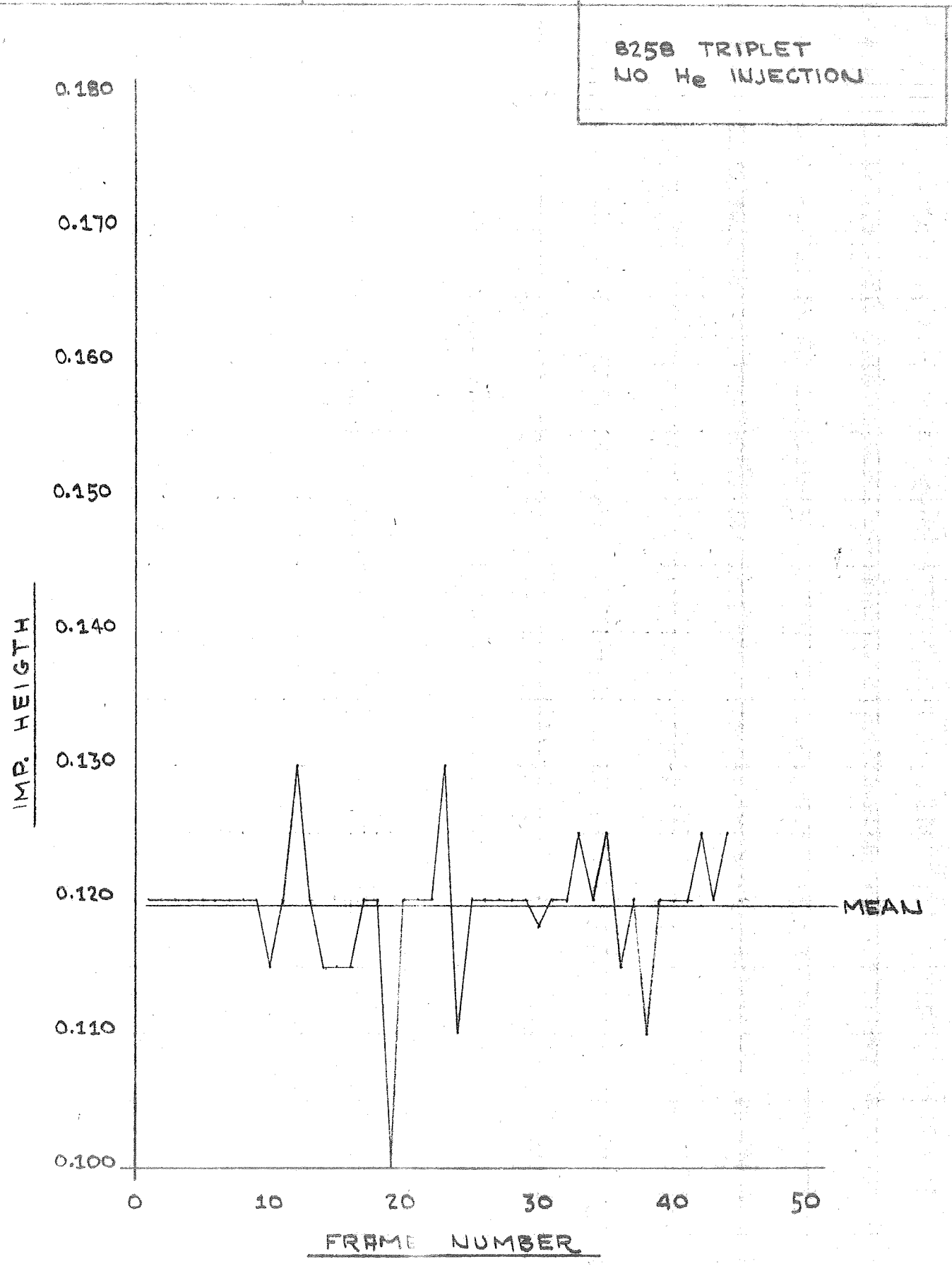
8258 TRIPLET
NO He INJECTION
0.180
0.170
0.160
0.150
0.140
0.130
0.120
0.110
0.100
IMP. HEIGTH
MEAN
0
10
20
30
40
50
FRAME NUMBER

FIGURE II-5

ORIFICE #1

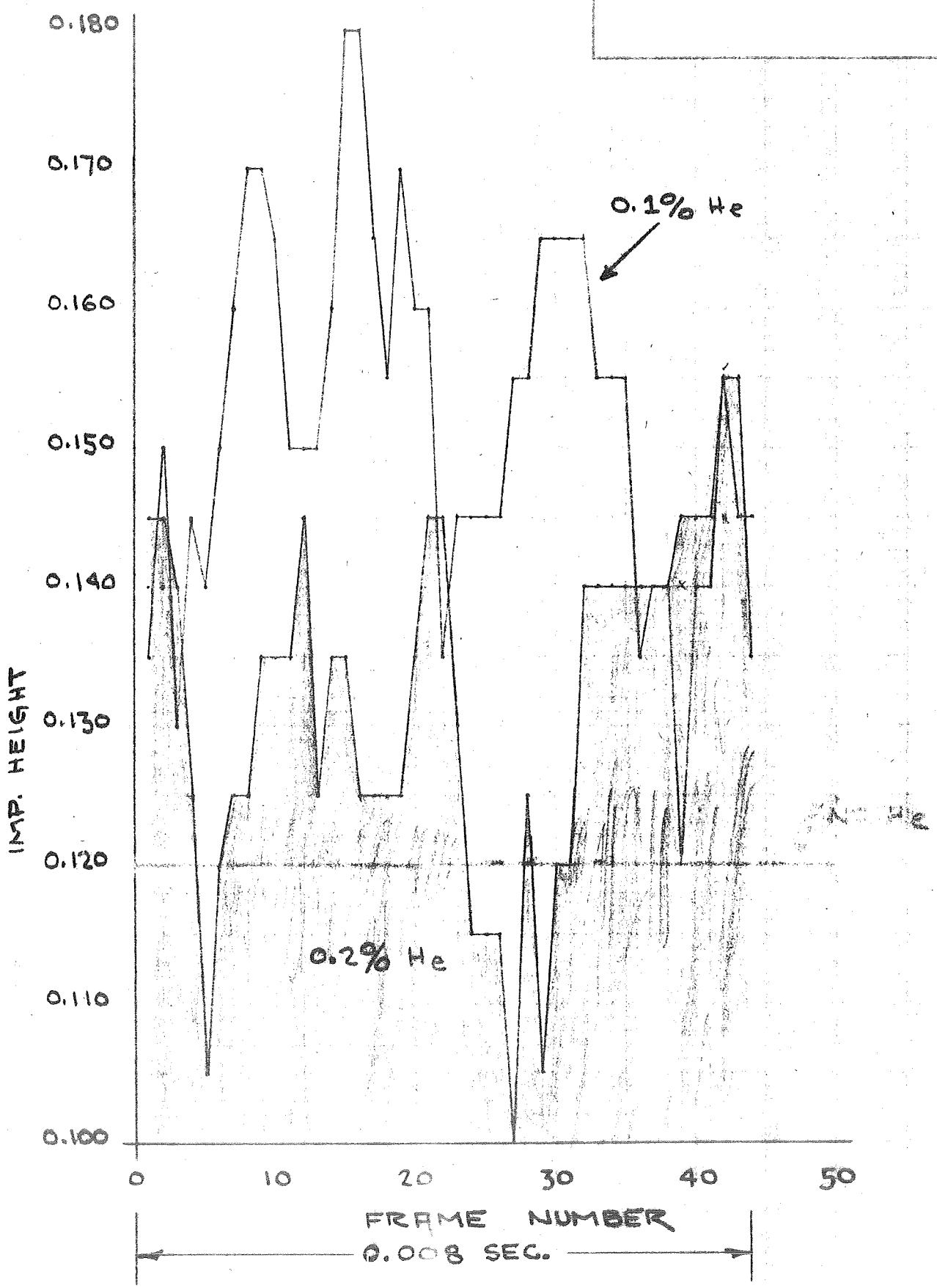

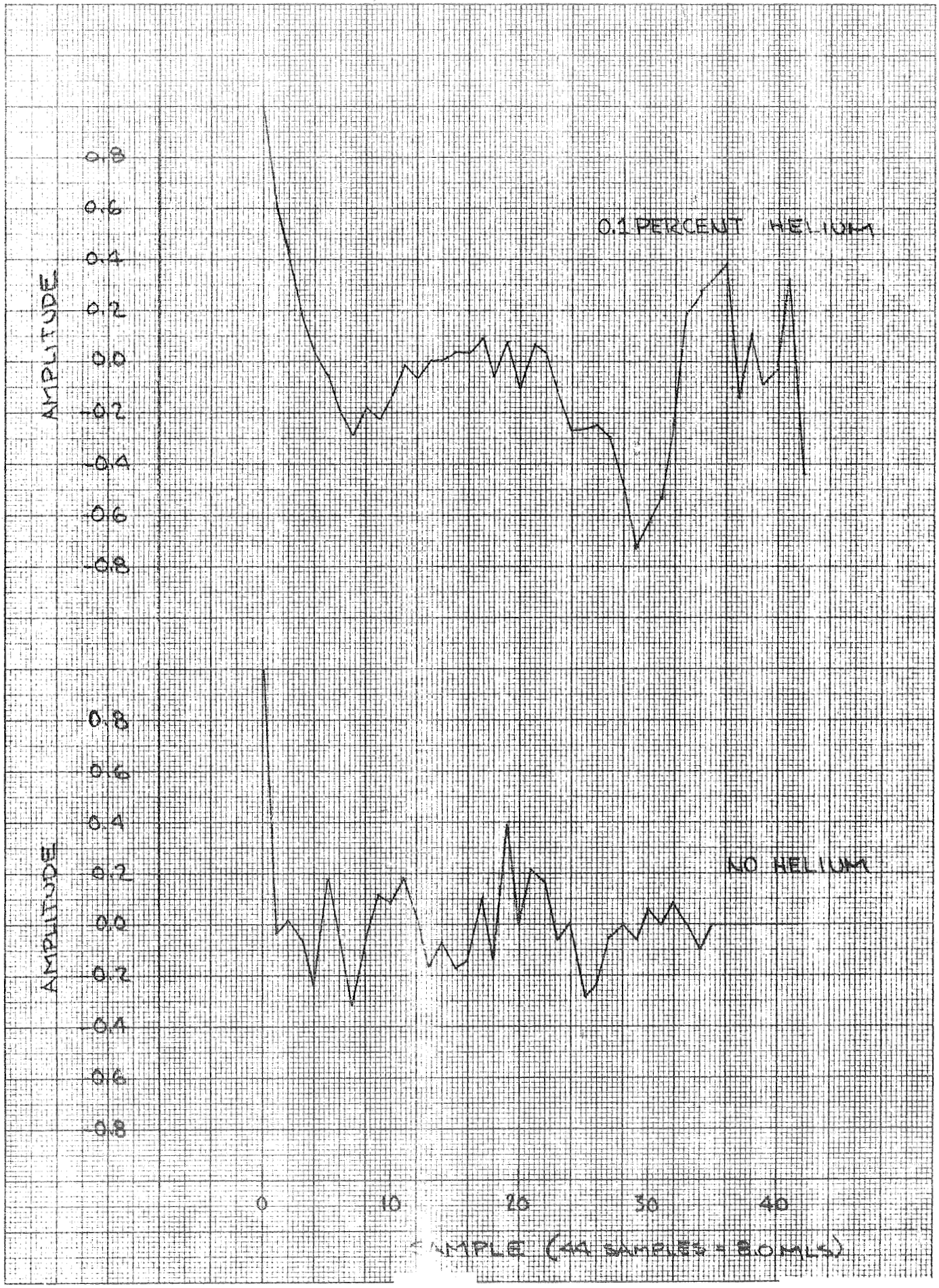
0.1 PERCENT HELIUM
NO HELIUM
AMPLITUDE
AMPLITUDE
0.8
0.6
0.4
0.2
0.0
-0.2
-0.4
-0.6
-0.8
0
10
20
30
40
SAMPLE (44 SAMPLES = 8.0 MILS)

FIGURE II-6

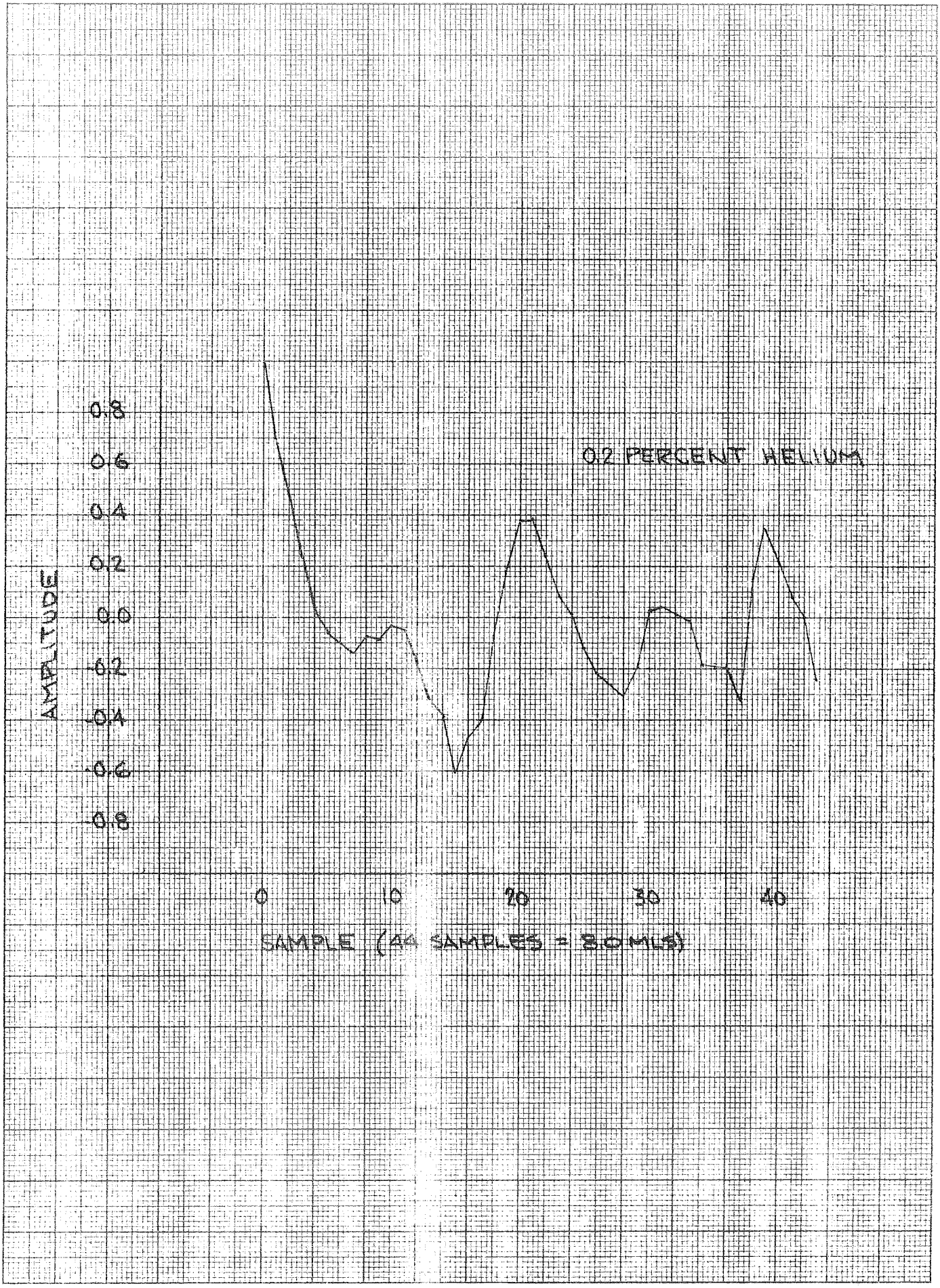
0.2 PERCENT HELIUM
AMPLITUDE
0.8
0.6
0.4
0.2
0.0
-0.2
-0.4
-0.6
-0.8
0
10
20
30
40
SAMPLE (46 SAMPLES = 80 MS)

FIGURE II-7

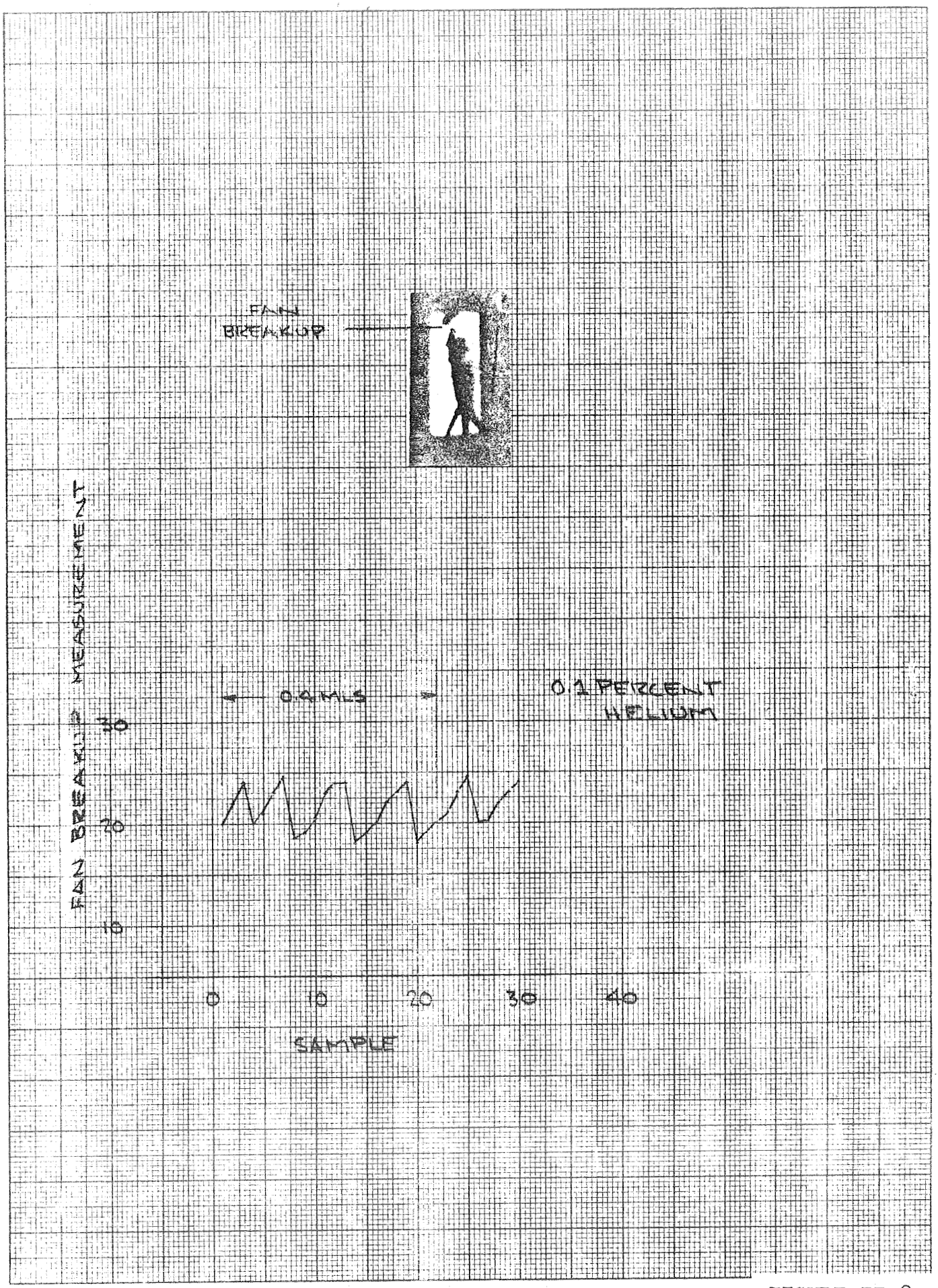
FAN BREAKOUT
FAN BREAKOUT MEASUREMENT
0.9 MLS
0.1 PERCENT HELIUM
30
20
10
0
10
20
30
40
SAMPLE

FIGURE II-8

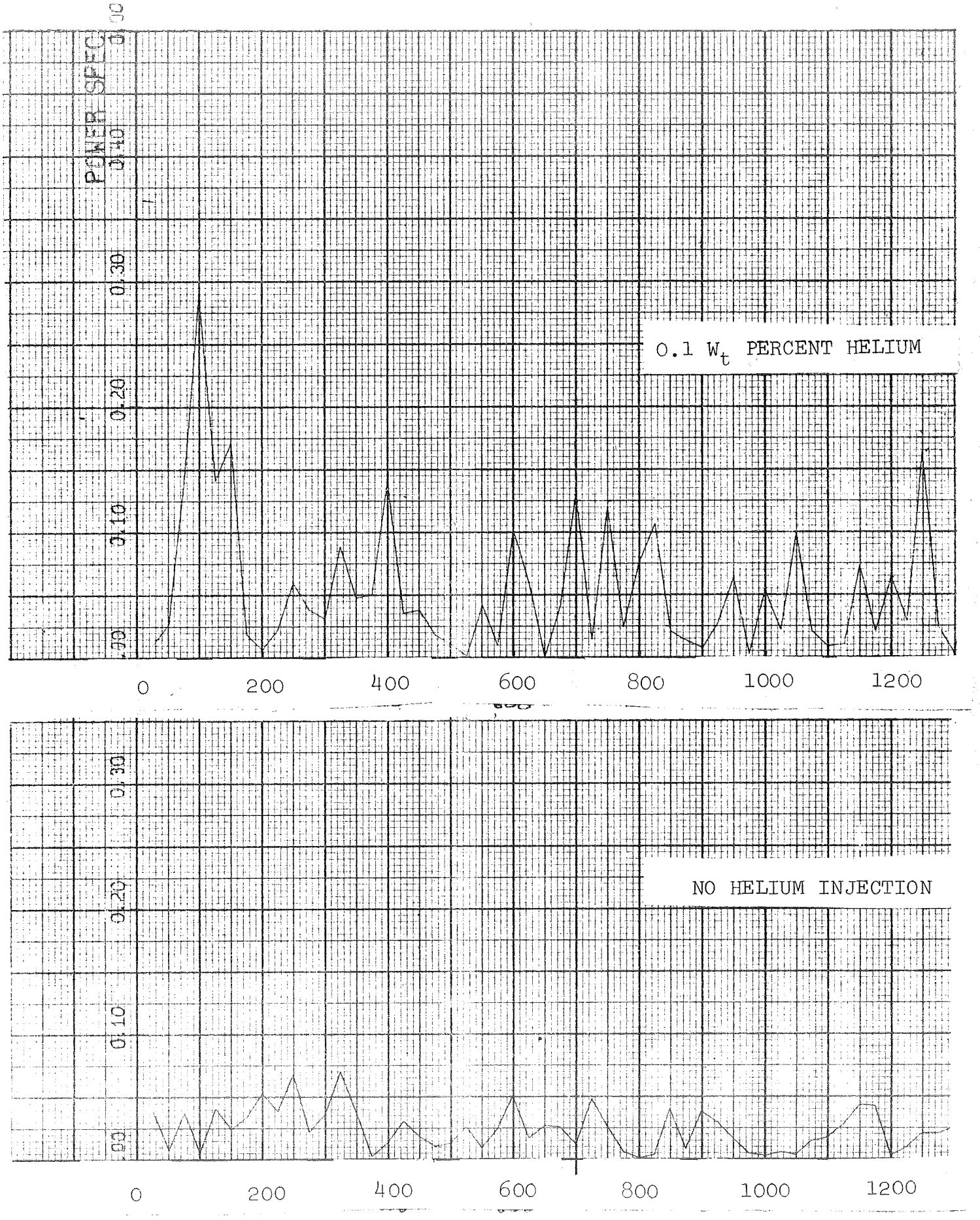
POWER SPEC
0.40
0.30
0.20
0.10
0.00
0.1 W_t PERCENT HELIUM
0
200
400
600
800
1000
1200
0.30
0.20
0.10
0.00
NO HELIUM INJECTION
0
200
400
600
800
1000
1200
FREQUENCY IN CPS

FIGURE II-9

VARIATIONS IN IMPINGIMENT HEIGHT (FROM PHOTOGRAPIC STUDIES)

AS COMPAIRED TO ENGINE CHAMBER PRESSURE (DEVELOPEMENT TEST)

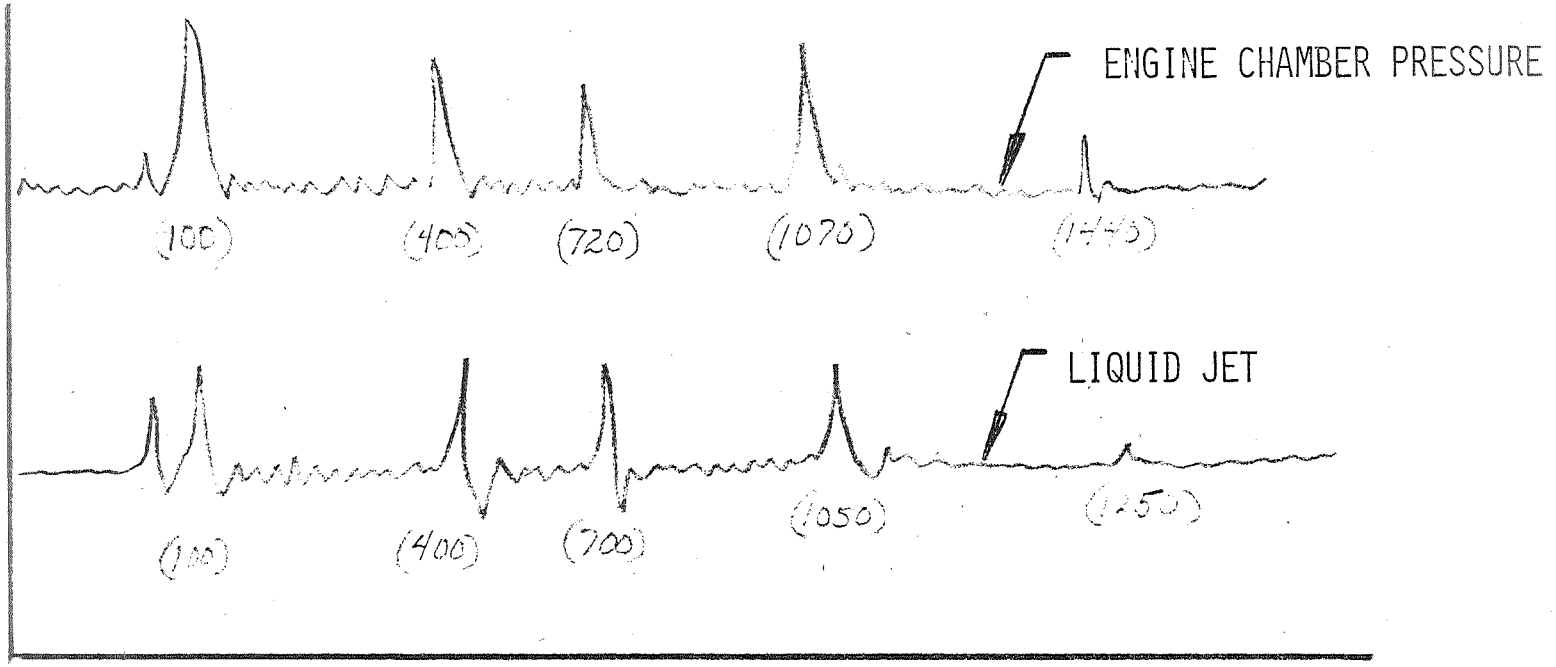

FREQUENCY

FIGURE II-10

APPENDIX III

TASK C - DEFINITION OF CONTROLLING PARAMETERS AND BASIC MECHANISMS INVOLVED

TASK C - POTENTIAL FEEDBACK MODELS

The correlation of the observed data provides an indication that, for the particular configuration to which these data apply, a definite relationship exists between the critical pressure drop and the gas evolution potential. Although the latter term cannot be quantitatively defined at this time, it is observed that periodic, low frequency oscillations will be maintained at levels below a given critical steady-state injector pressure drop when the fuel has been conditioned to a saturation point corresponding to 190 psi at a given temperature. These oscillations will not be maintained in the identical hardware and operating conditions if the saturation conditions are decreased to a value like 140 psi, which is lower than the interface pressure at the valve inlet but, of course, higher than the nominal chamber pressure of 120 psi. In addition, it appears from the successive movie frames that the fuel jet, impingement point and reaction zone luminosity are significantly affected by injection of helium. With these observations in hand, one can speculate on the potential interactions which can establish the feed back mechanism to sustain a periodic oscillatory phenomenon of more or less constant frequency. This frequency, ranging somewhere in the vicinity of 300 to 400 cps, can be computed as the flight time oscillation of the fuel jets by dividing the jet velocity by twice the distance from the orifice entrance to the impingement point.

Three possible feedback mechamisms have been hypothesized; namely:

1. The discharge coefficient for a fuel jet having a given helium gas evolution potential changes discontinuously at a given value of instantaneous back pressure or ΔP (flipping).

2. Triplet blow-apart, which changes the combustion rate and spatial location, occurs in a discrete manner as the instantaneous pressure drop or velocity of a fuel jet of given gas evolution potential varies.

3. The reaction zone and the liquid volume of the fuel orifices form a resonant system at given levels of gas evolution potentials. The latter quantity can be considered as a measure of fuel acoustic velocity. In this particular model, the higher ΔP would be considered strictly as increased resistance.

It might be helpful to elaborate briefly on some of the considerations which underlined these three models.

a. C_d Variation

No experimental data are available to us which would confirm the hypothesis that "flipping" of a jet of high gas evolution potential occurs discretely at given levels of pressure drop. To a large extent, this hypothesis evolved from the observations on the photographs. It should be noted in passing that Northrop of G.E. (Ref. Flow Stability of Small Jets; paper - ASME November 1958), found that the "flipping" characteristics of an orifice were significantly affected when it effluxed into a helium atmosphere compared to a nitrogen one.

b. Triplet Blow-Apart

It is well known from the work of other investigators that blow-apart of reactive jets can occur when sufficient time exists for the production of vapors prior to impingement. Therefore, one cannot rule out the possibility that liquid jets having such a high gas evolution potential as the ones which we are discussing could produce the same mechanism. It is not clear at the moment how the change in jet velocity would modify this particular type of blow-apart.

c. Combustion Feed System Interaction

It is, of course, possible that the combustion can couple with a fuel fluid volume to establish the right time relationship to sustain a continuous oscillation. In this case, the gas evolution potential of the fuel would establish the acoustic velocity of the fluid and the pressure drop across the orifice would be modeled as value of resistance. We know, of course, that the complete feed system does not enter into this coupling mechanism since more or less the same frequency is obtained in test cells having widely varying configurations; however, it is possible that a specific volume within the injector, such as the injector orifices, could establish such a coupling mechanism.

It is planned to examine these hypotheses in somewhat greater detail under Task C. It is ceear, howeve, that some additional experimental data will ultimately be required to isolate the particular feedback mechamism which is responsible for the occurrence of low frequency oscillations.

APPENDIX IV

TASK D - ANALOGUE MODEL ANALYSIS

A. SUMMARY

A critical examination of models was made with particular emphasis placed upon their ability to exhibit the "football" or low frequency oscillation phenomena. No effort was made to tailor a model which would produce this phenomena; but rather it was attempted to determine from the generalized model whether low frequency oscillations are produced under specific operating conditions. It is found that the model in its present form indicates favorable trends and is in reasonable fundamental agreement with experimental data. In particular, the "footballs" are noted; however, further effort and some model improvement will be required to obtain better correlation with experimental data. Sufficient correlation has been obtained to confirm the basic concepts upon which the model is based. When final proposed improvements are incorporated, the simulation will be an effective tool.

Analog computer results for several conditions are presented, illustrating the "football" phenomena and the values of pressure and transport delay time required for their formation.

Finally, a proposed program for model improvement is presented.

B. INTRODUCTION

The occurrence of pressure oscillations in feed systems and combustion chambers motiviated a theoretical study to devise a mathematical model which would simulate the observed behavior and which could subsequently be employed to obtain a better understanding of the phenomena.

Since information obtained by experiment is usually in the time domain, it was felt that a rocket engine simulation yielding time histories directly would be desirable. Equations incorporating known characteristic properties have been derived and simulated on the analog computer. This report describes the Bell Aerospace analog model and presents a proposed program for model improvement to obtain better prediction of engine-feed system behavior, as well as for use in general engine design and development.

C. DISCUSSION OF RATIONALE

A rocket engine system is composed of several coupled subsystems. Since it is not known which particular subsystem is the prime contributor to the observed intermittent low frequency instability, one must rely upon a simplified simulation of the entire system as a starting point. This forms a framework for continuous refinement of the subsystems until the most sensitive element is located. This philosophy formed the basis for the development of the mathematical model.

C. DISCUSSION OF RATIONALE (Cont)

A rationale of the methods used in the fulfillment of the requirements in the work statement will be presented. After each requirement a brief discussion of the equivalent mathematical and/or analog method used to meet this requirement is given.

1. Helium Saturated Propellants

It is assumed that the presence of helium (or any other gas) in the subsystem, line, valve, injector or combustion chamber is mathematically equivalent to a change of acoustic velocity in the subsystem. In this simplified simulation the generating mechanism of the process is not uniquely described. The present system is capable of investigating discrete changes of the acoustic velocity only; however the capability of making other parametric variations (such as possible orifice flipping, etc.) is present when the generating mechanism is prescribed. For a feed line or flow passage, the propagation of pressure waves will be significantly effected by the amount and distribution of free gas out of solution.

2. Pressure Drops and Volumes in Various Parts of the Injector

The injector must be considered a prime suspect in exciting low frequency oscillations. The detailed mathematical model of an injector is extremely complex. Therefore detailed electrical analogy of the injector was prepared and the frequency characteristics of this system evaluated. It was presupposed that if this electric analogy yielded a natural frequency in the 400 HZ range when reasonable values of acoustic velocity were used, effort could be initiated to define the redesign which would be required to shift the frequency of maximum amplitude out of this region. This analysis was performed on the digital computer. A description of the injector is given in Attachment III-A.

Prior tc this program the analog model assumed a perfect injector, i.e. having resistance elements only, with the injector volume reflected as a required fill time. Since no capacitance and inductance elements had been included, if "footballs" are observed in this analog model, one would have to conclude that the injector alone is not a possible source. The simulated pressure drop may conveniently be taken as any design value.

3. Pressure Drops and Volumes in Various Parts of the Propellant Feed Lines, Valve and Test Stand

a. Feed System

The propellant is assumed to be in a gas pressurized tank. It assumed that the supply pressure remains constant during any particular computer run. However, the tank pressure may have any

prescribed constant value. Subsequently, the feed line is assumed to be characterized by a fluid supplied from a source of constant pressure.

The distributed parameter method is used in describing the dynamic behavior of the feed line. This method is used because of the simplicity of the mathematical simulation, as well as the availability of "time delay modules" in the BAC analog computer facility. For a brief description of the time delay concept see Attachment III-B. The delay time is a function of propellant bulk modules (which is determined directly from acoustic velocity) and pipe length, diameter and wall thickness. Further clarification of this relationship is presented later. The simulation is capable of accepting any magnitude or combination of the aforementioned parameters.

b. Valve

In the mathematical description of the valve, it is assumed that the valve is a device which has a known volume requiring a finite fill time, with an entrance which opens at a prescribed rate requiring a finite opening time. The valve is assumed to be invariant to frequency; that is the flow rate is proportional to the square root of ΔP for all frequencies. For the LM investigation it was assumed that the valve opened in zero time. One can reason that in a simplified model of this kind this is not an unreasonable assumption.

c. Test Stand

Equations describing the possibility of fluid coupling with test stand dynamics were not derived. To investigate this possibility, one could resort to the frequency response characteristic of the analog model to determine what external frequencies would be required to induce system coupling. This can be done very simply by employing an electronic oscillator. Line pressure pulsations may be applied to the simulated feed line and the output recorded. The oscillator frequency will then be varied until serious feed system oscillations result. The actual test stand natural frequency should not coincide with the critical frequency obtained in the simulated condition.

4. Change in Operating Conditions

a. Mixture Ratio

Analysis indicates that in general one must speak of two types of mixture ratios: (1) the more conventional one described as the ratio of the time average oxidizer flow rate to the time average fuel flow rate, and (2) the ratio of the instantaneous mass concentration of oxidizer to mass concentration of fuel in the combustion chamber at any given time. The latter ratio must be computed while the former is obtained by so adjusting the valve or

orifice pressure drops to obtain the required time average ratio of the two propellants. The computation method is presented later in the report in the derivation of equations. In fact, it has been observed in the analytical model that the dynamic behavior may be a function of the time rate of change of mixture ratio.

b. Propellant Temperatures, Pressure and Acoustic Properties

Since dynamic combustion models are very involved and not firmly established, the decision was made to use precomputed steady state data. It is acknowledged that the steady state combustion properties are not truly representative of the unsteady process. However, steady state data are being used extensively with marked success in evaluating the unsteady processes in other applications, for example motion of aircraft.

A description of the thermochemical propellant data is given in Attachment III-C. Here are presented such properties as combustion temperature vs mixture ratio (based on mass concentration for each condition), characteristic velocity vs mixture ratio, slopes of combustion temperature and characteristic velocity vs mixture ratio, etc. Actually each of these properties are functions of chamber pressure; for simplicity these variations, however, were not included in an elementary model of this type. They are available, however, and will be included in a more accurate simulation. Solutions may be obtained with assumed or precomputed decreases in theoretical combustion temperatures and characteristic velocities.

c. Combustion Equations

A derivation of combustion equations is given in Attachment III-D. The time rate of change of pressure ratio under prescribed assumptions is computed.

d. Impingement Angle

A "first order" effect of impingement angle variation is obtained by variation of the "transit time", defined as the time required for the propellant to travel from the injector face to average point of impact. In the simulation, this transit time is represented by a "time delay" described in Attachment III-B. Here we assume that a given time is required for the propellant to reach the combustion zone or average impact point. Computer solutions may be obtained for any preset time delay.

e. Fuel and Oxidizer Propellant Leads

If one assumes that the propellant and oxidizer valves open simultaneously, then the time of arrival of each propellant at the injector face is a function of the total fill volumes of the valve plus conduit downstream from the valve gate to the entrance of

the injector. In addition, the corresponding volume of each passage to the injector face must be added. The corresponding flow rates, however, are functions of passage impedance which varies along the path. Although flow configuration is quite complex, it is definable. In the present simplified model, the propellant is assumed to flow at a constant average impedance until a volume equal to the void volume is obtained at which time it is assumed that the reference propellant is at the face of the injector. It was found, however, that if one replaces the aforementioned with a time delay equal to the fill time, no appreciable difference is noticeable in the resulting overall system response, for this simplified system.

D. DISCUSSION OF MODEL

Based on the previously presented discussion, equations were derived and simulated on the analog computer. Possible sources of instability may now become apparent when computer runs are made. Before proceeding to a direct comparison with the LM experimental data, a brief study of the trends resulting from selected changes in system parameters is in order.

1. Hard Starts or "Spike" Phenomena

If one is to have any confidence in the model, the more normally expected behavior must be predicted. The phenomena of hard starts or "Spikes" when a fuel lead is present is a classical example. When fuel lead is present, the model does indeed experience a sharp high initial rise in P_c. An explanation of this as well as other response characteristics may be obtained by observation of the $\dot{P}_c$ equation along with the thermochemical reaction curves. For convenience the equation is given below.

$$\dot{P}_c = \frac{R}{V} \dot{W}_c T(r) + W_c \frac{\partial T}{\partial r} \dot{r} + \frac{\partial P_c}{\partial c^*} \frac{\partial c^*}{\partial r} \dot{r} + \frac{\partial P_c}{\partial \rho} \frac{d\rho}{dr} \dot{r}$$

From Figure III-1 one concludes that for a fuel lead condition when ignition begins, all terms on the RHS are positive, hence $\dot{P}_c$ is positive, and the integral of $\dot{P}_c$ or P_c, begins to increase at a rapid rate. However, $\frac{\partial T}{\partial r}$ and $\frac{\partial c^*}{\partial r}$ increases to a maximum value when $r \approx 0.8$ and decreases rapidly until the sign changes at which time $\dot{P}_c$ may become negative, P_c will stabilize, and fluctuations may occur until $\dot{P}_c = 0$ is obtained. The magnitude attained by P_c during this process may be quite high, depending upon the rate of flow into the chamber. Figure III-1 further shows that for an oxidizer lead the mixture ratio starts at infinity, and for large mixture ratios the reference terms are negative and small and the design ratio may be reached without passing through a region of large positive values resulting in mild

CHARACTERISTICS OF HIGH PERFORMANCE CHAMBERS OPERATING AT OR VERY NEAR PEAK C*.

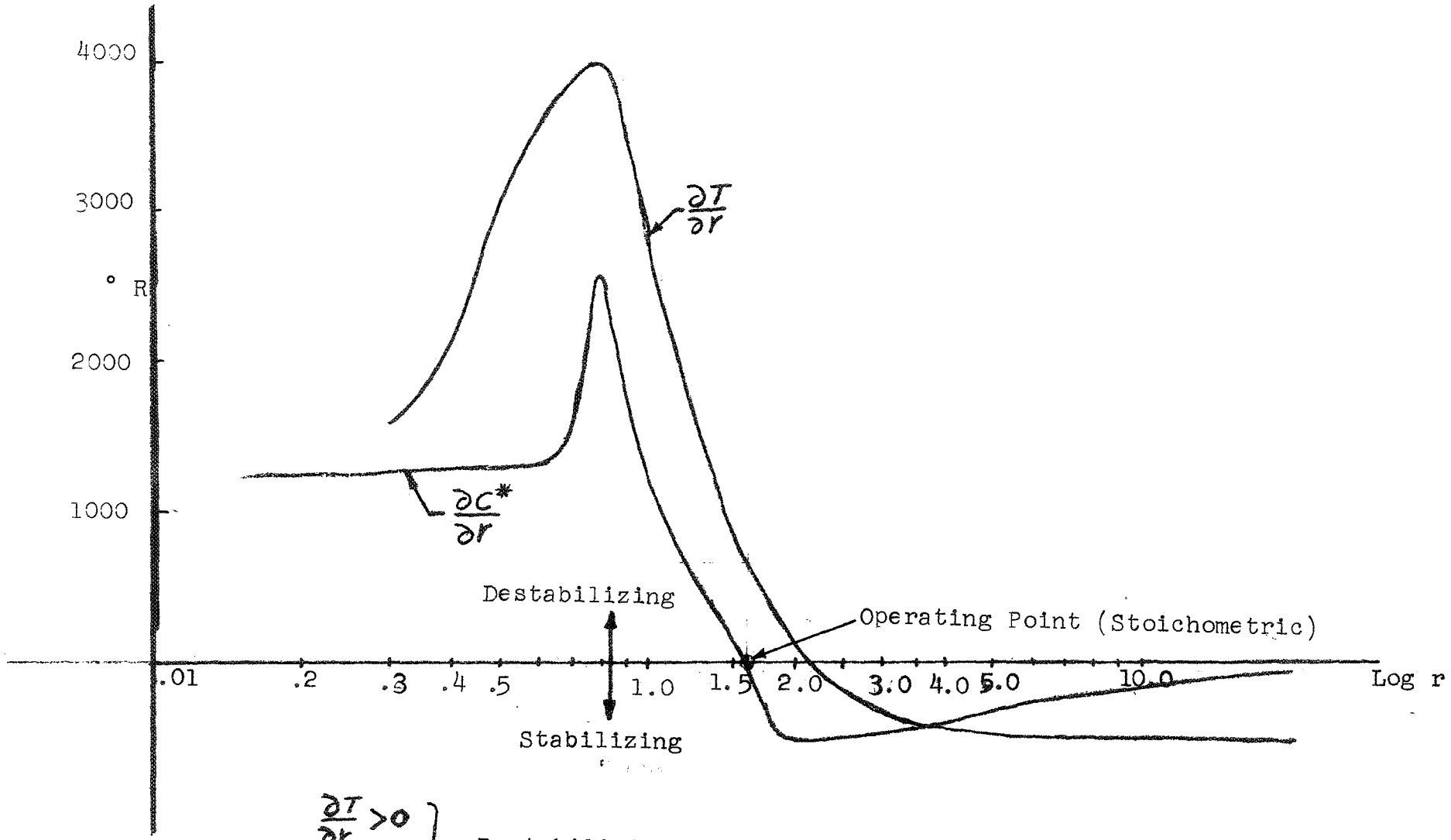

$\frac{\partial T}{\partial r} > 0$
$\frac{\partial C^*}{\partial r} > 0$
} Destabilizing

$\frac{\partial T}{\partial r} < 0$
$\frac{\partial C^*}{\partial r} < 0$
} Stabilizing

Note: Sensitivity depends upon slope of $\frac{\partial C^*}{\partial r}$, $\frac{\partial T}{\partial r}$ in neighborhood of Zero.

Fig III.1

steady increase in $\dot{P}_c$ and a more moderate increase of P_c, hence eliminating the spike. The preceeding discussion gives a rather unique explanation of a possible source of the hard start or spike exhibited in test when a fuel lead is present.

A more detailed discussion of the precomputed thermochemical data is given in Attachment III-C.

2. "Footballs"

a. Computer Results

An attempt was made to apply the model to the LM engine by inserting exact known system characteristics as follows:

(1) Engine Characteristics

A_t	= 16.331 in.^{2}	$\dot{W}_f$	= 4.379 #/sec
V_c	= 429 in^2	$\dot{W}_o$	= 7.055 #/sec
$*P_c$	= 120 in^2	*r	= 1.6
P_T	= 165 psi	Inj. ΔP	= 27 psi (fuel)
Valve ΔP =	5 psi	Inj. ΔP	= 23 psi (ox)

*Chamber pressure and mixture ratios are the results of simulation calculations.

(2) Feed Line Characteristics

The feed lines consist of a 1.5 in. diameter line 370 in. long for each propellant from the supply tank to the test stand. Also a line 1.25 in. diameter, 110 in. long for each propellant from the test stand to the valve. These feed lines were simulated by using the method presented in Attachment III-B. The various feed system impedances for the pertinent components were computed. From this the propellant pressure wave time was computed for incorporation into the time delay elements. The computations indicated that the system is found very sensitive to τ_t (time required for propellant to travel from face of injector to impace point plus sensitive time lag).

b. Chamber Volume Effectiveness

The results showed that the model appears to yield valid information but certain parameters appear not to be consistent with actual system configuration. When the effective chamber volume is decreased more realistic frequencies and τ_t values result. This step appears reasonable when one recalls that the actual reaction zone

in the chamber is considerably smaller than the chamber volume, and (2) the thermochemical data employed is based upon a volume composed only of gas or vapor actually being subjected to a thermalchemical exothermal reaction process which properly defines the reaction volume. Reducing this volume in the simulation to one-half the geometric volume yielded frequencies of approximately 400 Hz and propellant transit time of approximately 5 M.S. This frequency is in reasonable agreement with the observed frequency and the transit time is rather close to that expected. For example, assuming propellant exit velocities of 40 ft per second, the impact time is slightly less than 1 M.S. which allows approximately 4 M.S. for complete combustion to occur. Figure III-2 shows that a "football" is not present with t = 5.3 M.S. Figures III-3 - III-5 show the "football" magnitude progressively increases with increasing t where t = 5.4, 5.5 and 5.6, respectively. For these runs the mixture ratio was higher than design value. For t = 7.6 M.S. a post start "football" is present with the steady-state mixture ratio of the design value of 1.6 (Figure III-6). Notice that for the lower mixture ratio condition, the instability present in the P_c rise has been eliminated.

Feed line oscillations during injection fill are somewhat larger than those shown in test data. This is attributed to the lack of information on the magnitude of the damping constant which must be inserted in line dynamics loop as given in Attachment III-B.

A mathematical rationale of the "football" phenomena is presented in Attachment III-E.

c. Transient Volumetric Effects

As previously stated, the 400 Hz frequency could be produced by using an "effective" volume smaller than the actual chamber. This could imply that the frequency is a function of the actual "reaction" colume rather than the geometrical one. When the propellant enters the chamber initially combustion should occur through the entire volume and this volume becomes the "effective" volume. As P_c increases, the "effective" volume tends to decrease to its steady-state value. If this hypothesis is true, then one should expect a decrease in observed frequency during the Pc transient. Observation of test data reveals this to be true. However, for the analog model, the volume is assumed constant through the transient as well as the steady-state. When this effect is incorporated in the analog model, one may expect decreased amplitude and frequency during the Pc rise and better agreement with experimental data.

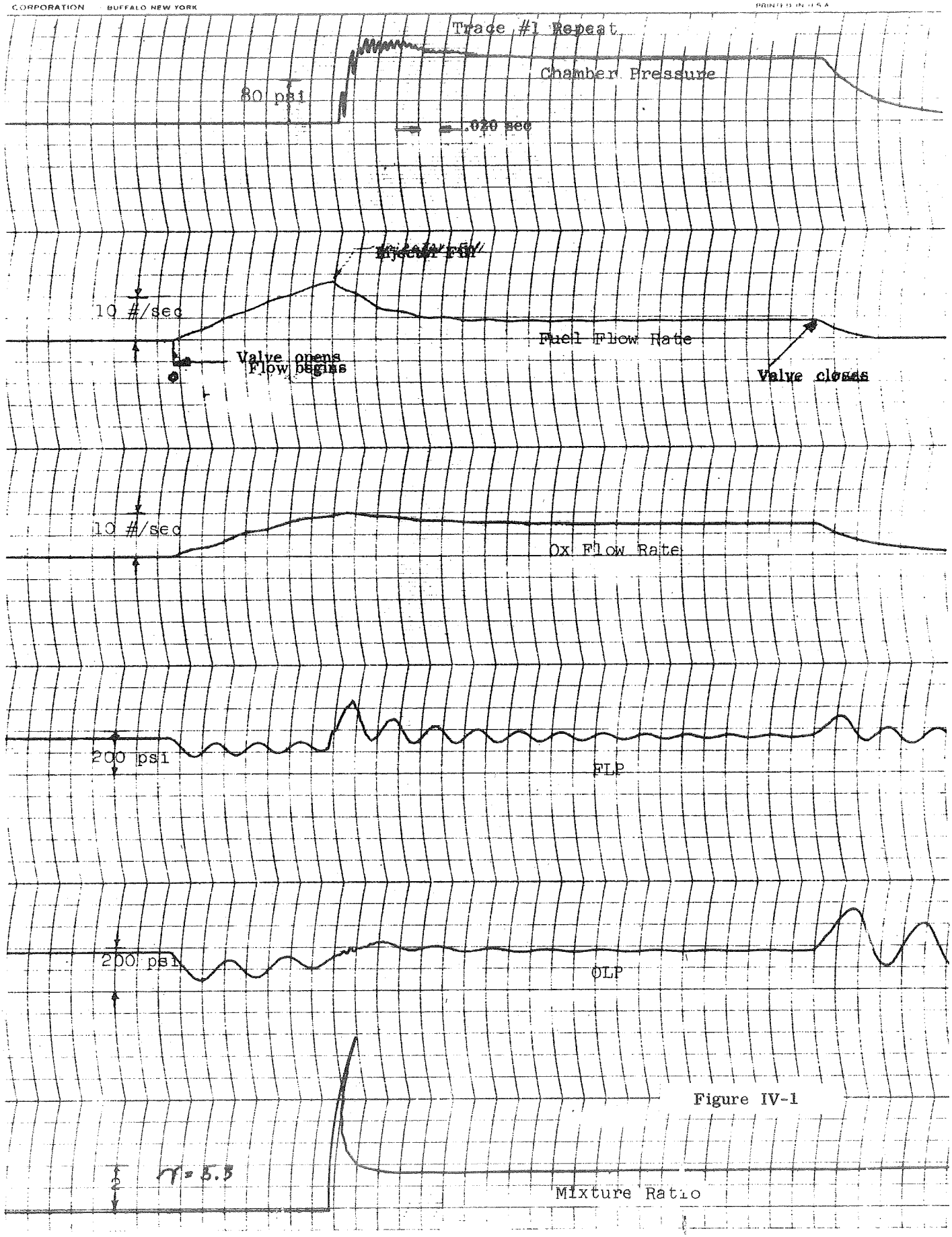
Trace #1 Repeat
Chamber Pressure
80 psi
.020 sec
10 #/sec
Fuel Flow Rate
Valve opens
Flow begins
Valve closes
10 #/sec
Ox Flow Rate
200 psi
FLP
200 psi
OLP
Mixture Ratio

Figure IV-1

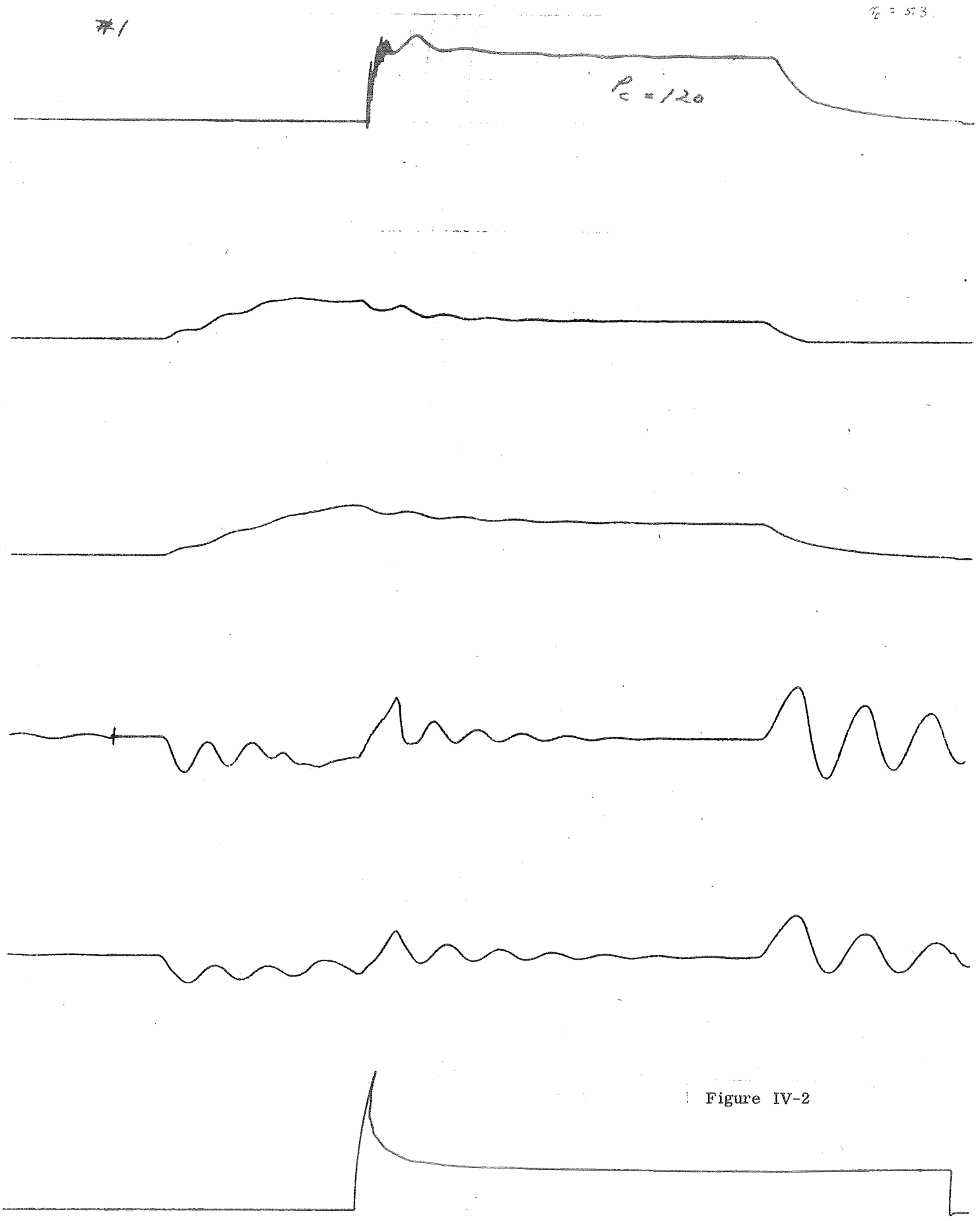

Figure IV-2

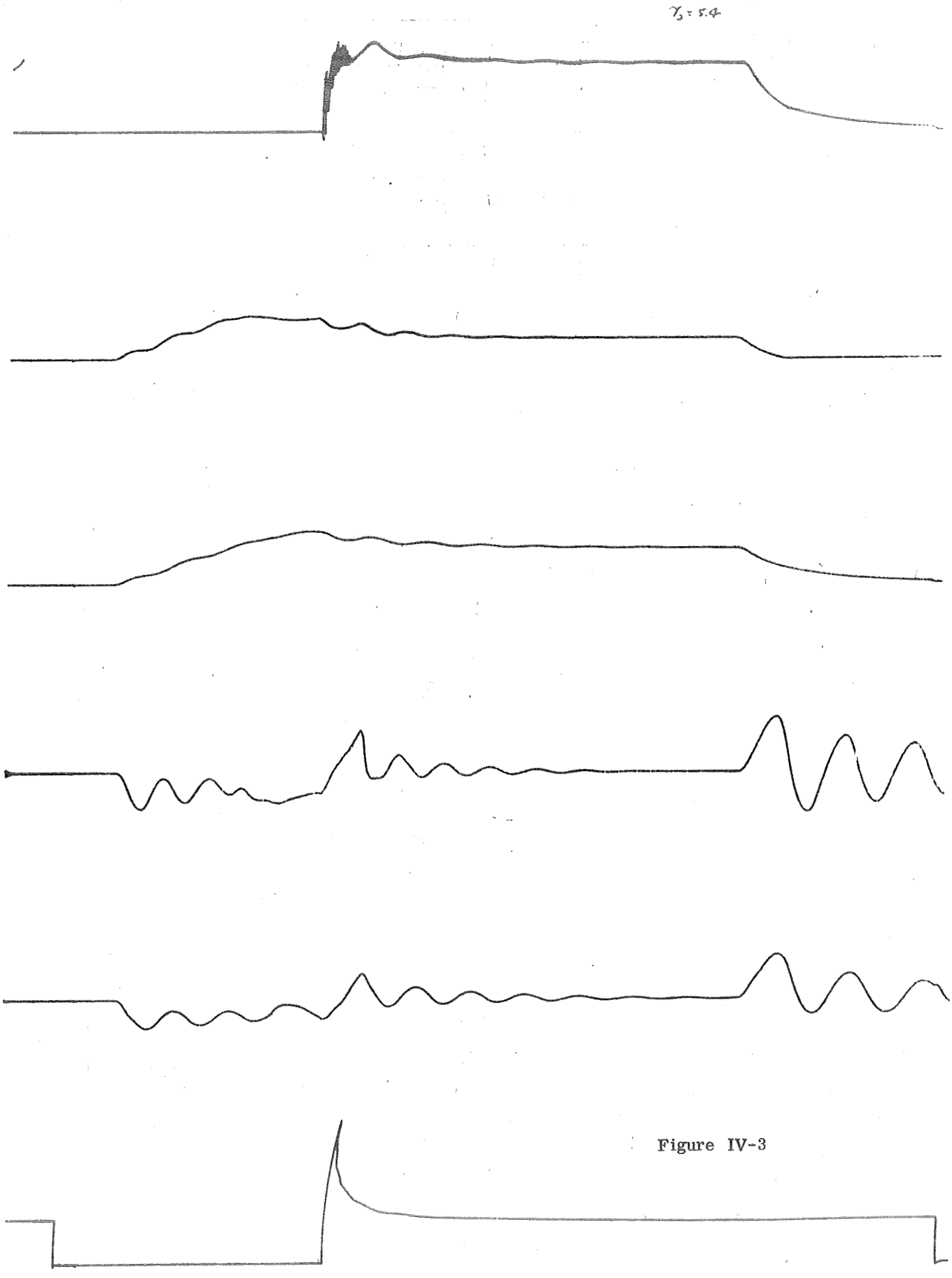

Figure IV-3

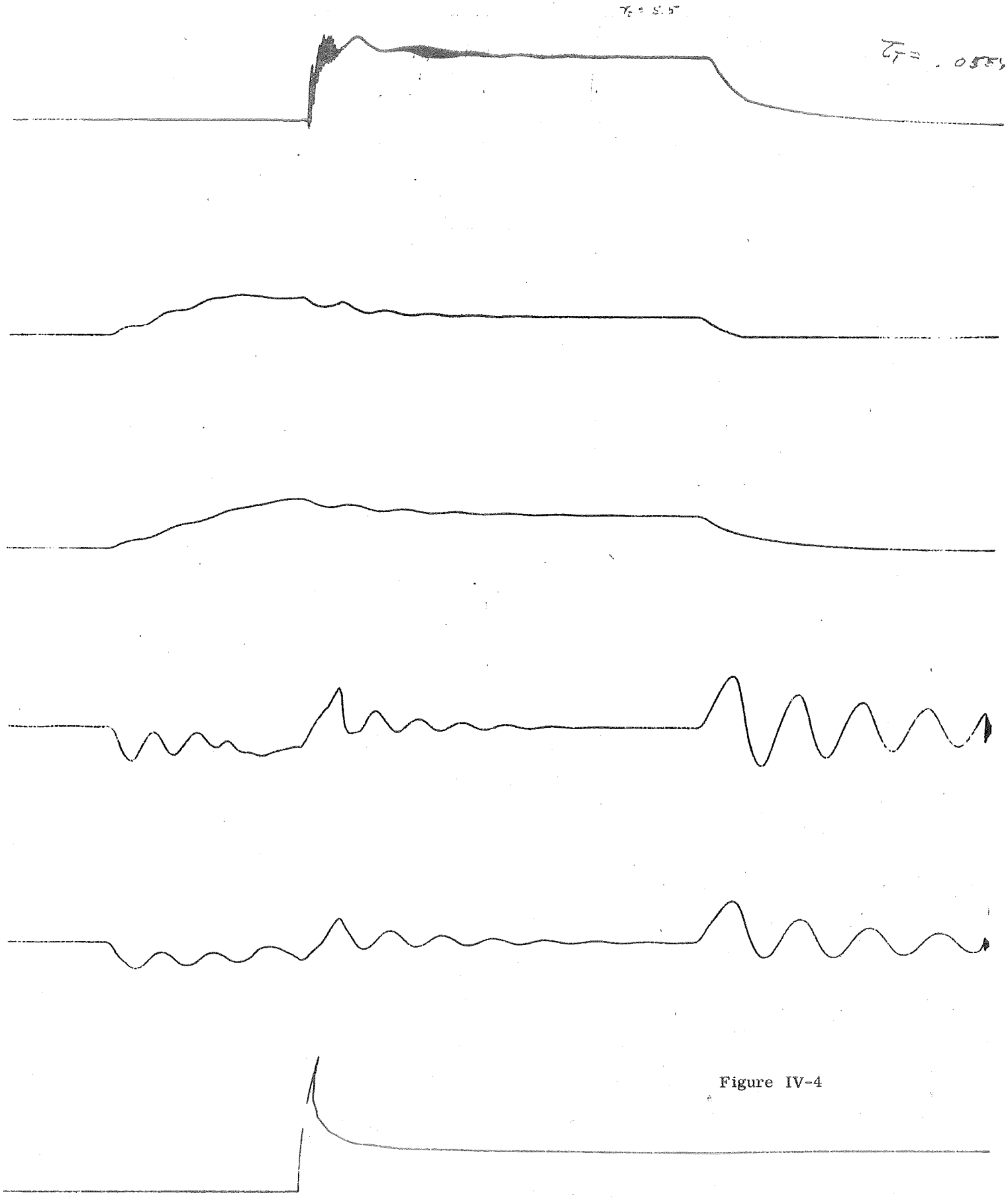

Figure IV-4

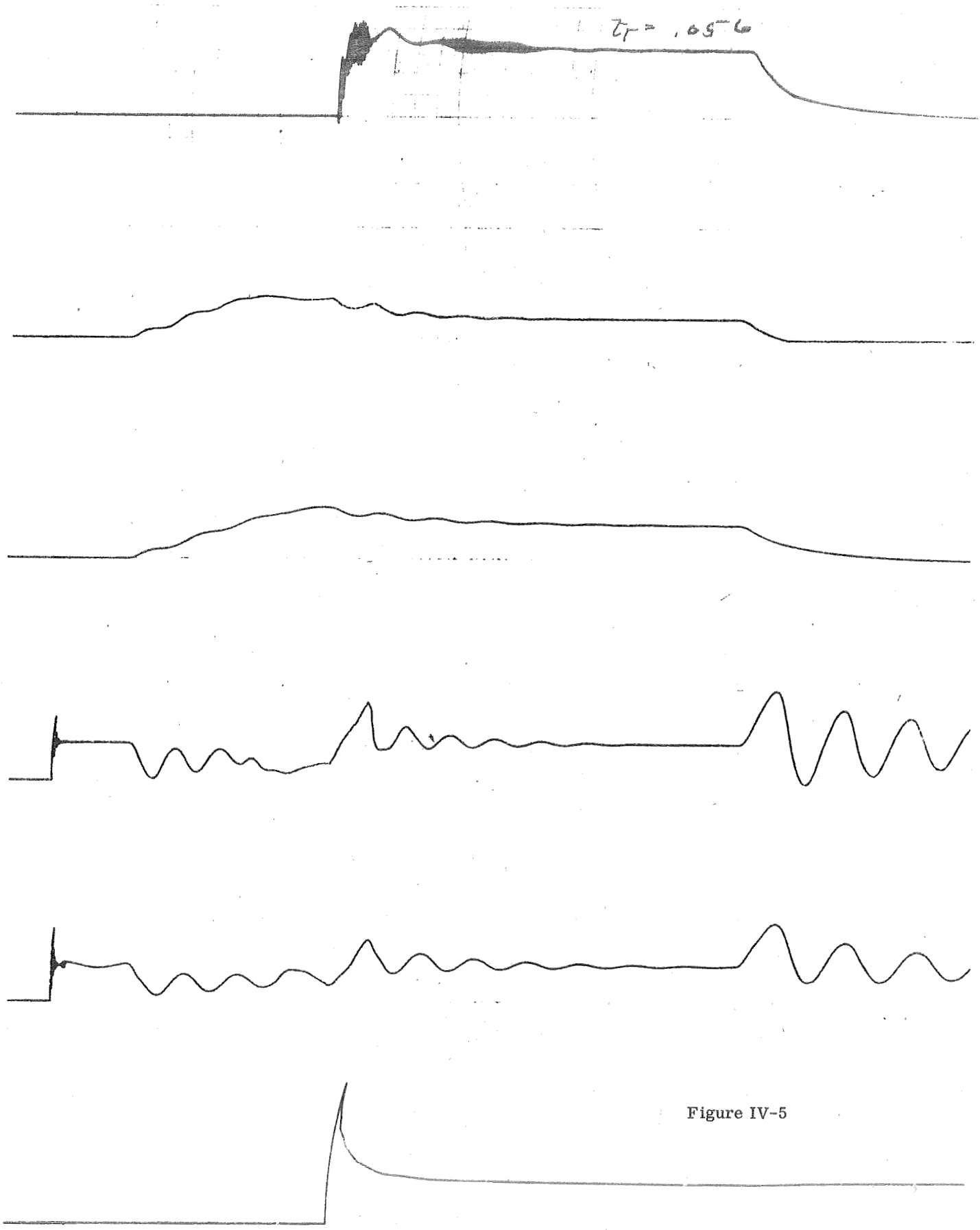

Figure IV-5

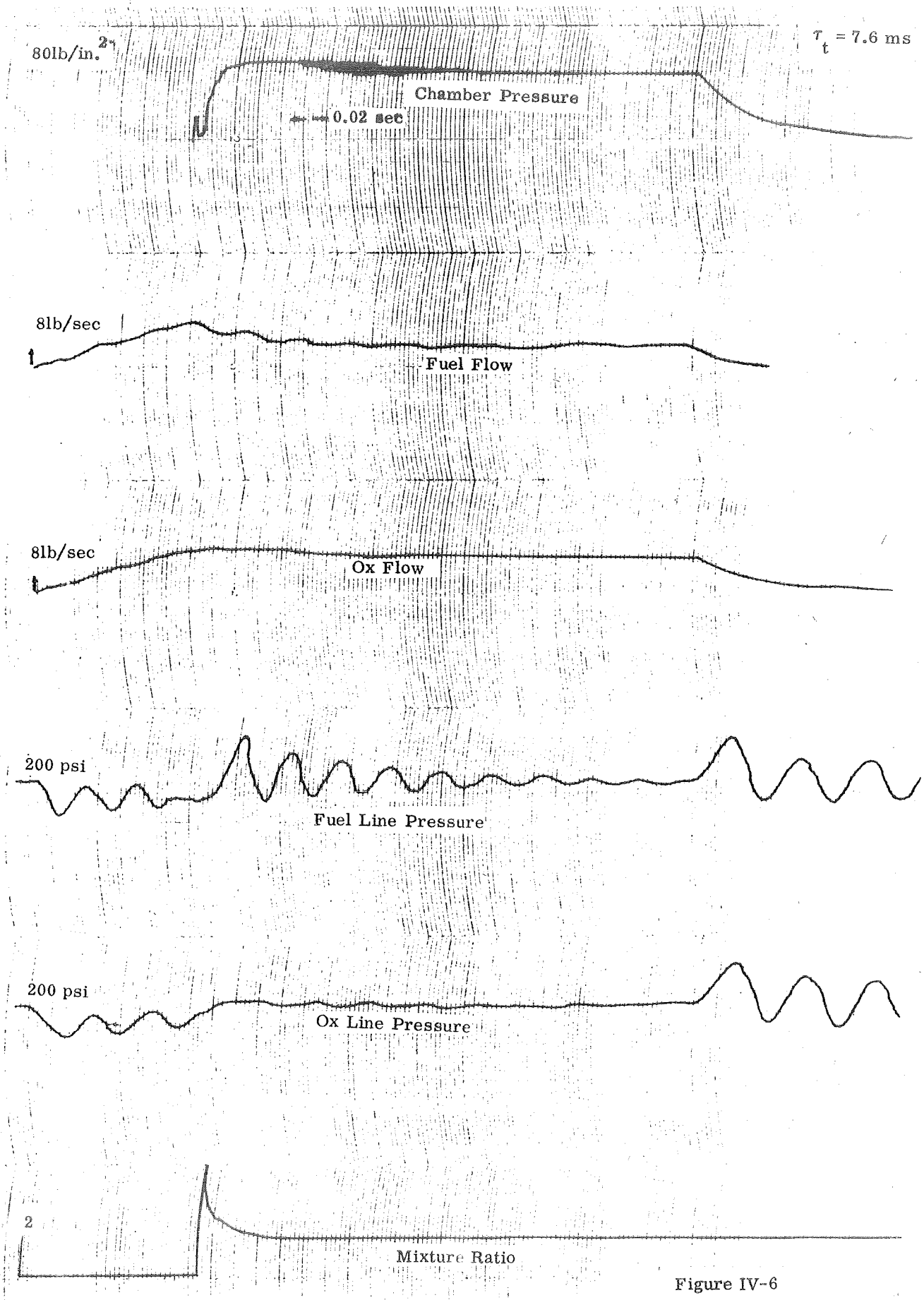
80lb/in.²
τ_t = 7.6 ms
Chamber Pressure
0.02 sec
8lb/sec
Fuel Flow
8lb/sec
Ox Flow
200 psi
Fuel Line Pressure
200 psi
Ox Line Pressure
2
Mixture Ratio

Figure IV-6

E. PROPOSED MODEL IMPROVEMENT PROGRAM

The existing Bell pressure fed rocket engine model is used to calculate the transient and steady-state performance of various rocket engine systems. It does this by breaking the propellant feed system into a number of segments or modules dictated by the particular design configuration, and calculating the flow and pressure in them. Subsequently, the feed system from tank to injector or valve is simulated by a cascade of individual modules. The valve simulation assumes valve opening is linear, while the injector is simulated by a pressure drop only. The transportation delay is determined by a time delay device which simulates the propellant flight time (between injector face and impingement point plus vaporization and burning time). The combustion process is a function of precomputed thermochemical data.

A detail digital model of the injector is available. Acoustic velocity and pressure drops at all major flow passages may be given any design values, and subsequently, impedance and frequency characteristics may be determined.

The present analog model indicates trends which are, in general, consistent with test results. Specific detailed correlation has not been attempted in Phase 1 of this effort, only a comparison of available preliminary analog results with test data was made. These comparisons indicate that the basic concepts set forth in the model are valid and that more detailed simulation, based upon the present model, is desirable.

Based upon studies made in Phase 1, the following recommendations are made.

Task A

Activate present analog model and obtain agreement with present experimental data point (condition for "football" as determined from present experimental data). Establish limits of simplified model.

Task B

1. Revise feed line representation to include two phase flow.
2. Revise injector representation to include storage of propellant in injector manifold, and gas evolution effects.
3. Revise injector representation to include resistance and inertia of injector orifices, including flipping condition.
4. Revise combustion zone time delay to be a function of jet velocity.

Task C

Activate this improved model and obtain agreement with present experimental data point. Extrapolate to other known data points if and when available.

ATTACHMENT III-A

DEFINITION OF LINEAR MODEL

The dynamic model is derived on the basis of an analogous impedance network satisfying continuity and energy conservation requirements, and represents the fuel feed system from the trim orifice downstream of the LM valve to the injector (Fig. 1) represented by Figure 2 and the analogous impedance network by Figure 3. In electrical terminology, voltage is analogous to perturbation pressure (p.s.f.), and current to perturbation volume velocity (Ft^3/sec).

The analogous network elements are simply evaluated as follows:

Resistance: $R = \frac{\tilde{p}}{S\tilde{v}}$

Inertance: $L = \rho_m \left(\frac{L_{eff}}{S}\right)$

Capacitance: $C = V/\rho_m C_m^2$

These are derived in most acoustics textbooks.

ρ_m = density of gas-liquid medium.

C_m = sonic velocity in gas-liquid medium.

V = volume of element.

L_{eff} = effective length of inductive element.

S = cross-sectional area of inductive element.

The response characteristics of the system are determined through the utilization of an IBM digital program capable of analyzing complex networks of the required form. At present the characteristics are demonstrated by the print-out of node voltages and phase for a given input voltage and frequency. This can be modified to produce input impedance functions as well as transfer functions.

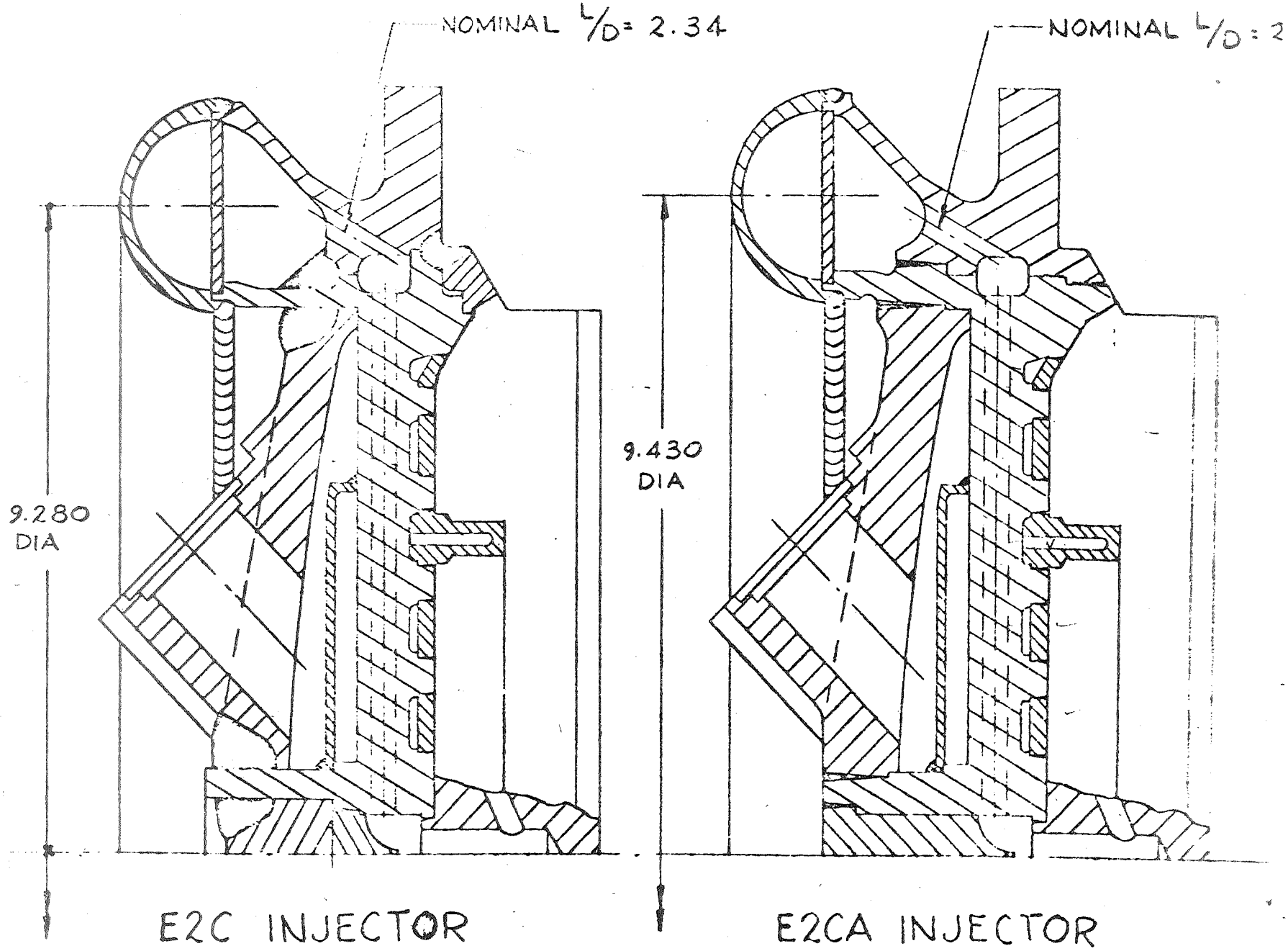

Figure 1. LM Ascent Engine Injector

LM ASCENT ENGINE INJECTOR SCHEMATIC

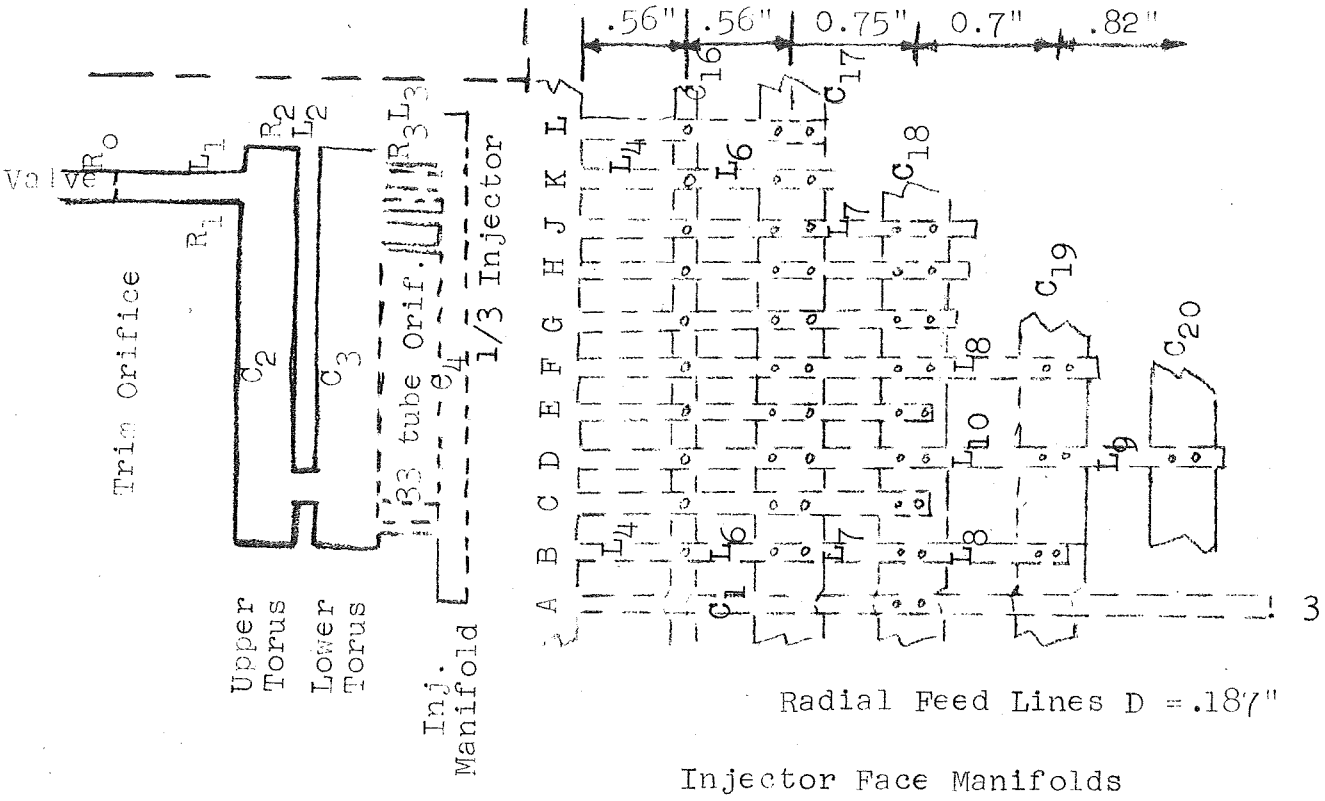

Injector Face Manifolds

1. Radial Feed Lines "A" supply Baffle Lead
2. Face Manifold "C_{18}" supplies Cooled Ring Baffle
3. Injector Orifices Omitted from Schematic

LM ASCENT ENGINE FUEL SYSTEM LINEAR DYNAMIC MODEL

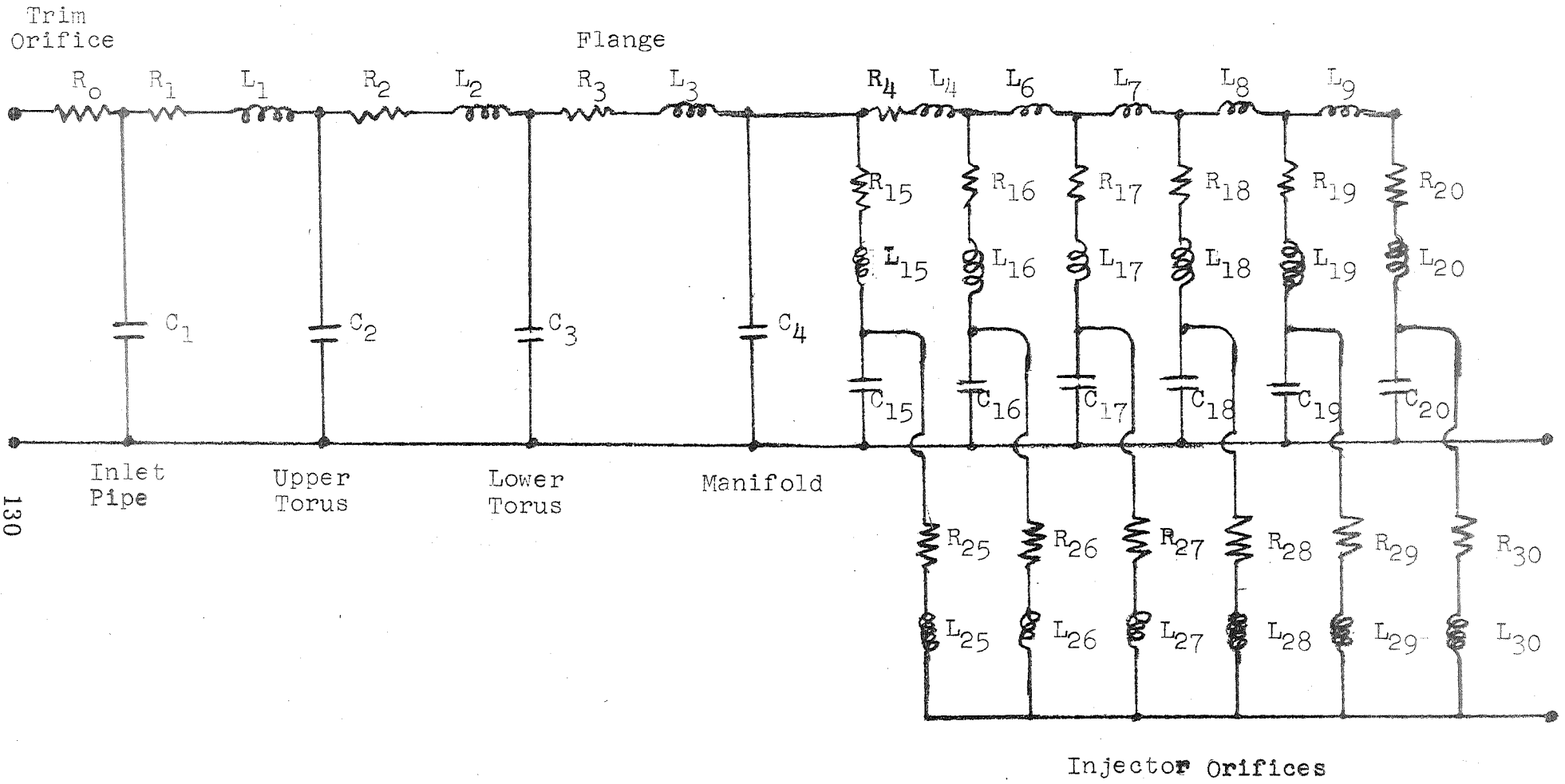

ATTACHMENT III-B

A. FEED SYSTEM THEORY

Applying the continuity and momentum equations to a fluid flowing at low velocity in a cylinder or pipe yields the following equations

$$-\frac{\partial V}{\partial x} = \frac{1}{\beta_c}\frac{\partial P}{\partial t} \qquad (1)$$

$$-\frac{\partial P}{\partial x} = \rho\frac{\partial V}{\partial t} \qquad (2)$$

Combining Equations (1) and (2) yields the wave equation since their solution when applied to systems of this type have been found to describe traveling waves observed in a wide variety of distributed - parameter systems. However in feed systems, it is often convenient to consider pressure and flow effects at each end and to determine the relationships P_a, W_a, P_b, W_b. This consideration gives rise to the four terminal network concept shown below.

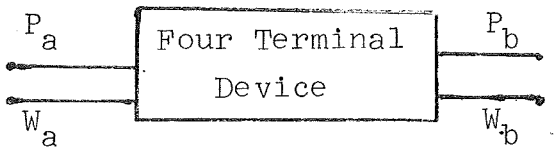

Two of the four variables may be considered as independent while the other two are independent, as long as both do not occur at the same end.

With,

$$\tau = L\sqrt{\rho/\beta_c} \qquad Z = \sqrt{\frac{\rho\beta_c}{A^2}}$$

$$C_s = \sqrt{\beta_e/\rho} \qquad Y = \frac{1}{Z}$$

$$\frac{1}{\beta_e} = \frac{1}{\beta} + \frac{2r}{Et}$$

and a line resistance term (linearized) given in terms of pressure drop as

$$\Delta P = \frac{Kf}{A} \dot{W}$$

Kf = equivalent pipe friction coefficient.

The solution of Equations (1) and (2) yields the two following difference equations in operator form where ($\bar{}$) represents the Laplace transform:

$$\bar{P}_2 + \frac{\mu}{S} Z \bar{W}_2 = \bar{P}_1 e^{-\tau\mu} + \frac{\mu}{S} Z \bar{W}_1 \quad (3)$$

$$\bar{P}_1 + \frac{\mu}{S} Z \bar{W}_1 + \bar{P}_2 e^{-\tau\mu} + \frac{\mu}{S} Z \bar{W}_2 \quad (4)$$

where

$$\mu = \sqrt{S^2 + gK_f S} \quad (5)$$

Writing Equation (5) as,

$$\mu = S \left(1 + \frac{K_f g}{S}\right)^{\frac{1}{2}} \quad (6)$$

and noting that,

$$\left(1 + \frac{K_f g}{S}\right)^{\frac{1}{2}} = 1 + \frac{K_f g}{2S} + \ldots\ldots \quad (7)$$

Retaining only the first two terms of the expansion, Equation (6) becomes

$$\mu = S + \frac{K_f g}{2} + \ldots. \quad (8)$$

Using Equation (8) in Equations (3) and (4) yields

$$\bar{P}_2 + Z \bar{W}_2 \left(1 + \frac{K_f g}{2S}\right) = e^{-\frac{K_f g \tau}{2S}} \left[P_1 e^{-\tau S} = Z \bar{W}_1 e^{-\tau S} \left(1 + \frac{K_f g}{2S}\right)\right] \quad (9)$$

$$\bar{P}_1 + Z\,\bar{\dot{W}}_1\left(1 + \frac{K_f g}{2S}\right) = e^{-\frac{K_f g \tau}{2}}\left[\bar{P}_2 e^{-\tau S} + Z\,W_2\, e^{-\tau S}\left(1 + \frac{K_f g}{2S}\right)\right] \quad (10)$$

Recalling that $e^{-\tau s}$ in the complex plane is equivalent to a time delay "τ" in the time domain, and $(1 + \frac{K_f g}{S})$ may be approached by an electronic network an analog simulation of Equations (9) and (10) is made and the presently used approximation is shown in Figure 1.

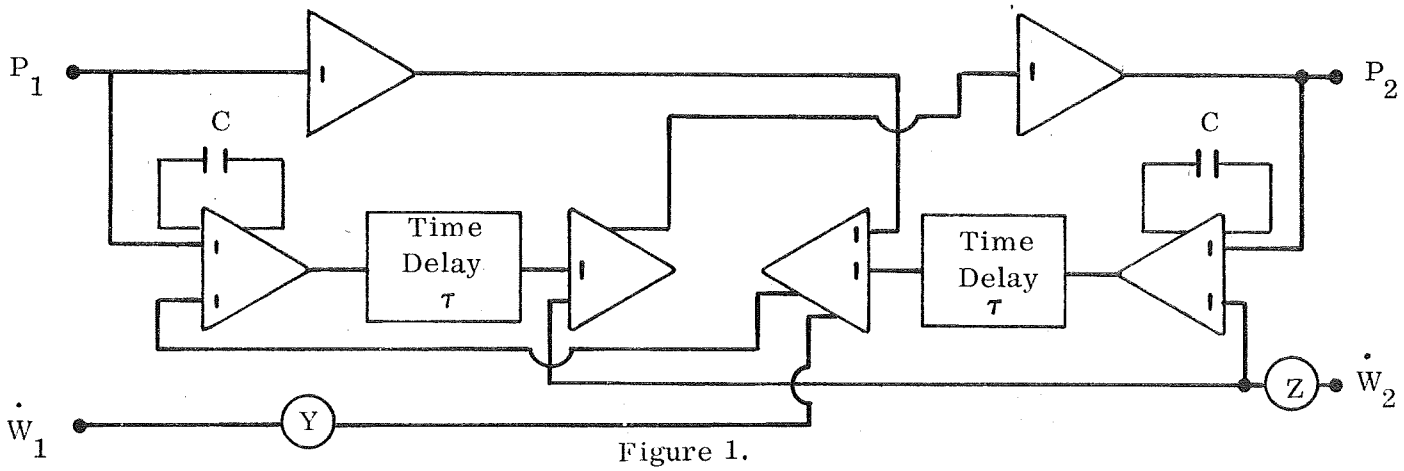

Figure 1.

A more detailed description of the time delay concept and device is given later.

Figure 1 characterizes one line segment for a prescribed impedance z and admittance Y. A useful practical condition arises when P_1 is the supply tank pressure (or other source of constant pressure) and one is not interested in W_1, then Figure 1 reduces to Figure 2.

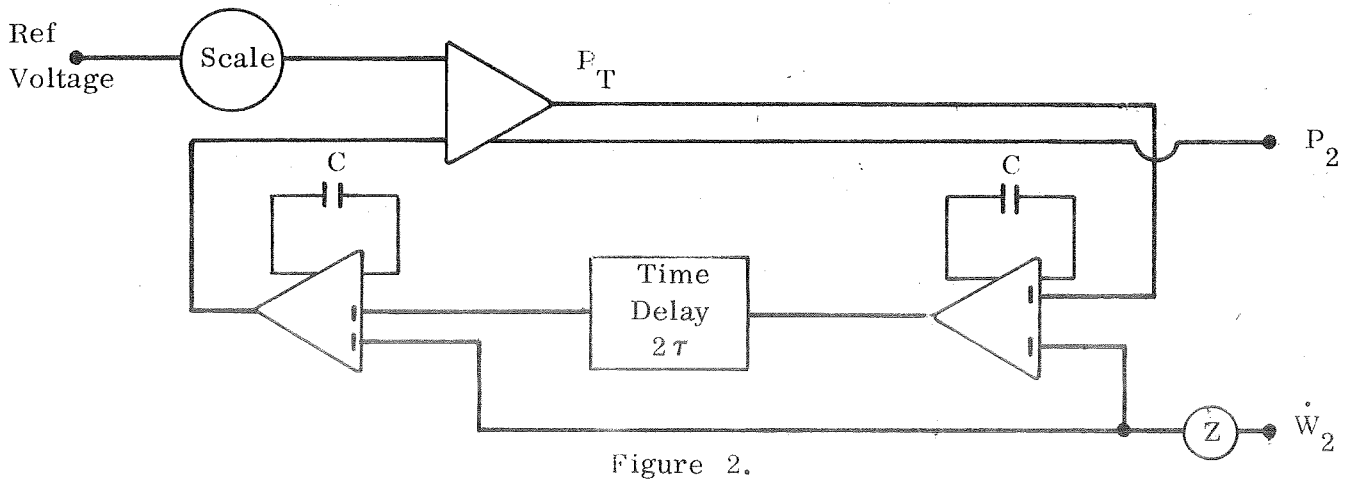

Figure 2.

The simulation shown in Figure 2 has been used extensively and has proven to agree very well with experimental results. The capacilance values "C" must be empirically determined.

VALVE INJECTOR SIMULATION

Propellant flow rate is assumed to be given by

$$\frac{L}{Ag}\ddot{W} = P_2 - P_c - K\dot{W}^2$$

where:

$$K = \frac{1}{2\,g\,C_D^{\,2}A_v^{\,2}}$$

In the present simulation C_D is assumed constant. Since a finite time is required to open the valve, "A_v" is zero at $t = 0$ and increases linearly to its nominal value in "t_v" sec, the opening time. Injector fill time is simulated by delaying the flow rate to the combustion chamber entrance, or to the injector orifice outlet by a time τ_t. This is the time required to produce a volumetric flow (using the internal injector impedance) equal to the volume of the injector. The simulation of this loop is shown in Figure 3.

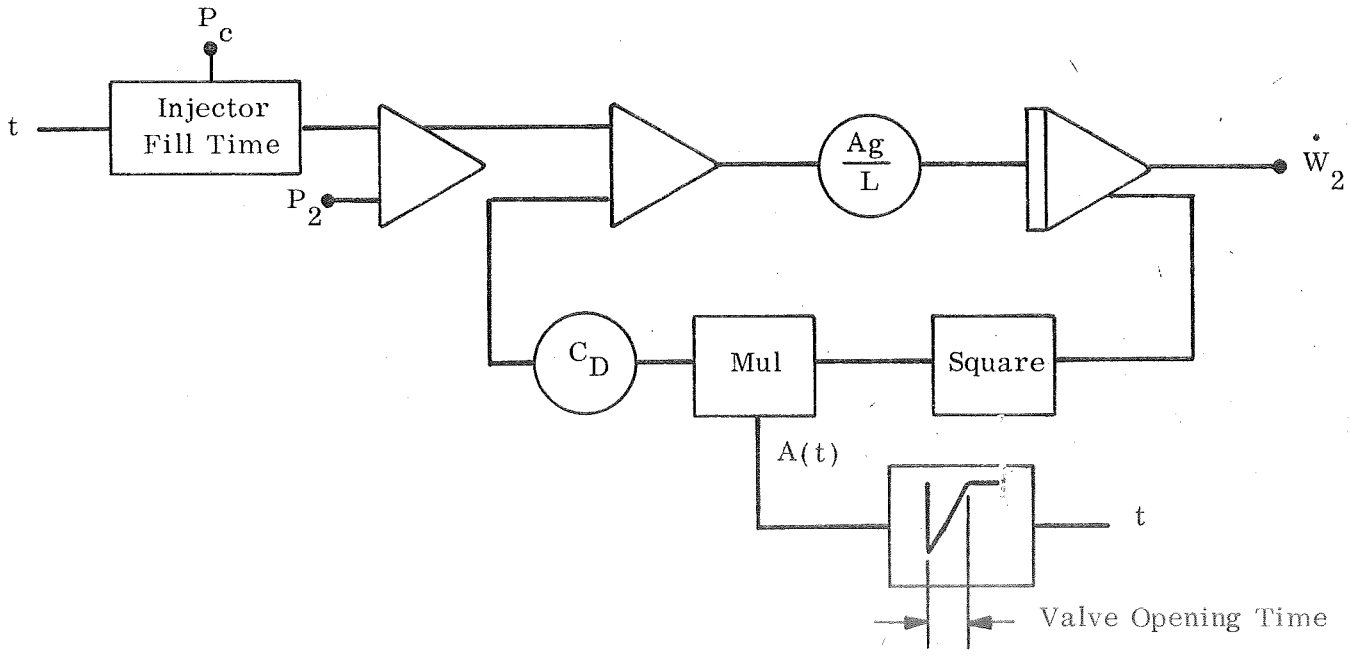

Figure 3.

TIME DELAY DEVICE

Pressure waves travel at a known velocity down a pipe. Hence a finite time (τ seconds) is required for the valve to reach the opposite end and τ seconds will be required for its return. If the magnitude of the wave is constant or does not vary during transit, it will be reflected back with the same intensity as it had when transmitted. Thus if a wave is sent down a pipe 2τ seconds will be required for its return. The transmitter only knows what is happening at the present time. Hence if P (t) represents the pressure at the present time and 2τ seconds must laps before the return of the preview wave, the actual pressure at the present time will always be equal to the pressure 2τ seconds earlier. An event of this type may be represented as follows:

$$\left.\begin{array}{l}\text{Pressure at} \\ \text{Present Time}\end{array}\right\} = \left\{\begin{array}{l}\text{Pressure at } 2\tau \\ \text{second earlier}\end{array}\right.$$

or in mathematical language

$$P(t) = 0 \quad \text{for } t \text{ less than } 2\tau$$

$$P(t) = P\ (t - 2\tau) \quad \text{for } t \text{ greater than } 2\tau$$

A time delay device performs this process. A disturbance is put into the device and the same disturbance comes out of the device but delayed by 2τ seconds. If an attenuation factor k is known, by calculation or test, then the formula becomes

$$P(t) = 0 \text{ for } t < 2\tau$$

$$P(t) = k\ P(t - 2\tau); \quad \text{for } t > 2\tau$$

It must be remembered however that the characteristic velocity (speed of sound, if one assumes that the pressure travels at sonic speed along the pipe) must be constant. When the elasticity of the pipe is considered the wave will travel at a speed considerably less than the sonic speed.

Time delay computers are available and are used extensively for the analysis of rocket engines here at Bell.

ATTACHMENT III-C

THERMOCHEMICAL DATA

Thermochemical calculations are usually in a form from which the several derivatives or slopes required for evaluation of Equation (8) may readily be determined. In particular this has been done for the N_2O_4/50-50 UDMH-N_2H_4 combination, and results are presented in the following figures. Figure 1 shows T and C* versus r_c curve. Figure 2 shows $\partial T/\partial r_c$ versus r_c (note the change in sign for $r_c > 2$). This sign inversion becomes significant since in Equation (8) Attachment III-D the second term on the right becomes negative. The magnitude of P_c is a function of the sign of this parameter. For t = 0+ the positive sign implies fuel lead, while the negative sign implies oxidizer lead. Physically this means that if M_c is large enough, fuel lead will yield high P_c for t = 0+ while oxidizer lead yields more moderate values. This is a plausible explanation of the tendency of hard starts (spiking) to be associated with fuel lead.

Note further that if M_c is small enough or if $\dot{r}_c$ is small at t = 0+ the theoretical hard start condition may be removed. The foremention conclusions have been verified experimentally.

Figure 3 shows $\partial \rho / \partial r_c$ versus r_c and indicates a sign change at $r_c = 1.3$. For fuel lead or fuel-rich mixture the slope is positive, hence stabilizing; for oxidizer lead or oxidizer-rich mixture the slope is negative, or destabilizing. The magnitude is also a function of P_c.

Figure 4 shows P_c versus ρ for various mixture ratios and indicates that $\partial P_c/\partial \rho$ is practically independent of mixture ratio for $r_c > 1$. and $0.2 < \rho < 0.07$.

The previously described data are used to evaluate engine performance and stability boundaries.

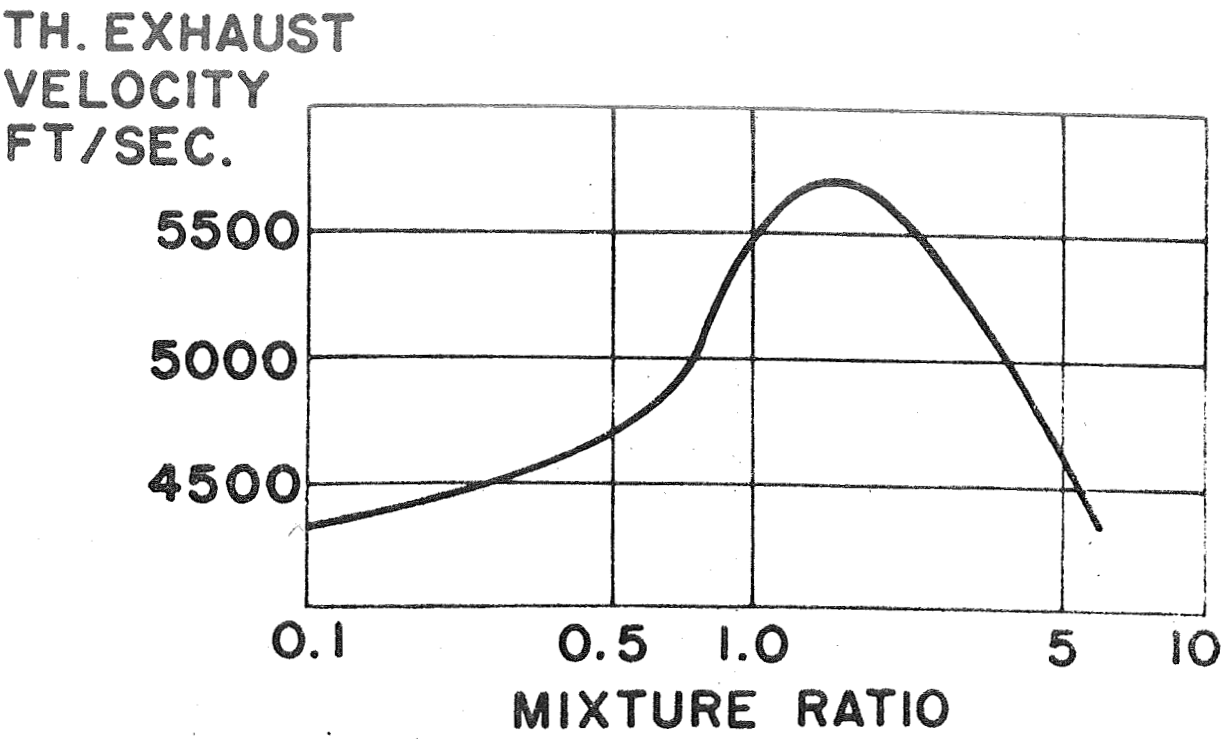
TH. EXHAUST
VELOCITY
FT/SEC.
5500
5000
4500
0.1
0.5
1.0
5
10
MIXTURE RATIO

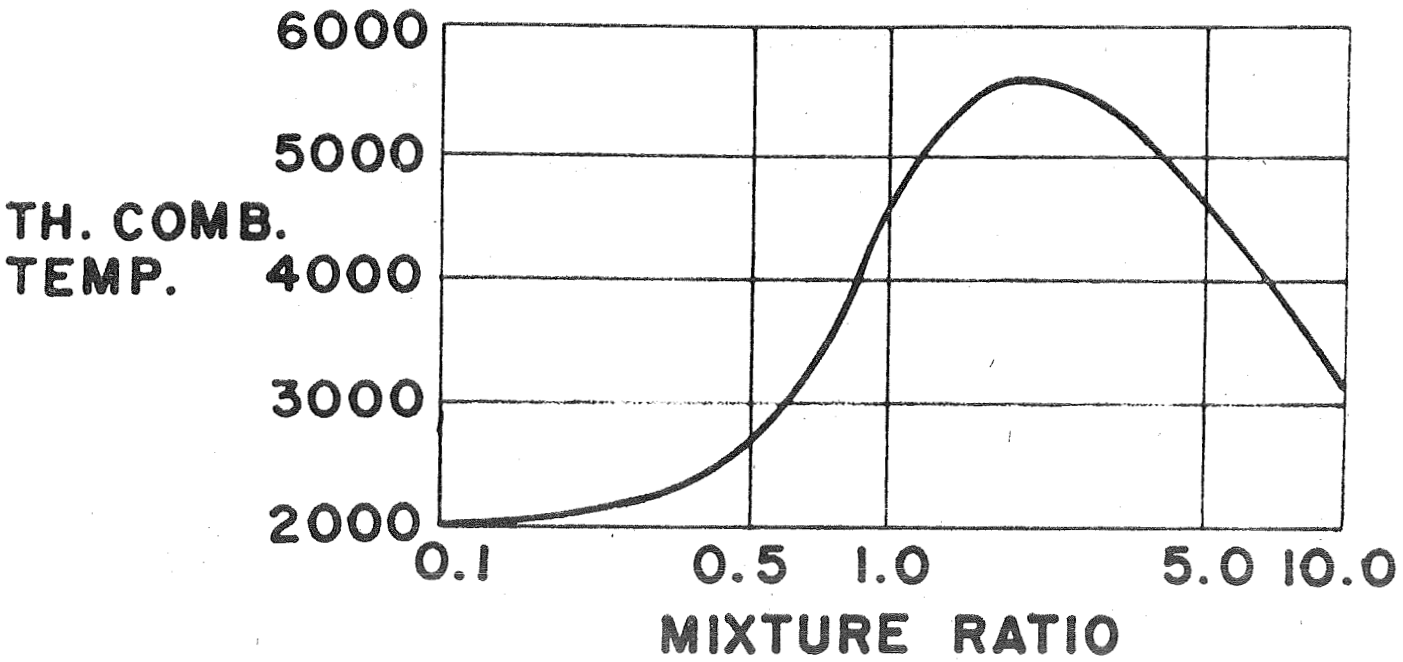
6000
5000
TH. COMB.
TEMP.
4000
3000
2000
0.1
0.5
1.0
5.0
10.0
MIXTURE RATIO

FIGURE 1

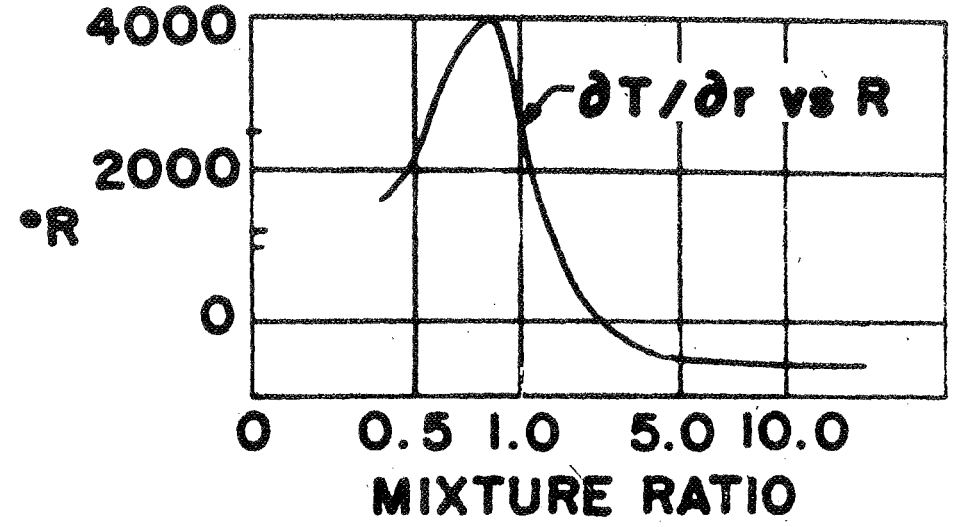
4000
2000
°R
0
∂T/∂r vs R
0 0.5 1.0 5.0 10.0
MIXTURE RATIO

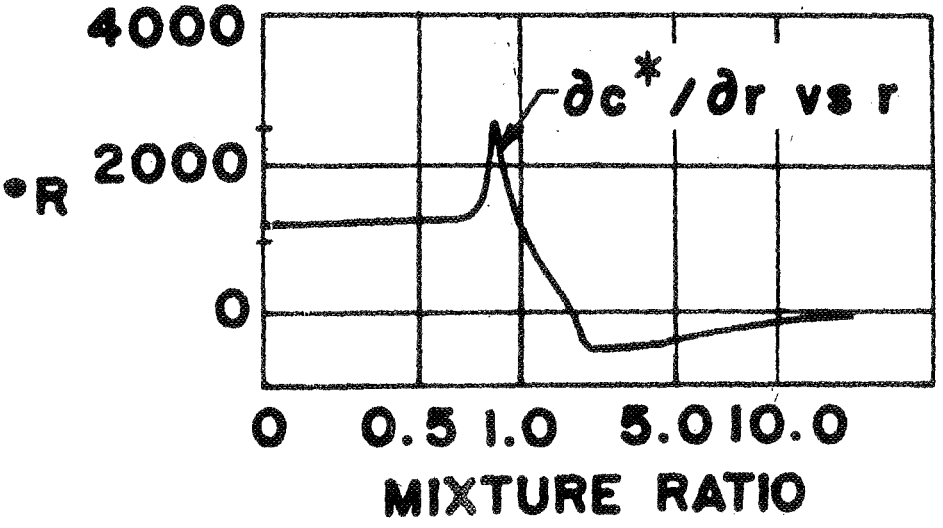
4000
2000
°R
0
∂c*/∂r vs r
0 0.5 1.0 5.0 10.0
MIXTURE RATIO

FIGURE 2

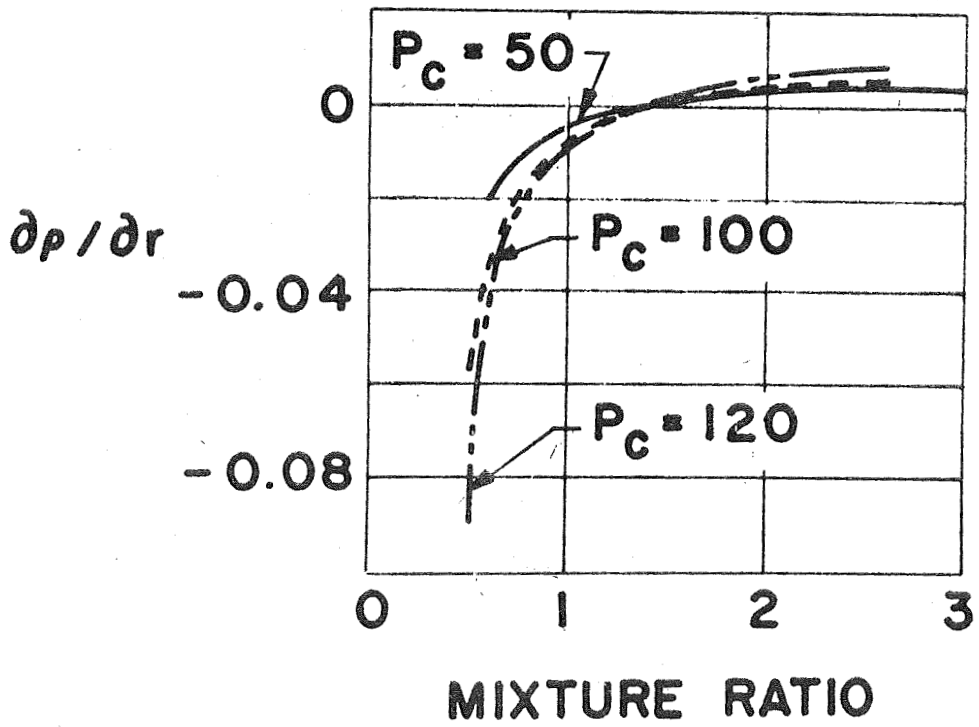
P_c = 50
P_c = 100
P_c = 120
0
-0.04
-0.08
$\partial p / \partial r$
0
1
2
3
MIXTURE RATIO

FIGURE 3

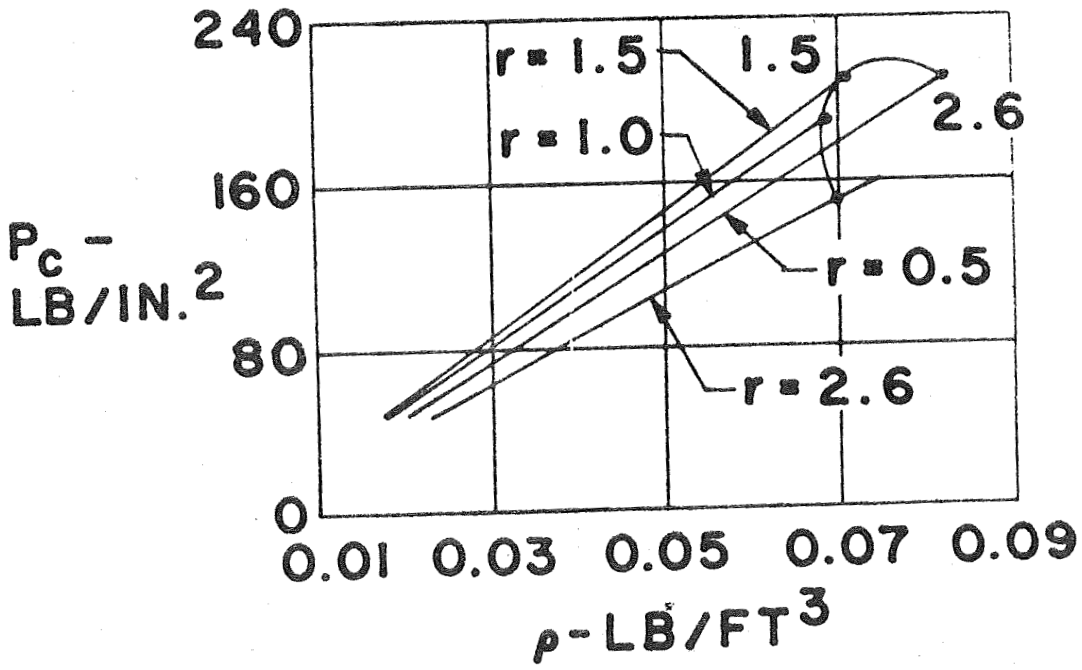
240
160
80
0
P_c - LB/IN.^{2}
r = 1.5
1.5
r = 1.0
2.6
r = 0.5
r = 2.6
0.01
0.03
0.05
0.07
0.09
ρ - LB/FT^3

FIGURE 4

ATTACHMENT III-D

A. DERIVATION OF EQUATIONS

Primary consideration will be given to obtaining chamber pressure time response as well as low frequency stability characteristics. For the present, homogeneous mixing throughout the chamber is assumed. The perturbed chamber pressure variation is assumed to be the sum of other parameter variations and is written as:

$$\Delta P_c = \frac{\partial P_c}{\partial M_c} \Delta M_c + \frac{\partial P_c}{\partial T} \Delta T + \frac{\partial P_c}{\partial \rho} \Delta \rho + \frac{\partial P_c}{\partial C^*} \Delta C^* \qquad (1)$$

The equilibrium equation or equation of state is assumed to be defined by a modified version of the perfect gas law. This modified version is used since static conditions do not exist in the chamber as a result of chemical reaction and flow through the chamber. The equation is written as:

$$P_c V = M R T$$

or more generally

$$P_c (t) V = R M_c (t - \tau_m) \cdot T (t - \tau_t) \qquad (2)$$

The τ_t term is a time delay function and implies that pv at the present time equais M_c RT at τ_t units of time earlier. (See Attachment III-B) This approach allows one to study the process by varying τ_t which is an indication of thermal and combustion lags in the chemical process.

Dividing Equation 1 by Δt and assuming,

$$\lim_{\Delta t \to 0} \frac{\Delta P_c}{\Delta t} = \frac{d P_c}{dt}$$

yields

$$\dot{P}_c = \frac{\partial P_c}{\partial M_c} \dot{M}_c + \frac{\partial P_c}{\partial T} \dot{T} + \frac{\partial P_c}{\partial \rho} \dot{\rho} + \frac{\partial P_c}{\partial C^*} \dot{C}^* \qquad (3)$$

Thermochemical calculations have shown that temperature variation is strongly influenced by mixture ratio. This variation is approximated as,

$$\Delta T = f(r_c) = \frac{\partial T}{\partial r_c} \Delta r_c; \quad r_c = \frac{W_o}{W_f} \text{ (ratio by mass)} \qquad (4)$$

Equation (4) with respect to time becomes

$$\dot{T} = \frac{\partial T}{\partial r_c} \dot{r}_c \qquad (5)$$

Similarly we have

$$\dot{p} = \frac{\partial \rho}{\partial r_c} \dot{r}_c \qquad (6)$$

and

$$\dot{C}^* \frac{\partial C^*}{\partial r_c} \dot{P}_c \qquad (7)$$

combining Equations (2), (3), (4) and (5) with Equation (1) yields:

$$\dot{P}_c = \frac{R}{V} \dot{M}_c (t - \tau_m) T + M_c (t - \tau_m) \frac{\partial T}{\partial r_c} \qquad (8)$$

$$+ \frac{V}{R} \frac{\partial \rho}{\partial r_c} \frac{\partial P_c}{\partial \rho} + \frac{V}{R} \frac{\partial P_c}{\partial C^*} \frac{\partial C^*}{\partial r_c} \dot{r}_c$$

Observation reveals that the partial derivative terms on the right of Equation (8) are the slopes of curves available from thermochemical calculations. These slopes may readily be obtained Attachment III-C and used as data inputs to the computer required for obtaining P_c (t).

It must be emphasized here that mixture ratio in Equation (8) is defined as the mass ratio of oxidizer to fuel concentration in the chamber and not the mass flow rate ratio as the more conventional definition implies. This definition is important for two reasons: First, the thermochemical calculations are based on

the definition, and second, extreme fluctuations in mixture ratio may exist in the chamber while the average flow rate deviation in the liquid state is negligible. The latter reason may be better understood when one recalls that the actual mass in the chamber, from which combustion characteristics are obtained, is quite small. Consequently, small fluctuations in liquid flow rates in the injector are capable of producing large instantaneous changes in mixture ratio in the chamber. The distinction is also important when fuel lead and oxidizer lead effects are evaluated.

B. PROPELLANT FLOW EQUATIONS

Continuity and mass conservation demands

$$\dot{M}_c = \dot{M}_t - \dot{M}_c \tag{9}$$

Assuming the nozzle is choked for the entire process

$$\dot{M}_c = \frac{Ag}{C^*} P_c (t - \tau_t) \tag{10}$$

Using (9) and (10) we have

$$M_c = \int \left[\dot{M}_T - \frac{A_t g}{C^*} P_c (t - \tau_t) \right] dt \tag{11}$$

Flow through the injector for oxidizer and fuel respectively is given as:

$$\dot{M}_{oT} = K_o (\Delta P_{io})^a \quad \dot{M}_{fT} = K_f (\Delta P_{if})^b \tag{12}$$

$a \approx b \approx 1/2$

By definition:

$$\dot{M}_c = \dot{M}_{oc} + \dot{M}_{fc} \tag{13}$$

$$\dot{M}_T = \dot{M}_{oT} + \dot{M}_{fT} \tag{14}$$

$$\dot{r}_c = \frac{d}{dt} \left(\frac{W_o}{W_f} \right) = \frac{W_o - r_c \dot{W}_f}{W_f} \tag{15}$$

C. SCHEMATIC OF ANALOG SIMULATION

A schematic diagram of the analog simulation is shown in Figure 5. The figure as shown represents a "module" since the line dynamics are represented in a form suitable for attachment to another propellant line yielding a model suitable for multi-engine system analysis. The stability derivatives occurring in Equation (8) were inserted in the analog loop by use of function generators available for this purpose. Time delay modules were used to simulate time delay effects in the supply line dynamics and thermodynamic loop. The resulting major loop (module) is employed to investigate step response as well as low frequency instability.

This module concept has been used for evaluation of coupling in multi-engine systems.

BELL ENGINE SYSTEM MATHEMATICAL MODEL

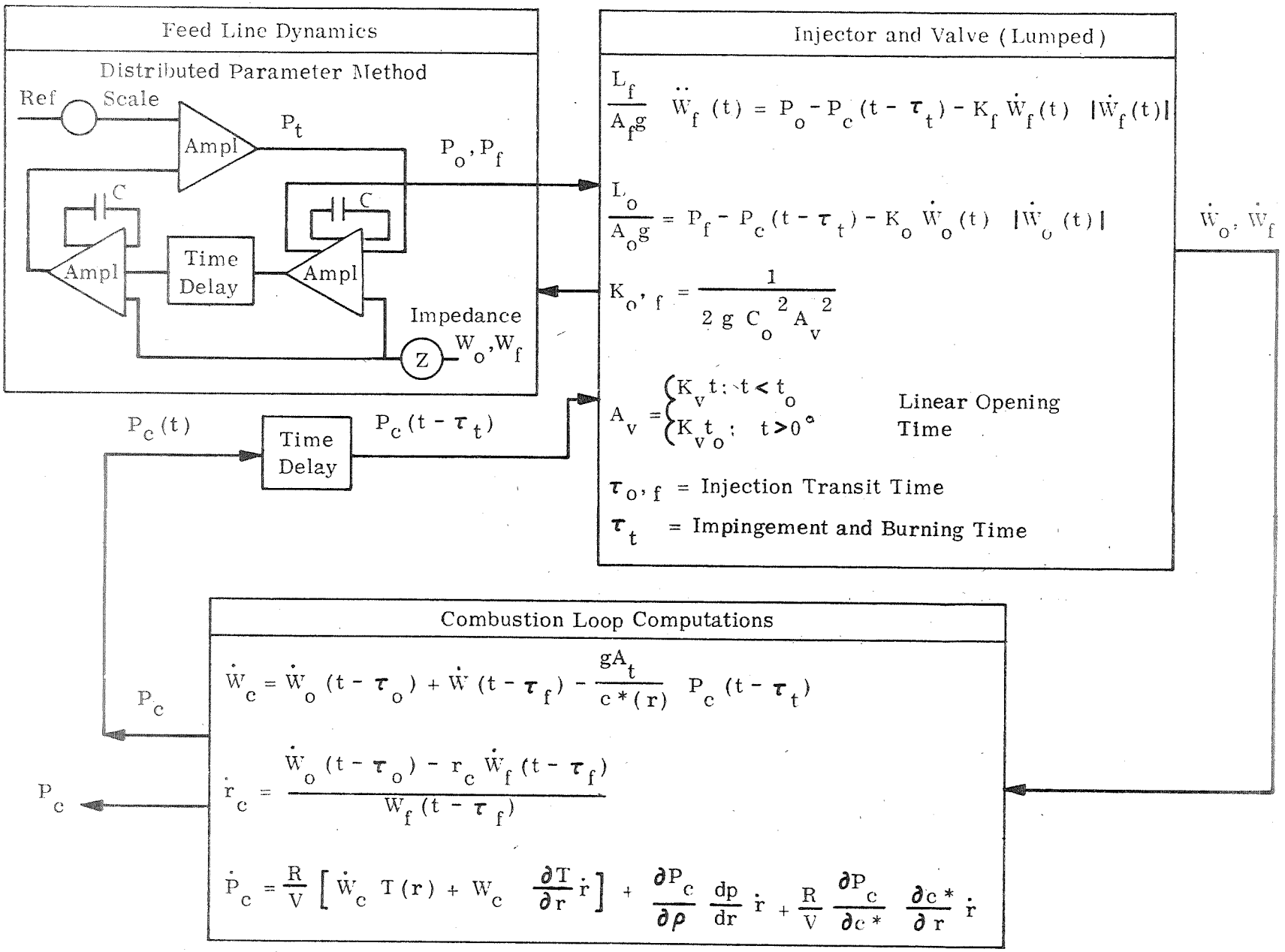

Figure 5.

ATTACHMENT III-E

FUEL DISTURBANCE SENSITIVITY (MATHEMATICAL EXPLANATION)

Experience has shown that intermittant flow disturbances in the fuel feed line produces chamber pressure oscillations. The equations will now be examined to determine whether some information may be obtained which will explain this phenomena.

Assume that the engine is operating in the steady-state, or $\dot{r} = 0$. Then $\dot{P}_c$ becomes,

$$V.1 \qquad \dot{P}_c = \frac{R}{V} \dot{W}_c T$$

Since the system is in the steady state

$$(a) \quad \dot{W}_o (t - t_o) = \dot{W}_o (t)$$

$$(b) \quad \dot{W}_f (t - t_f) = \dot{W} (t)$$

$$(c) \quad P_c (t - t_t) = P_c (t)$$

consequently $\dot{W}_c$ is given as

$$V.2 \qquad \dot{W}_c = - \frac{g A_t}{C^*} P_c \quad \text{where } \mathcal{W} = \dot{W}_c + \dot{W}_f$$

Using V.2 in V.1 and simplifying yields,

$$V.3 \qquad \tau \dot{P}_c + P_c = K$$

$$\text{where: } \tau = \frac{Ve^*}{RgA_t} \qquad K = \frac{\mathcal{W} C^*}{RgA_t}$$

Since, (imposing conditions V.1 (a), (b) and (c))

$$V.4 \qquad \dot{r}_c = \frac{\dot{W}_o - r_c \dot{W}_f}{W_f} = \frac{1}{W_f} \left[\dot{W}_o - r_c \dot{W}_f \right]$$

or

$$W_f \dot{r}_c = \left[\dot{W}_o - r_c \dot{W}_f \right]$$

And

$$\text{V.5} \quad \frac{W_f}{\dot{W}_f} \dot{r}_c + r_c = \frac{\dot{W}_o}{\dot{W}_f} \quad \text{(a first order differential equation)}$$

Notice that W_f in Equation V.5 is the weight concentration of propellant in the chamber. If $\dot{r}_c = 0$ we then have the identity $r_c = r_c$. If W_o is perturbed the identify still holds $r_c \equiv r_c$. Thus varying W_o produces a small change in r_c. However, if W_f is disturbed, then r_c at any subsequent time must be determined by solving the first order differential equation. As an example, if W_f is a "time" constant, equation V.5 may then be written as,

$$\frac{}{W_f}$$

$$\text{V.6} \quad \tau \dot{r}_c + r_c = \bar{r}$$

where $\tau = \frac{W_f}{\dot{W}_f}$

$\frac{\dot{W}_o}{\dot{W}_f} = \bar{r}$ (the time average mixture ratio).

Note that in the steady state, $\dot{r}_c = 0$, we have

$$r_c = \bar{r}$$

or the mixture ratio by weight in the chamber does indeed equal the average mixture ratio.

Let us now assume that r_c is capable of changing more rapid than $\bar{r}$ so much so that $\bar{r}$ may be assumed constant as r_c is disturbed. This is equivalent to assuming that large instantaneous changes may be made in very short time intervals in r_c with little or negligible change in average mixture rate weak function compared to $\bar{r}$, or that $\bar{r}$ is "almost" constant the solution to the differential equation V.6 becomes,

$$\text{V.7} \quad r_c = \bar{r} + C \; e - \frac{1}{\tau} t$$

where C is an arbitrary constant.

To obtain an estimate of C differentiate Equation V.7 and assume for initial condition, $r_c = 0$ when $t = 0$, we have,

$$C = \tau \dot{\bar{r}}$$

Equation V.7 now becomes,

$$\text{v.8} \qquad r_c = \bar{r} + \tau \dot{\bar{r}} \, e^{-\frac{t}{\tau}}$$

For this linearized condition the mixture ratio by weight in the chamber is related to the average mixture ratio in a peculiar manner. The time constant τ which governs the nature of transient response as given by Equation V.8 is independent of the oxidizer properties which appear only in the $\bar{r}$ and $\dot{\bar{r}}$ terms. Thus for an oxidizer disturbance, τ is not grossly affected and the resulting r_c change as a function of time will be mild. However, if a disturbance occurs in the fuel line τ is altered and subsequently the magnitude and decay rate are affected resulting in a more drastic change in r_c, or a dynamic situation is initiated. This discussion gives a rather weak mathematical picture of the phenomena, but tends to agree with observed data.